NASA CR-134588

OUT-OF-PILE CREEP BEHAVIOR OF URANIUM CARBIDE

by

T. R. Wright and M. S. Seltzer

BATTELLE
Columbus Laboratories

prepared for

NATIONAL AERONAUTICS AND SPACE ADMINISTRATION

NASA Lewis Research Center
Contract NAS 3-16776
Cleveland, Ohio 44135

NASA CR-134588

OUT-OF-PILE CREEP BEHAVIOR OF URANIUM CARBIDE

by

T. R. Wright and M. S. Seltzer

BATTELLE
Columbus Laboratories

prepared for

NATIONAL AERONAUTICS AND SPACE ADMINISTRATION

NASA Lewis Research Center
Contract NAS 3-16776
Cleveland, Ohio 44135

FOREWORD

The following report was prepared by personnel of Battelle's Columbus Laboratories, Columbus, Ohio, and describes original work performed under Contract NAS 3-16776.

The contract was awarded to Battelle-Columbus by the NASA-Lewis Research Center. Technical monitoring was provided by Mr. G. K. Watson of the NASA-Lewis Research Center.

Dr. T. R. Wright served as Program Manager at Battelle's Columbus Laboratories.

The contract was performed over the period from July 1, 1972, to June 30, 1973.

TABLE OF CONTENTS

Table of Contents (Continued)

LIST OF TABLES

LIST OF FIGURES

List of Figures (Continued)

List of Figures (Continued)

OUT-OF-PILE CREEP BEHAVIOR OF URANIUM CARBIDE

by

T. R. Wright and M. S. Seltzer

ABSTRACT

Compression creep tests were performed on various UC-based fuel materials having a variation in both density and composition. Specimens were prepared by casting and by hot pressing. Steady-state creep rates were measured under vacuum at 1400 to 1800 C in the stress range 500-4000 psi. All data could be fit by an expression of the form: $\dot{\varepsilon} = A\sigma^n \exp^{-Q_c/RT}$. Values for the stress exponent were in the range $1.3<n<2.3$ while Q_c varied from 23.1 to 79.6 kcal/mole.

SUMMARY

Compression creep tests have been performed on fully dense and 75 percent dense specimens of $UC_{1.01}$, $UC_{1.01}$ + 4 weight percent W and $U_{0.9}Zr_{0.1}C_{1.01}$ + 4 weight percent W, on 85 percent dense specimens of the latter two compositions, and on fully dense specimens of $UC_{1.05}$. Steady-state creep rates for fully dense samples were measured in the range of 1400 - 1800 C under a vacuum of 1.33×10^{-3} N/m^2 (1×10^{-5} torr) while tests on low density specimens were conducted at 1400 and 1550 C in a vacuum of $6.65 + 10^{-4}$ N/m^2 (5×10^{-6} torr). The data for fully dense $UC_{1.01}$ could best be fit by an expression of the form $\dot{\varepsilon} = 1773\ \sigma^{6.024} \exp\left(\frac{106.5}{RT}\right)$, where $\dot{\varepsilon}$ is the steady-state creep rate in h^{-1}, σ is the applied stress in MN/m^2, and the creep activation energy is given in kcal/mole. The stress dependence for creep of $UC_{1.05}$ decreased with decreasing temperature because of second-phase precipitation; therefore, a unique creep activation energy could not be

established for this U/C ratio. At all temperatures, the creep strength of $UC_{1.05}$ exceeded that of $UC_{1.01}$. For example, at 1700 C steady-state creep rates for $UC_{1.05}$ were about one-fourth those for $UC_{1.01}$, but at 1400 C the creep rates were about three orders of magnitude less. At 1700 C, creep rates for uranium carbide alloys are some four orders of magnitude lower than those for unalloyed $UC_{1.01}$.

All data for low-density specimens could be fit by an expression of the form: $\dot{\varepsilon} = A\sigma^n \exp^{-Q_c/RT}$ where $\dot{\varepsilon}$ is the creep rate, A is a constant, σ is the applied stress, n is the stress exponent, Q is the creep activation energy, and T is the absolute temperature. Values for the stress exponent were in the range $1.3<n<2.3$ while Q_c varied from 23.1 to 79.6 kcal/mole.

INTRODUCTION

The following research program was undertaken to assist NASA in obtaining information on the mechanical behavior of potential uranium carbide-base nuclear fuels of the type being considered for use in thermionic space power reactors. Since the proposed thermionic nuclear power generation devices are to operate at temperatures above 1400 C for times up to 50,000 hours, the mechanical response of all components of the system to small stresses can result in creep strains which could profoundly affect the operating characteristics of the devices. Fission gas generated in the fuel is one source of stress which could cause the fuel to swell. In order to design a fuel containment system that would minimize the damage caused by this swelling, it was necessary to know the creep strength of the fuel, which in this case is uranium monocarbide (UC), unalloyed and alloyed with tungsten or ZrC or both, and containing various amounts of porosity.

The overall objective of the program was to determine the out-of-pile (unirradiated) creep behavior of uranium carbide-base nuclear fuels of the types being considered for thermionic space power reactors. The creep properties of these fuel materials were required for the analytical

modeling techniques to be used to predict the long-term performance of the reactor fuel elements. In addition, knowing the creep properties of the fuels would help in interpreting the results of actual irradiation tests.

The creep properties of four uranium carbide-base fuel materials were determined at approximately 1400 C, 1550 C, and 1700 C. The four fuel materials were (a) unalloyed uranium monocarbide, nominally $UC_{1.01}$, (b) unalloyed uranium monocarbide, nominally $UC_{1.05}$, (c) uranium-monocarbide plus 4 weight percent tungsten, and (d) uranium-10 mole percent zirconium monocarbide plus 4 weight percent tungsten. Location of the alloys of interest on the W-U-C compositional diagram is shown in Figure 1.

The materials were fabricated into creep test specimens of specified density levels, nominally 100 percent dense castings, and powder compacts 85 and 75 percent dense. These were characterized metallographically and analytically prior to creep testing. Creep tests were run at 1400 C, 1550 C, and 1700 C at stresses ranging upward from 3.4 MN/m^2 (500 psi). The initial low loads applied were increased progressively until measurable creep was obtained and then, depending upon the creep rate obtained, the creep measured at two or three additional stresses for each specific material and temperature. The entire test matrix is shown in Table 1. Results were analyzed for the effects of porosity, temperature, and alloy content upon creep strength. Activation energies were determined.

In order to achieve the stated objectives of this research, the program at Battelle's Columbus Laboratories was divided into three separate tasks covering specimen fabrication, creep testing, and data analysis. The results obtained on each of these tasks are presented in this report.

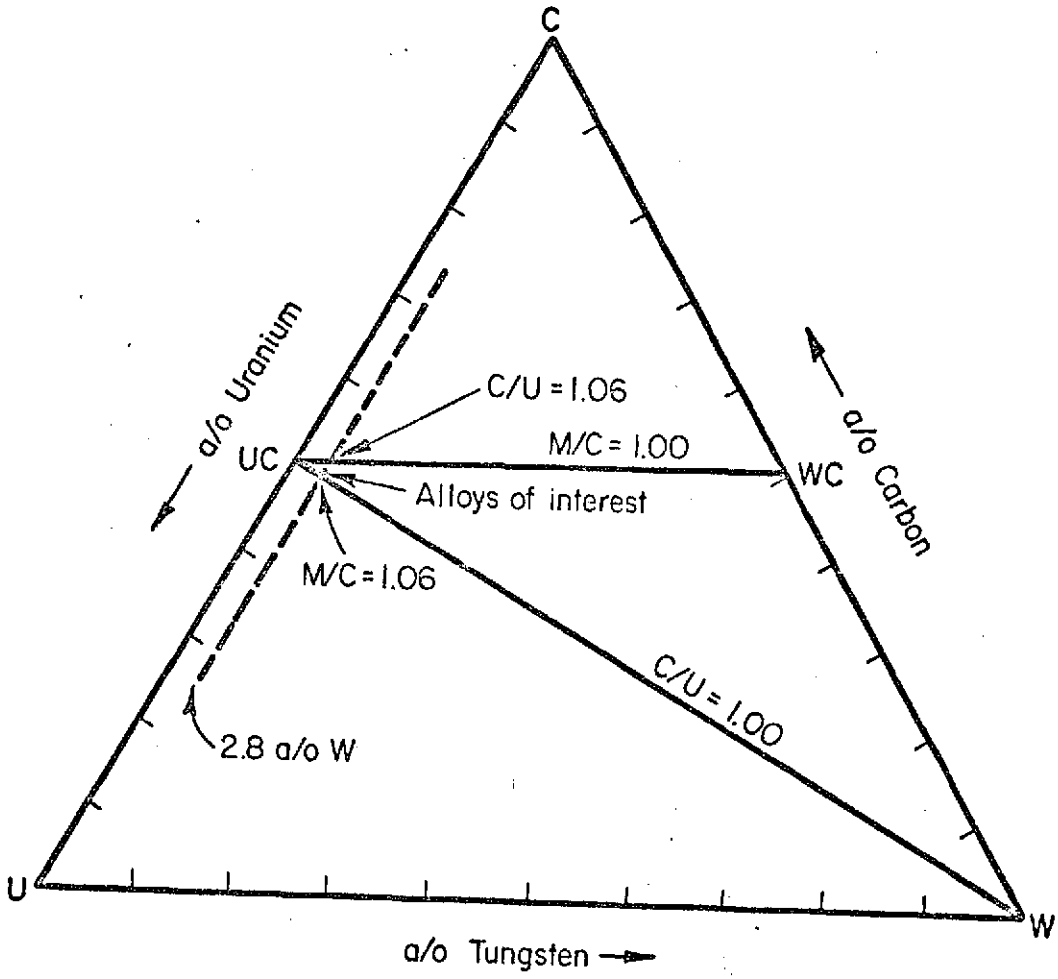

FIGURE 1. LOCATION OF ALLOYS OF INTEREST

TABLE 1. TEST MATRIX FOR DETERMINATION OF THE CREEP STRENGTH OF UC ALLOYS AT 1400 TO 1700 C

Alloy Composition	Density % of Theoretical	Number of Tests at Different Stresses Temperature		
		1400 C	1550 C	1700 C
$UC_{1.01}$	100	4	4	4
$UC_{1.01}$ + 4 w/o W	100	4	4	4
$U_{0.9}Zr_{0.1}C_{1.01}$ + 4 w/o W	100	4	4	4
$UC_{1.01}$	75	3	3	
$UC_{1.01}$ + 4 w/o W	75	3	3	
$U_{0.9}Zr_{0.1}C_{1.01}$ + 4 w/o W	75	3	3	
$UC_{1.01}$ + 4 w/o W	85	2	2	
$U_{0.9}Zr_{0.1}C_{1.01}$ + 4 w/o W	85	2	2	
$UC_{1.05}$	100	4	-	4

TASK I. PREPARATION OF SPECIMENS

D. P. Moak and E. O. Speidal

I. INTRODUCTION

The objective of this task was to prepare the 75, 85, and 100 percent dense creep specimens required by the testing program matrix. The 100 percent dense specimens were synthesized by arc-melting and drop-casting techniques. A sufficient number of castings also were prepared to provide material for the powder metallurgy preparation of the 75 and 85 percent dense specimens. Control specimens for each specimen type were prepared for the determination of stoichiometry, purity, homogeneity, microstructure, and grain size.

II. STARTING MATERIALS

The starting materials employed were nuclear grade depleted uranium, spectrographic grade carbon, iodide zirconium, and high-purity tungsten prepared by chemical vapor deposition from the fluoride. These materials were characterized by determining the level of impurity contents. Optical emission spectroscopy was used for metallic impurities, vacuum fusion for gaseous impurities, and combustion techniques for determining the carbon contents. The results of the starting materials characterizations are shown in Table 2.

The depleted uranium was high in carbon but this presented no problem in preparing the UC or UC alloys. The oxygen contents were all below the 200 ppm target with the zirconium containing the most oxygen at 108 ppm. In all cases, nitrogen and each of the metallic impurity contents were below the 100 ppm target.

TABLE 2. IMPURITY CONTENT OF STARTING MATERIALS

Starting Materials	Impurity Content,[a] ppm by weight															
	C	O	H	N	B	Si	Mn	Fe	Mg	Cr	Ni	Al	Mo	Cu	Ca	Sn
Depleted Uranium	740	58	4	8	0.7	30	5	70	<1	15	25	10	5	2	ND[b]	ND
Tungsten	6	44	<0.5	<4	ND	ND	ND	ND	ND	ND	ND	ND	ND	<1	<1	ND
Carbon	--	83	9	16	ND	ND	ND	50	ND	ND	ND	ND	ND	ND	ND	ND
Zirconium	18	108	6	<2	ND	<5	ND	70	<5	<10	10	10	ND	30	<5	5

(a) Other metallic impurities were sought by optical emission spectroscopy but none were found.

(b) ND - not detected.

III. SPECIMEN PREPARATION

High-Density Materials

The raw materials were mixed into charges in which each constituent had been added after weighing to at least three significant digits. The charges were prealloyed and reacted in a "button melting furnace" in which a flat "button" is melted and turned over and remelted at least seven times to insure homogeneity without opening the furnace. The prealloyed button was then transferred to a drop-casting furnace in which the button was remelted and dropped through the bottom of the hearth into a thin-walled graphite mold. The size of the casting was 0.53 cm (0.21 in.) diameter by 6 cm (2-1/2 in.) to 7.5 cm (3 in.) long.

The 100 percent dense creep specimens were prepared initially. One casting of each of the four compositions described in Table 1 was sufficient to provide 6 creep specimens of each composition. The specimens were ground to the creep specimen size of 0.43 cm (0.17 in.) diameter by 0.86 cm (0.34 in.) long using a diamond wheel and undiluted cutting oil as the coolant. All specimens were degreased with acetone, rinsed with ethyl alcohol, and stored under argon prior to creep testing.

Additional castings to provide material for the preparation of low-density specimens by powder metallurgy techniques also were prepared.

Low-Density Material

Approximately 150 g of $UC_{1.01}$ and 300 g each of $UC_{1.01}$ + 4 w/o tungsten and $U_{0.9}C_{1.01}$ + 4 w/o tungsten were prepared by drop casting. The castings were crushed by hand within an inert atmosphere glove box to minus 325 mesh (<44μ). The powder particle size was further reduced by ball milling under nanograde hexane for 8 hours in a stainless steel mill with tungsten carbide balls. The hexane was removed by vacuum extracted. Based on past experience, the as-milled powder particle size was expected to be less than 20 microns.

Several attempts were made initially to hot press specimens at 1800 C, varying time, pressure, and pressing technique. In all cases, sintering to higher than the required 75 and 85 percent densities occurred, presumably due to the finely divided and hence active state of the ball-milled powders. Because densities in excess of 94 percent of theoretical were obtained in all cases by direct hot pressing, an alternate fabrication method was devised.

Ball-milled alloy powders of all three compositions were sintered 3 hours at 1800 C, crushed to minus 270 mesh (<53 microns) and hot pressed at 1800 C into 75 and 85 percent dense cylindrical pellets nominally 2.5 cm (1 in.) diameter by 1 cm (0.4 in.) long. At the pressing temperature, 69 MN/m^2 (10,000 psi) pressure was applied until a predetermined die cavity volume was reached. The resultant bulk densities were as follows:

Alloy	Pressed Density, g/cm^3	Percent of Cast Density
$UC_{1.01}$	9.99	74.7
$UC_{1.01}$ + 4 w/o W	10.4 and 11.6	76.6 and 85.0
$(U_{0.9}\ Zr_{0.1})\ C_{1.01}$ + 4 w/o W	9.71 and 11.0	85.7 and 86.0.

Pellets nominally 0.47 cm (0.19 in.) diameter by 1 cm (0.4 in.) long were electro-discharge machined from the above-pressed slugs and finished to the final 0.43 cm (0.17 in.) diameter by 0.86 cm (0.34 in.) length test specimen by grinding under undiluted cutting oil. The finished specimens were washed ultrasonically in trichloroethane and in ethyl alcohol. Following the washing cycle, all specimens were vacuum outgassed at 1000 C and 1.3×10^{-4} N/m^2 (10^{-6} torr) and stored under high-purity argon until required for creep testing.

IV. SPECIMEN CHARACTERIZATION

High-Density Material

All of the nominally 100 percent dense specimens were initially characterized by measuring the density. This was accomplished by physical dimension and weight measurements. These results are shown in Table 3.

TABLE 3. AVERAGE BULK DENSITY OF CAST CARBIDE CREEP SPECIMENS

Nominal Composition	Average Density, g/cm^3 (min. - max.)
$UC_{1.01}$	13.32 (13.17-13.37)
$UC_{1.05}$	13.27 (13.21-13.37)
$UC_{1.01}$ + 4 w/o W	13.61 (13.37-13.71)
$(U_{0.9}Zr_{0.1})\ C_{1.01}$ + 4 w/o W	12.83 (12.74-12.94)

The average density results are perhaps somewhat low as some edge chipping was experienced on most of the specimens. These results do indicate, however, that no large shrinkage voids are present in the specimens.

A control specimen from the top and bottom of each casting was examined metallographically and these results are shown in Figures 2 through 5. Figure 2a shows the structure obtained near the top of the

$UC_{1.01}$ casting. The estimated carbon content is 4.85 to 4.90 w/o and the average ASTM grain size number is 2.6. The bottom of the casting shows a lower carbon content that is very close to the stoichiometric composition. No free uranium, however, was observed. The grain size shown in Figure 2b is approximately ASTM 3.9, average. This area, however, is from the lower portion of the casting and may exhibit some preferential grain orientation from the bottom of the mold. Grains located near the outer edge of the casting are somewhat larger; therefore, a grain size of 2.6 is considered to be more representative of the creep specimens prepared.

Figure 3 illustrates the microstructures of the top and bottom control specimens from the $UC_{1.05}$ casting. Both the top and bottom specimens contain ∿5.0 w/o carbon based upon the quantity of UC_2 platelets that are visible. As with the $UC_{1.01}$ casting, the grain size of the $UC_{1.05}$ casting is smaller at the bottom. The grain size believed representative of the creep specimen is approximately ASTM 2.0.

The microstructures shown in Figure 4 are representative of the $UC_{1.01}$ + 4 w/o W casting. The mottled structures shown are typical of this composition which make meaningful grain size measurements difficult. Although carbon content cannot be accurately determined metallographically, no evidence of free uranium or higher order carbides such as U_2C_3 and UC_2 was found.

Figure 5 shows the $(U_{0.9}Zr_{0.1})\ C_{1.01}$ + 4 w/o W casting microstructures. The apparent two-phase structure results from coring during solidification. The white phase is rich in ZrC, while the darker phase is UC-rich. Once again, the determination of grain size and carbon content by metallographic techniques is not meaningful.

Chemical characterization of the as-cast compositions was conducted and the results presented in Table 4. The alloy compositions were determined by wet chemical analysis techniques. Impurities were determined by inert gas fusion, mass spectrometry, and optical emission spectroscopy. The carbon

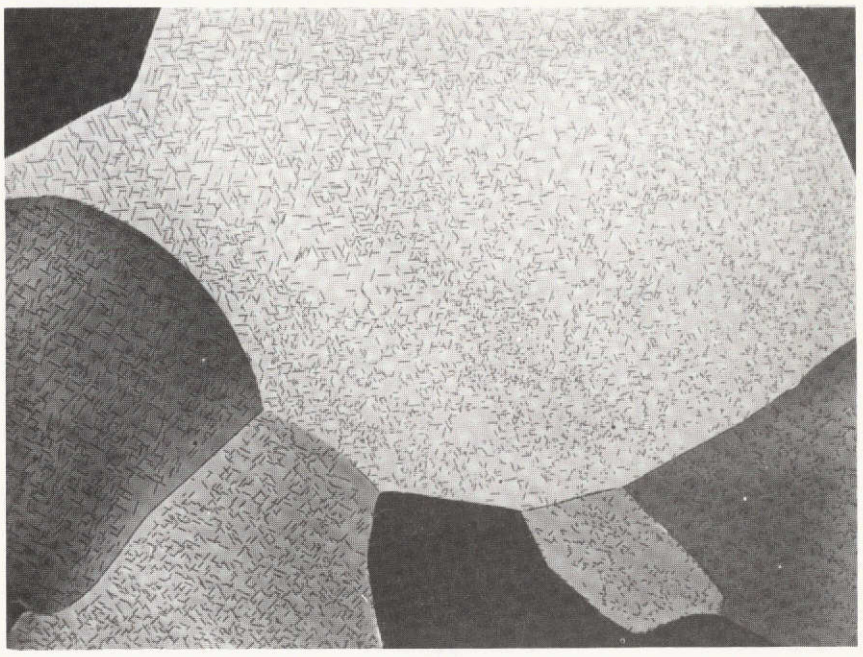

250X (a) Top 2G506

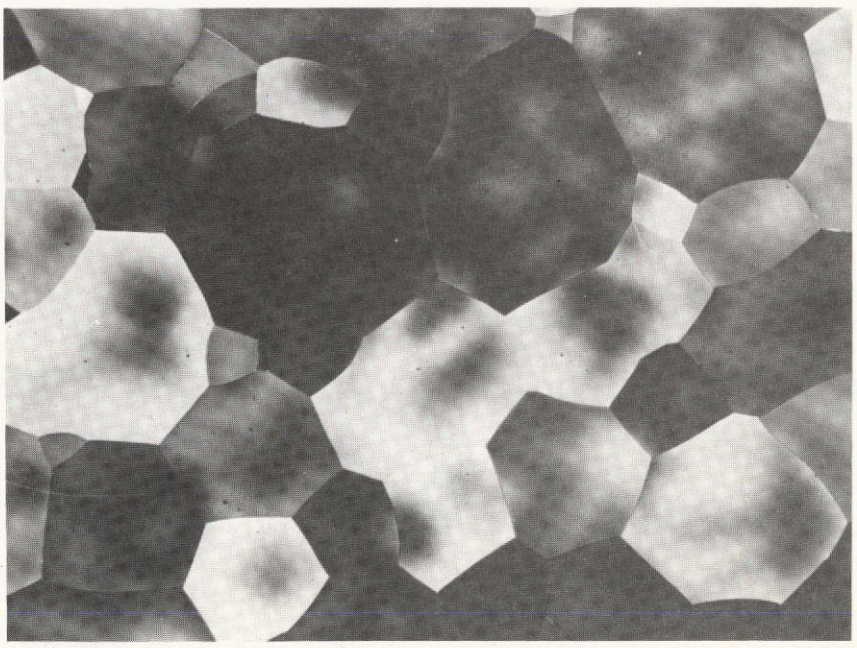

250X (b) Bottom 2G507

FIGURE 2. $UC_{1.01}$ CASTING (100% DENSE SPECIMENS)

Etchant: Equal parts H_2O, HNO_3, $HC_2H_3O_2$

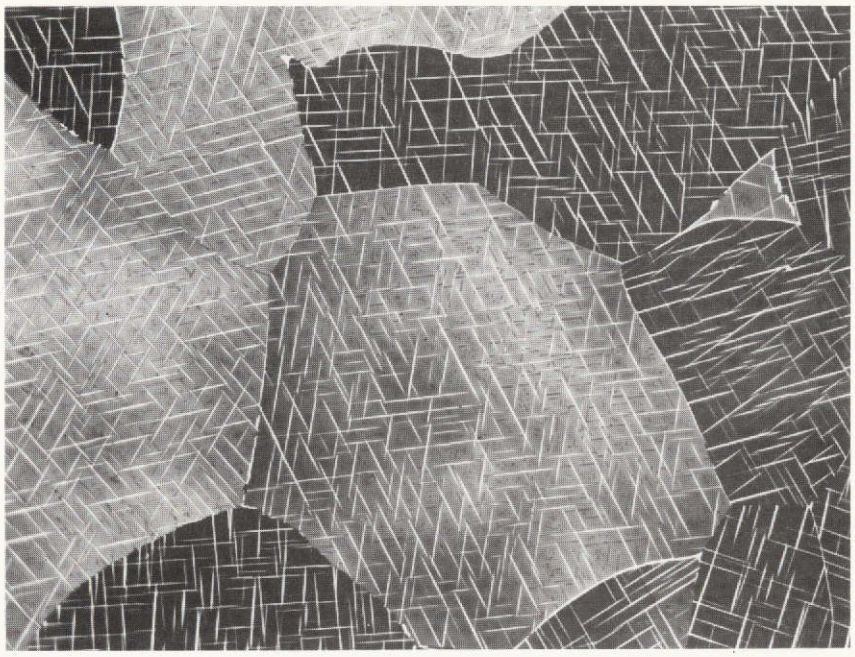

250X (a) Top 2G508

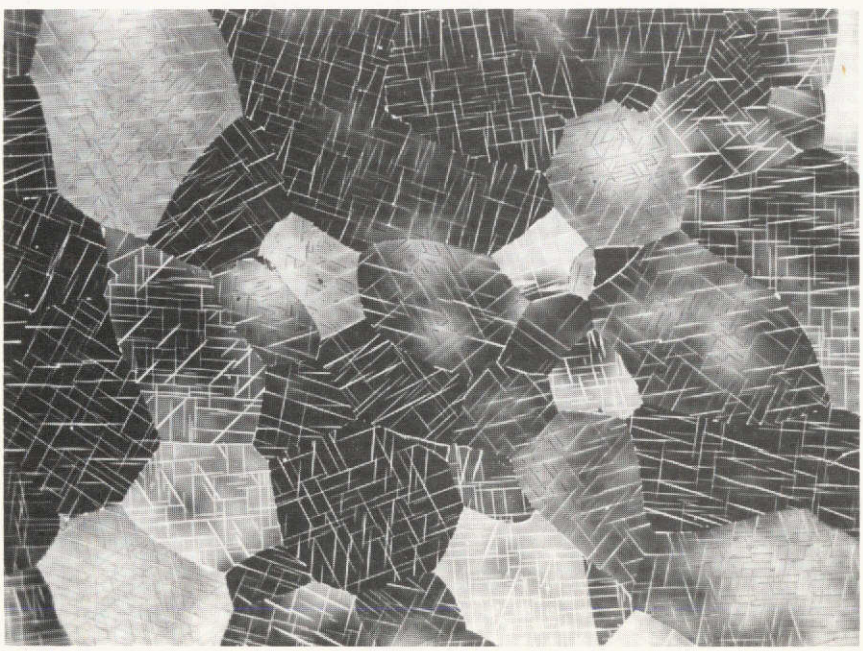

250X (b) Bottom 2G509

FIGURE 3. $UC_{1.05}$ CASTING (100% DENSE SPECIMENS)

Etchant: Equal parts H_2O, HNO_3, $HC_2H_3O_2$

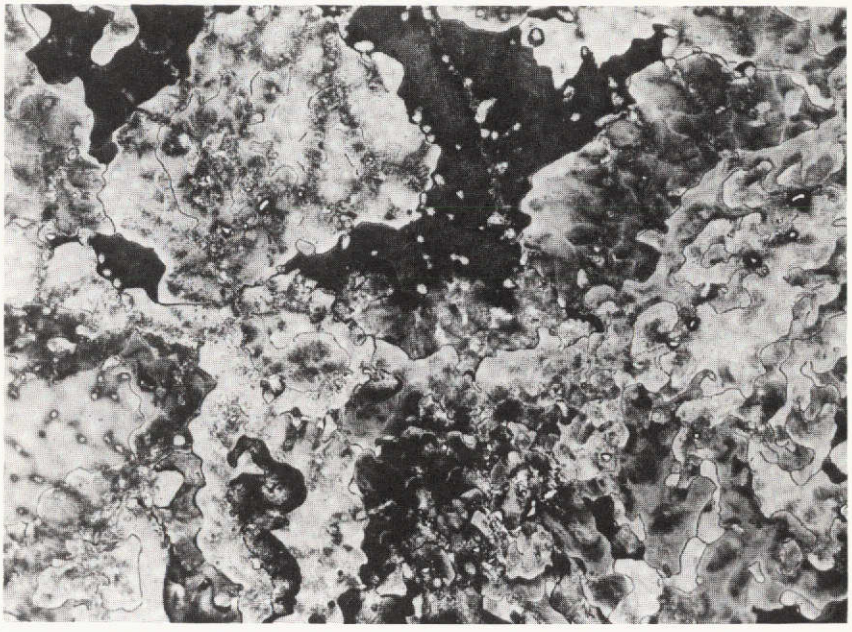

250X (a) Top 2G504

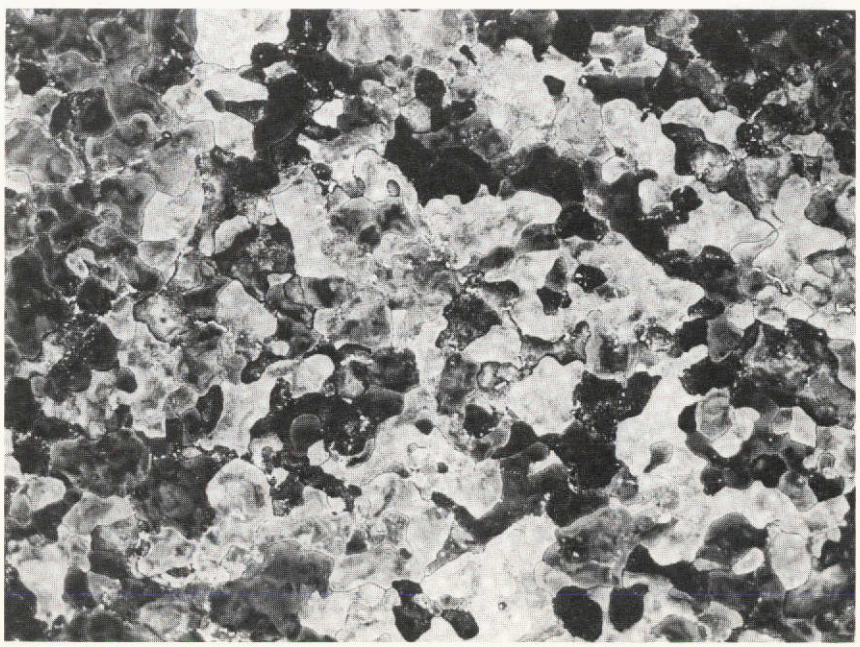

250X (b) Bottom 2G505

FIGURE 4. $UC_{1.01}$ + 4 w/o W CASTING (100% DENSE SPECIMENS)

Etchant: Equal parts H_2O, HNO_3, $HC_2H_3O_2$

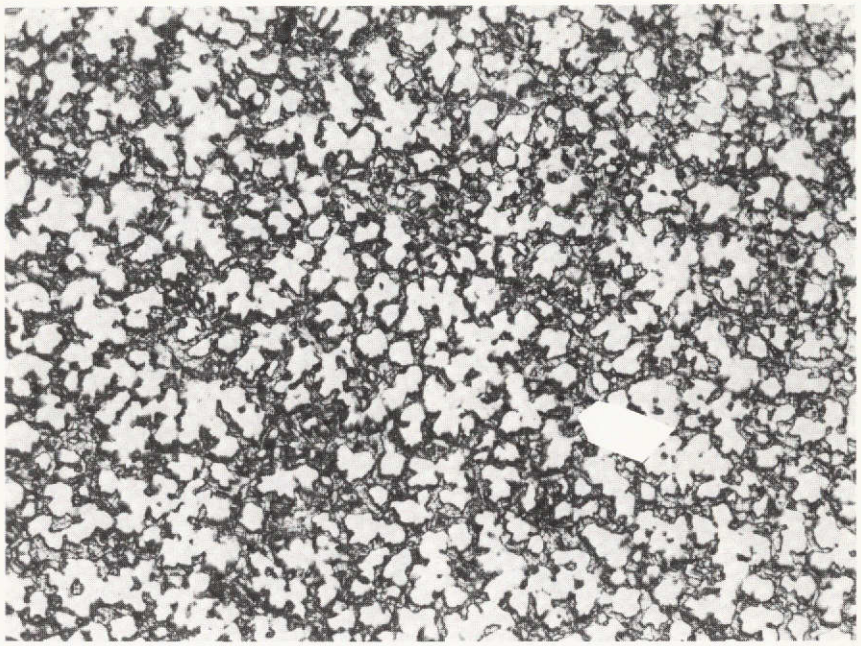

250X (a) Top 2G515

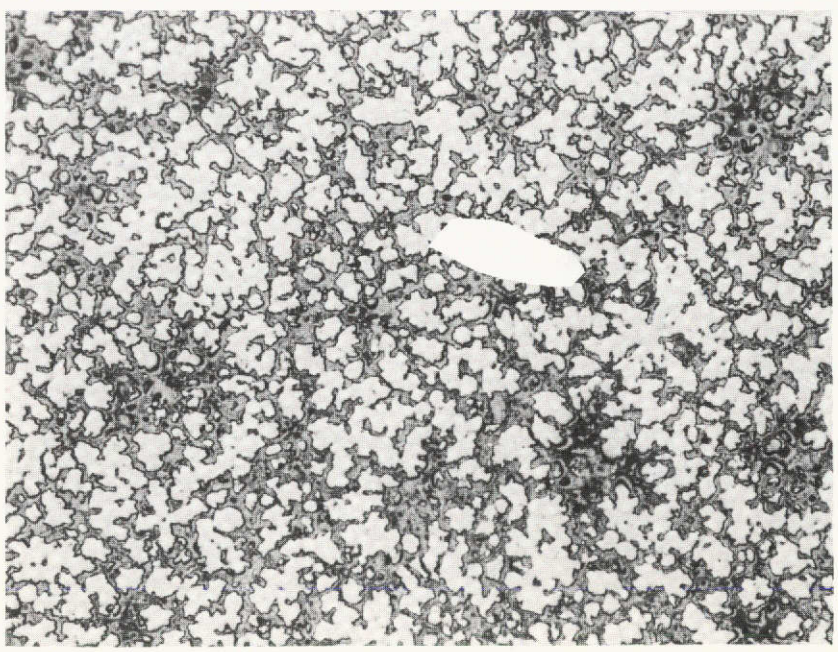

250X (b) Bottom 2G516

FIGURE 5. $(U_{0.9}Zr_{0.1})C_{1.01}$ + 4 w/o W CASTING (100% DENSE SPECIMENS)

Etchant: Equal parts H_2O, HNO_3, $HC_2H_3O_2$

TABLE 4. CHEMICAL CHARACTERIZATION RESULTS ON AS-CAST FUELS

Element	Analyzed Content, ppm (w)			
	$UC_{1.01}$	$UC_{1.05}$	$UC_{1.01}$ + 4 w/o W	$(U_{0.9}Zr_{0.1})C_{1.01}$ + 4 w/o W
C*	4.88	5.05	4.75	5.73
W*	--	--	4.01	3.78
Zr*	--	--	--	3.42
O	613	67	35	94
H	15	< 0.5	< 2	2
N	73	407	11	70
B	--	0.3	--	--
Si	--	15	--	--
Fe	--	20	--	--
Ni	--	5	--	--
Mo	--	1	--	--
Cu	--	2	--	--

* In weight percent.

contents of the ternary and quaternary carbides are slightly higher than the target levels but, as indicated earlier, no metallographic evidence of higher order carbides was found. This suggested that the alloys were within the desired ternary phase field.

The high level of oxygen in the $UC_{1.01}$ and nitrogen in the $UC_{1.05}$ seemed questionable as all alloys were prepared from the same starting stock and by exactly the same procedures. Metallic impurities were determined only in the $UC_{1.05}$ composition and are quite low. Other metallic impurities were sought by optical emission spectroscopy but were not found. These results were expected to be typical of the impurities present in the other alloys.

Low-Density Material

The densities of the low-density specimens measured after vacuum outgassing are listed in Table 5. If uncertainties of ±0.001 g, ±0.0025 cm (±0.001 in.), and 0.025 cm (±0.001 in.) were assigned respectively to the weight, diameter, and length measurements made on the individual pellets, then a maximum error of ±0.2 g/cm^3, or ±1.5 percent (±1.6 percent for the U-Zr-C-W alloy), could be expected in the calculated densities.

It was noted that only two pellets deviated more than ±0.2 g/cm^3 from the averages of the measured pellet densities. In both cases, the measured densities were low and could result from chipping of the edges rather than indicating a real variation in porosity.

Chemical and vacuum fusion analysis of control pellets indicated the results shown in Table 6. Other impurity elements determined by optical emission spectroscopy are shown in Table 7.

Microstructural characteristics of the materials are shown in the photomicrographs of Figures 6 through 10. It is particularly noted that the tungsten addition to the uranium carbide, containing excess carbon, has tied up this carbon as well-distributed UWC_2 leaving stoichiometric

TABLE 5. MEASURED BULK DENSITIES OF LOW-DENSITY CREEP TEST SPECIMENS

Specimen No.	Nominal Composition	Density		Deviation from Avg.		Avg.	
		g/cm^3	%(a)	g/cm^3	%(a)	g/cm^3	%(a)
PA 1	$UC_{1.01}$	10.2	76.1	+0.1	+0.5		
PA 2		10.0	74.9	-0.1	-0.7		
PA 3		10.0	74.5	-0.1	-1.1		
PA 4		10.0	75.]	-0.1	-0.4		
PA 5		10.2	76.6	+0.1	+0.1	10.1	75.6
PA 6		10.1	75.7	0	+0.1	±0.2	±1.5
PA 7		9.8	73.7	-0.3	-1.9		
PA 8		10.0	74.6	0	-1.0		
PA 9		10.3	77.0	+0.2	+1.4		
PB 1	$UC_{1.01}$ + 4 w/o W	10.3	75.9	-0.1	-0.5		
PB 2		10.4	76.7	0	+0.3		
PB 3		10.4	76.3	0	-0.1		
PB 4		10.4	76.6	0	+0.2		
PB 5		10.5	76.9	+0.1	+0.5	10.4	76.4
PB 6		10.5	77.1	+0.1	+0.7	±0.2	±1.5
PB 7		10.4	76.7	0	+0.3		
PB 8		10.5	77.3	+0.1	+0.9		
PB 9		10.5	77.1	+0.1	+0.7		
PB 11	$UC_{1.01}$ + 4 w/o W	11.7	85.7	0	-0.3		
PB 12		11.7	86.2	0	+0.2		
PB 13		11.7	86.2	0	+0.1	11.7	86.0
PB 14		11.7	86.1	0	+0.1	±0.2	±1.5
PB 15		11.7	85.9	0	-0.1		
PB 16		11.6	85.4	-0.1	-0.6		
PC 1	$(U_{0.9}Zr_{0.1})C_{1.01}$ + 4 w/o C	9.7	76.0	0	+0.4		
PC 2		9.6	74.5	-0.1	-1.1		
PC 3		9.8	76.6	+0.1	+1.0		
PC 4		9.5	73.8	-0.2	-1.8		
PC 5		9.8	76.2	+0.1	+0.6	9.7	75.6
PC 6		9.8	76.5	+0.1	+0.9	±0.2	±1.6
PC 7		9.7	75.8	0	+0.2		
PC 8		9.8	76.1	+0.1	+0.5		
PC 9		9.9	77.2	+0.2	+1.6		
PC 11	$(U_{0.9}Zr_{0.1})C_{1.01}$ + 4 w/o C	11.2	87.0	0	-0.3		
PC 12		11.1	86.4	-0.1	-0.9		
PC 13		11.2	87.2	0	-0.1	11.2	87.3
PC 14		11.2	87.4	0	+0.1	±0.2	±1.6
PC 15		11.2	87.6	0	+0.3		
PC 16		11.2	87.6	0	+0.3		

(a) Percent of average cast density: 13.36 g/cm^3 for $UC_{1.01}$; 13.61 g/cm^3 for $UC_{1.01}$ + 4 w/o W; 12.83 g/cm^3 for $(U_{0.9}Zr_{0.1})C_{1.01}$ + 4 w/o W.

TABLE 6. CHEMICAL ANALYSIS OF LOW-DENSITY PELLETS

Element, w/o	Nominal Alloy Composition		
	$UC_{1.01}$	$UC_{1.01}$ + 4 w/o W	$(U,Zr)C_{1.01}$ + 4 w/o W
Uranium	--	91.6	87.8
Tungsten	--	3.95	3.97
Carbon	4.82	4.90	5.16
Oxygen	0.239	0.260	0.327
Hydrogen	0.006	0.002	0.009
Nitrogen	0.004	0.011	0.010
Zirconium	--	--	3.32

TABLE 7. IMPURITY CONTENT OF LOW-DENSITY CONTROL PELLETS

Impurity, ppm	Nominal Alloy Composition		
	$UC_{1.01}$	$UC_{1.01}$ + 4 w/o W	$(U,Zr)C_{1.01}$ + 4 w/o W
Silicon	100	100	100
Iron	200	1000	1000
Magnesium	2	<1	1
Chromium	50	50	50
Nickel	20	50	50
Aluminum	200	20	20
Molybdenum	<1	<1	<1
Tin	2	<1	<1
Copper	100	30	50
Zinc	10	<10	<10
Titanium	20	10	<5
Cobalt	1	1	2
Calcium	40	5	5
Beryllium	1	1	1
Boron	2	2	2

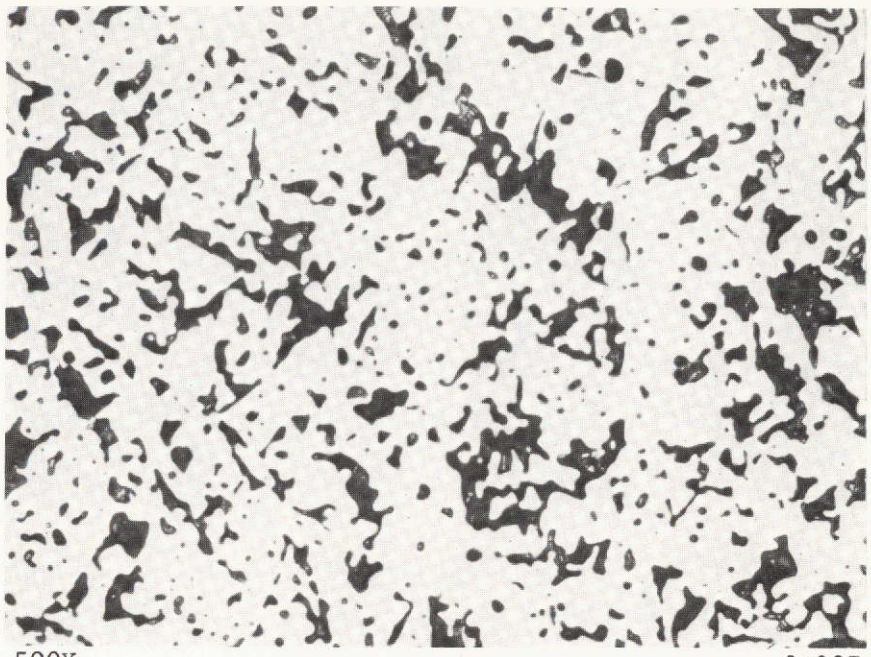

500X 2G907

(a) As Polished

500X 2G909

(b) Etched: Equal Parts Water, Nitric, and Acetic Acids

FIGURE 6. MICROSTRUCTURE OF 75 PERCENT DENSE $UC_{1.01}$ ALLOY

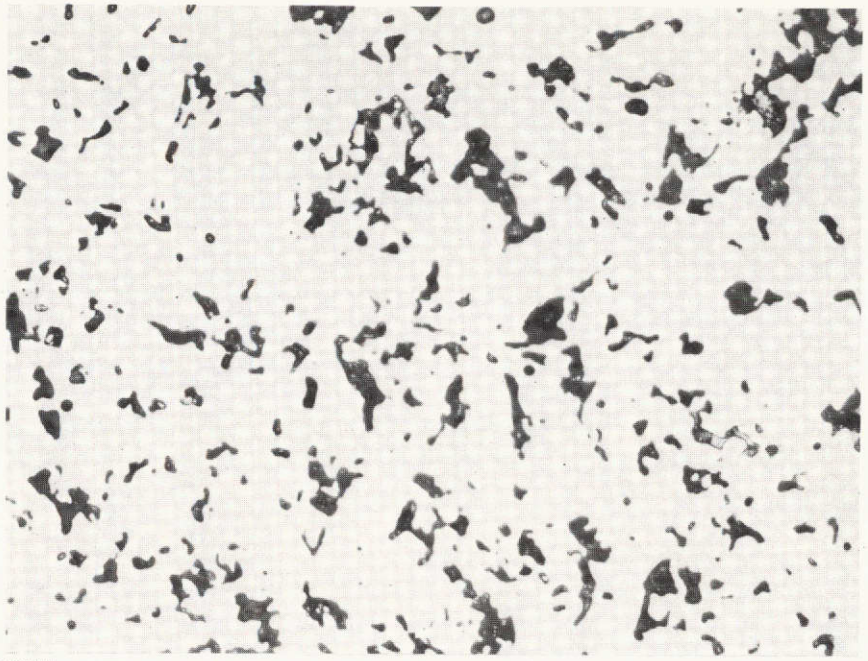

500X 2G910

(a) As-Polished

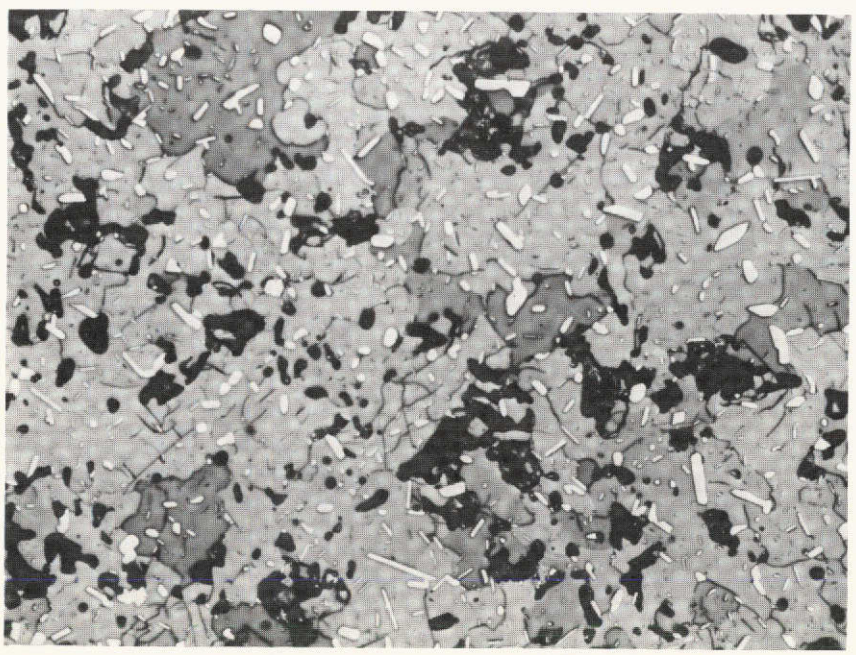

500X 2G911

(b) Etched: Equal Parts H_2O, HNO_3, HAc

FIGURE 7. MICROSTRUCTURE OF 75 PERCENT DENSE $UC_{1.01}$ + 4 W/O W ALLOY

Note: This material was extremely susceptible to moisture damage during metallographic preparation which caused the grey stringers quite evident near the center of the photomicrograph (b).

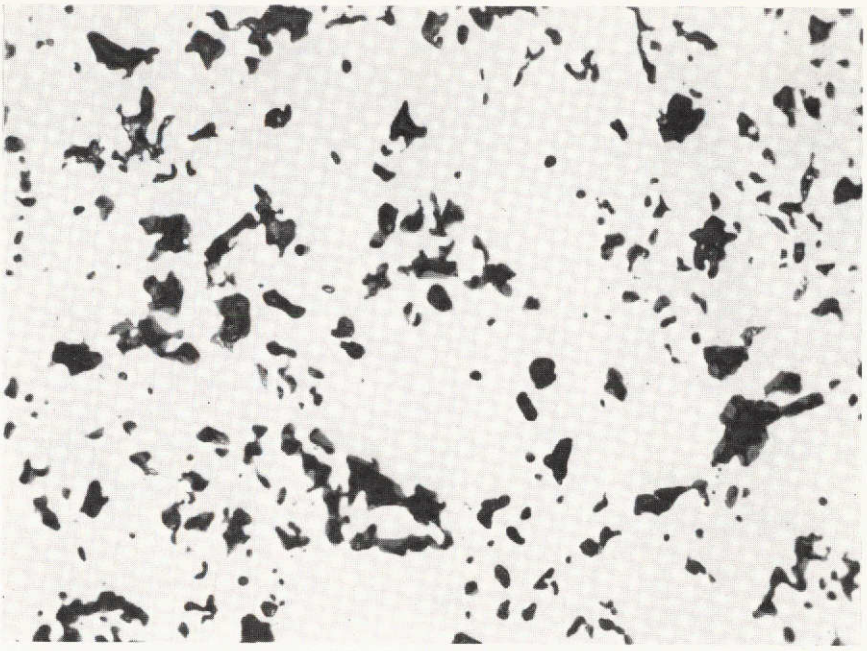

500X 2G913

(a) As Repolished After Etching

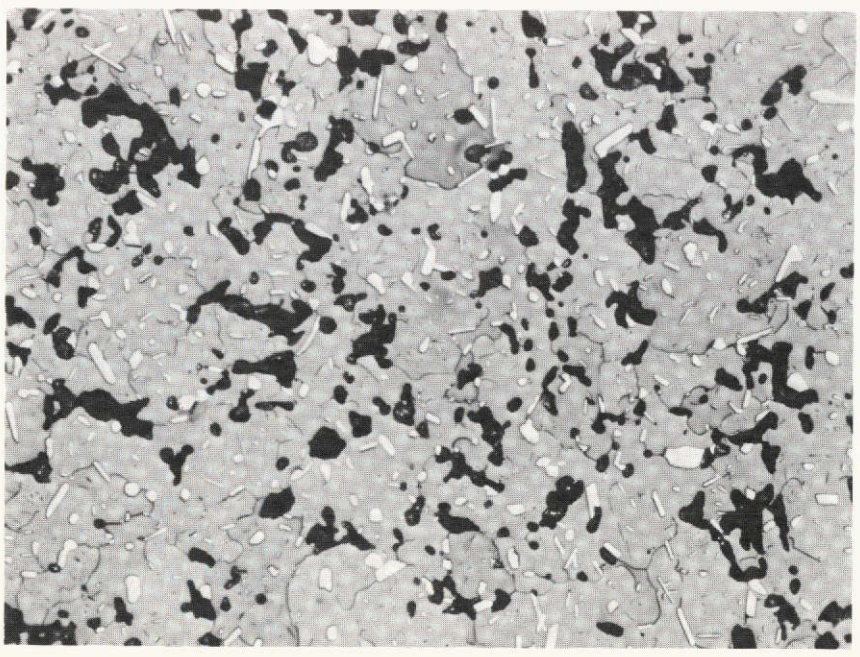

500X 2G914

(b) Etched: Equal Parts H_2O, HNO_3, HAc

FIGURE 8. MICROSTRUCTURE OF 85 PERCENT DENSE $UC_{1.01}$ + 4 W/O W ALLOY

Note: This material was quite susceptible to moisture damage during metallographic preparation which caused the grey"phase" seen at the edges of pores in (a).

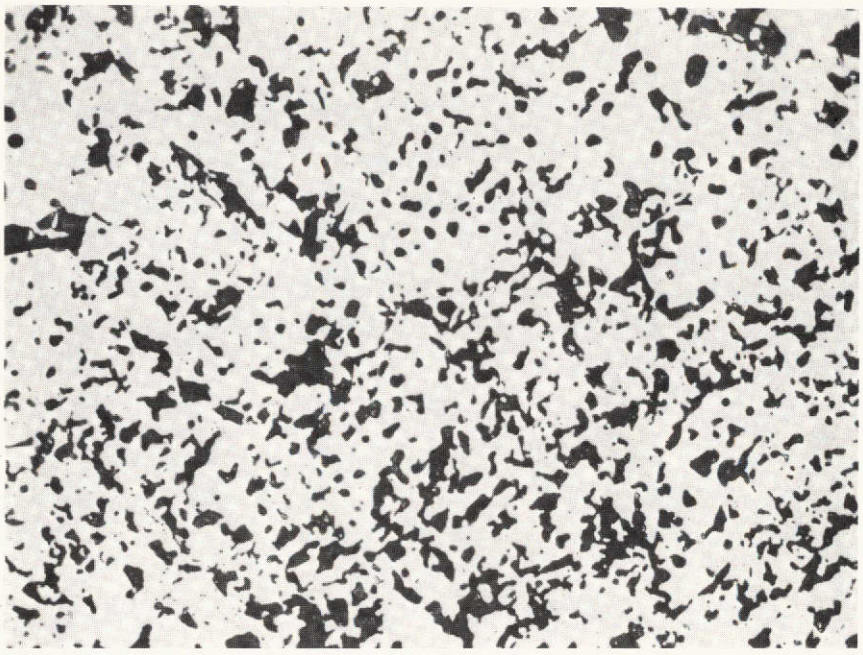

500X 2G917

(a) As-Polished

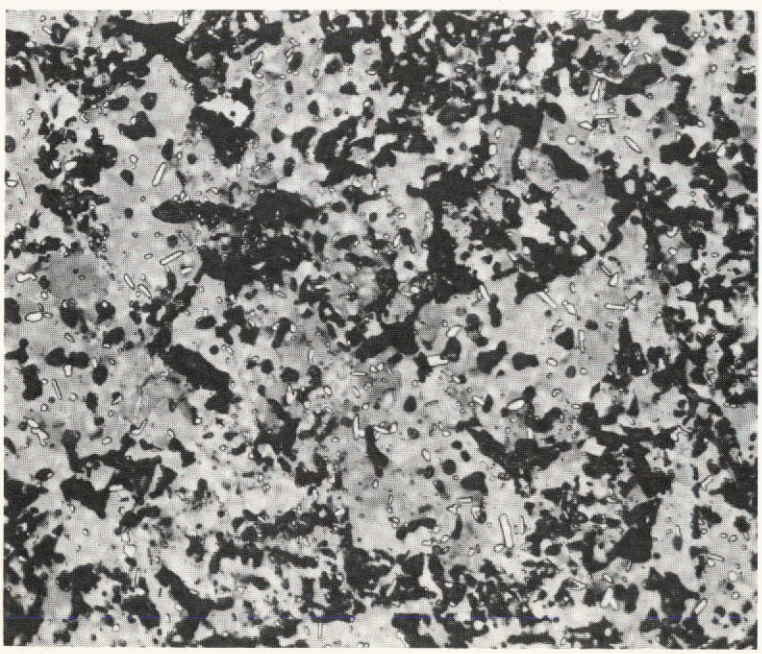

500X 2G919

(b) Lightly Etched: Equal Parts H_2O, HNO_3, HAc

FIGURE 9. MICROSTRUCTURE OF 75 PERCENT DENSE $(U_{0.9}Zr_{0.1})C_{1.01}$ + 4 W/O W ALLOY

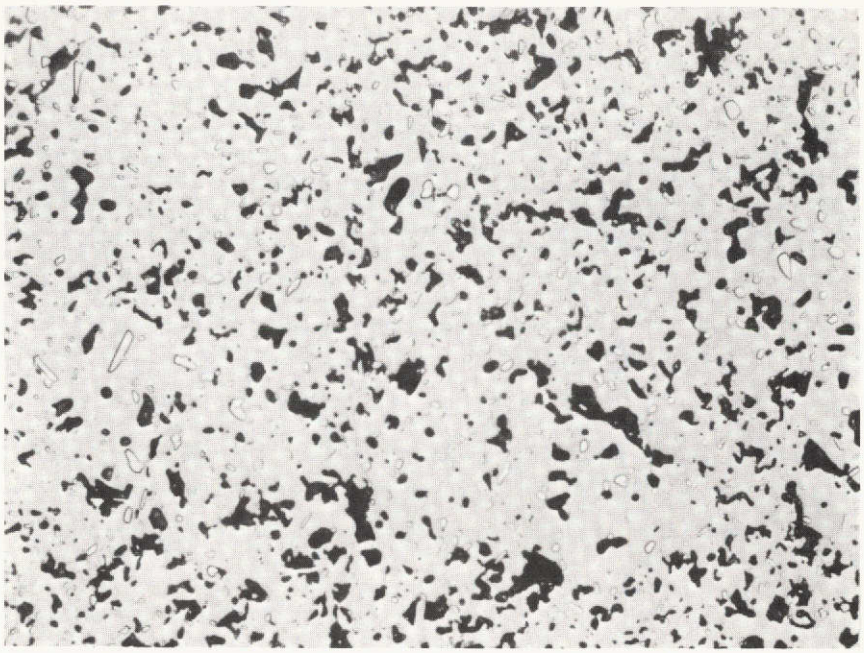

500X 2G922

(a) As-Polished and Lightly Etched to Show UWC_2 Phase (White)

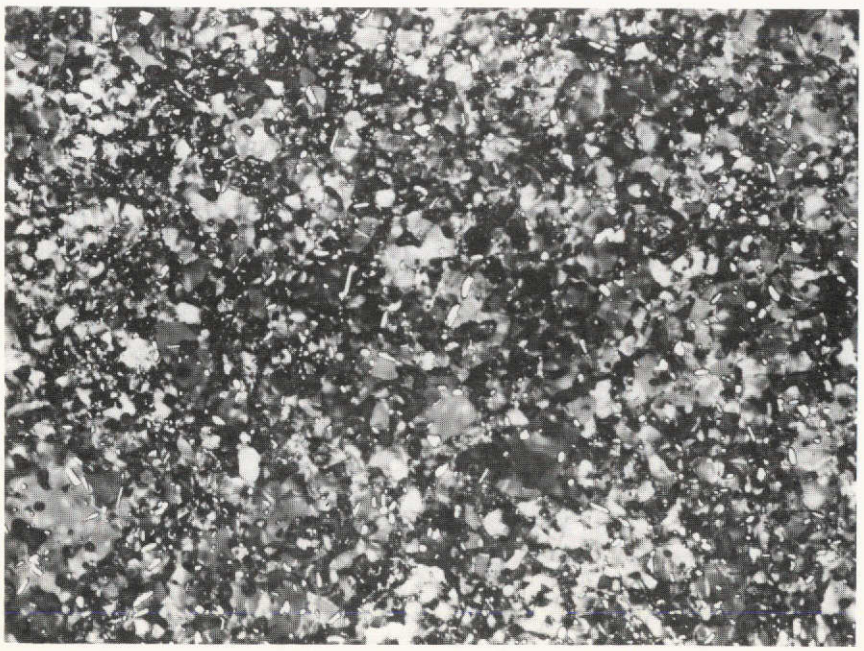

500X 2G923

(b) Heavily Etched: Equal Parts H_2O, HNO_3, HAc

FIGURE 10. MICROSTRUCTURE OF 85 PERCENT DENSE $(U_{0.9}Zr_{0.1})C_{1.01}$ + 4 W/O W ALLOY

UC as the matrix material. It was noted during processing that this material was quite "sinterable".

The presintering of the ball-milled powders before the recrushing and final hot pressing resulted in some isolated porosity as a part of the total porosity. It would appear that the amount of this residual porosity within the grains varies with the "sinterability" (or "refractoriness") of the basic matrix material. Intergranular porosity should be more stable during creep than that located at grain boundaries. If this is true, the above procedure may represent a method of preparing a structurally stable low-density fuel.

TASK II. CREEP TESTING

M. S. Seltzer and B. A. Wilcox

I. INTRODUCTION

Compression creep testing in vacuum of at least 1.33×10^{-3} N/m^2 (10^{-5} torr) was undertaken on all UC-base specimens over the temperature range 1400 C to 1700 C and stress range 4.55 to 69.0 MN/m^2 (660 to 10,000 psi). The specific stresses chosen were those which produced measurable creep rates in reasonable lengths of time. Stress cycling was performed on fully dense specimens in order to obtain about four steady-state creep rates per specimen at a given temperature. This technique was also used to a limited extent for the 75 and 85 percent dense specimens. In some cases, apparent changes in microstructure and density of low-density specimens during creep testing served to limit the amount of useful data which could be obtained from a given specimen. Therefore, some low-density specimens were tested at a single temperature and stress.

II. EXPERIMENTAL PROCEDURES

Compression creep testing was performed in two different vacuum creep furnaces. The fully dense samples were tested in a creep unit which operates at constant stress in a vacuum of 1.33×10^{-3} N/m^2 (10^{-5} torr). The system employs tungsten rams and LVDT arms. Previous studies at Battelle showed that uranium carbide may indent tungsten at the temperatures and stresses of interest in this study. Therefore, disks of "Bracermet", a cast eutectic alloy of refractory metal and carbide, were placed between the specimens and the platens during testing.

Strain over the specimen gage length alone was measured by determining the difference in deflection between the tungsten platens above and below the specimen. Tungsten push rods transmitted the deflection to a linear variable differential transducer located above the loading frame. Deflections of 12.77×10^{-5} cm (5×10^{-5} in.) could be measured, and the strain was recorded continuously. Chart speeds from 2.54 cm/sec (1 in/sec) to 0.254 cm/hr (0.1 in/hr) permit detailed recording of instantaneous, primary, and steady-state creep behavior. A sighting port allowed direct observation of the specimen (and strain measurement by optical means if necessary).

A constant-stress system ensured that the initial stress did not vary by more than 0.5 percent as the specimen was strained over several percent, without the necessity of adding load at regular intervals. Temperature was recorded continuously with a control of at least ±5 C over the specimen gage length. The specimens being tested were in the form of right cylinders with a height of 0.86 cm (0.34 in.) and diameter 0.43 cm (0.17 in.).

The leak rate of the constant stress creep unit could not be lowered below the level at which some oxidation of fully dense carbide samples occurred. Therefore, all testing of low-density specimens was performed in another creep unit that had a much lower creep rate and operated at a vacuum of 6.65×10^{-4} N/m^2 (5×10^{-6} torr). This unit employed a tungsten compression cage to allow application of a tensile load on the end blocks to put a compressive load on the specimen. As with the other creep unit, strain was recorded continuously using an LVDT system. A constant stress condition was maintained by the addition of weights to the unit with time. The leak rate of this system was sufficiently low, 0.6μm/hr, so that no oxidation was detected on any of the low-density specimens after annealing for 72 hours at 1750 C.

III. DATA PRESENTATION

Details of the tests conducted on nearly theoretically dense carbide specimens are included in Table 8 while data for the tests with low-density

TABLE 8. TEST INFORMATION FOR 100% DENSE, CARBIDE SPECIMENS TESTED IN VACUUM OF 1.33×10^{-3} N/m^2 (1×10^{-5} TORR)

Composition	Temp., °C	Stress, psi	Stress, MN/m^2	Strain on Loading*, %	Total Strain, %	Steady State Creep Rate, hr^{-1}	Total Time at Temp., hr
$UC_{1.01}$	1700	750	5.18	0.00	0.14	7.50×10^{-5}	21.2
$UC_{1.01}$	1700	1000	6.9	0.05	1.27	5.00×10^{-4}	8.3
$UC_{1.01}$	1700	1750	12.1	0.19	1.37	8.90×10^{-3}	0.67
$UC_{1.01}$	1700	2750	19.0	0.78	2.14	1.15×10^{-1}	0.14
$UC_{1.01}$	1550	1370	9.45	0.00	0.60	1.30×10^{-4}	68.0
$UC_{1.01}$	1550	2000	13.8	0.00	2.31	1.60×10^{-3}	30.7
$UC_{1.01}$	1550	3000	20.7	0.48	4.10	1.95×10^{-2}	1.1
$UC_{1.01}$	1550	4000	27.6	0.70	2.60	1.35×10^{-1}	0.15
$UC_{1.01}$	1400	2000	13.8	0.03	3.31	1.64×10^{-4}	99.3
$UC_{1.01}$	1400	2750	19.0	0.04	0.65	6.00×10^{-4}	5.7
$UC_{1.01}$	1400	4000	27.6	0.11	1.45	1.75×10^{-2}	0.75
$UC_{1.01}$	1400	5000	34.5	0.29	1.37	6.00×10^{-2}	0.20
$UC_{1.05}$	1700	1000	6.9	0.00	2.46	1.31×10^{-4}	63.7
$UC_{1.05}$	1700	1300	8.95	0.02	0.99	3.50×10^{-4}	22.8
$UC_{1.05}$	1700	2000	13.8	0.04	0.72	4.00×10^{-3}	1.5
$UC_{1.05}$	1700	3000	20.7	0.26	1.44	3.90×10^{-2}	0.33
$UC_{1.05}$	1400	4000	27.6	0.01	0.49	5.67×10^{-5}	40.3
$UC_{1.05}$	1400	5000	34.5	0.02	0.28	1.15×10^{-4}	24.0

* Strain in first two minutes.

TABLE 8. Continued

Composition	Temp., °C	Stress, psi	Stress, MN/m^2	Strain Loading*, %	Total Strain, %	Steady Creep Rate, hr^{-1}	Total Time at Temp., hr
$UC_{1.05}$	1400	6000	41.4	0.01	0.50	1.56×10^{-4}	24.7
$UC_{1.05}$	1400	8000	55.2	0.04	1.92	5.40×10^{-4}	24.3
$UC_{1.05}$	1400	10,000	69.0	0.04	1.02	1.14×10^{-3}	6.7
$UC_{1.05}$	1550	3000	20.7	0.00	0.56	2.40×10^{-4}	24.0
$UC_{1.05}$	1550	5000	34.5	0.06	1.02	1.90×10^{-3}	4.17
$UC_{1.05}$	1550	8000	55.2	0.15	1.31	1.32×10^{-2}	0.83
$UC_{1.01}$-4w/oW	1700	4000	27.6	0.00	0.53	1.00×10^{-4}	46.4
$UC_{1.01}$-4w/oW	1700	5000	34.5	0.01	0.86	3.08×10^{-4}	25.0
$UC_{1.01}$-4w/oW	1700	7000	48.3	0.04	0.67	7.50×10^{-4}	7.6
$UC_{1.01}$-4w/oW	1700	9000	62.1	0.09	2.00	2.17×10^{-3}	7.6
$U_{0.9}Zr_{0.1}C_{1.01}$-4w/oW	1700	4000	27.6	0.07	0.82	9.75×10^{-5}	42.0
$U_{0.9}Zr_{0.1}C_{1.01}$-4w/oW	1700	6000	41.4	0.02	0.49	2.11×10^{-4}	25.3
$U_{0.9}Zr_{0.1}C_{1.01}$-4w/oW	1700	9000	62.1	0.07	0.71	4.00×10^{-4}	12.3
$U_{0.9}Zr_{0.1}C_{1.01}$-4w/oW	1600	8000	55.2	0.00	0.13	1.40×10^{-5}	71.8
$U_{0.9}Zr_{0.1}C_{1.01}$-4w/oW	1600	10,000	69.0	0.01	0.14	2.50×10^{-5}	45.9
$U_{0.9}Zr_{0.1}C_{1.01}$-4w/oW	1800	2000	13.8	0.01	0.14	6.67×10^{-5}	18.0
$U_{0.9}Zr_{0.1}C_{1.01}$-4w/oW	1800	3000	20.7	0.03	0.45	1.41×10^{-4}	23.0
$U_{0.9}Zr_{0.1}C_{1.01}$-4w/oW	1800	5000	34.5	0.02	0.89	3.20×10^{-4}	24.0

* Strain in first two minutes.

TABLE 8. Continued

Composition	Temp., °C	Stress, psi	Stress, MN/m^2	Strain Loading*, %	Total Strain, %	Steady Creep Rate, hr^{-1}	Total Time at Temp., hr
$U_{0.9}Zr_{0.1}C_{1.01}$-4w/oW	1800	8000	55.2	0.03	0.75	8.40×10^{-4}	8.0
$U_{0.9}Zr_{0.1}C_{1.01}$-4w/oW	1700	5000	34.5	0.02	0.25	4.11×10^{-5}	45.2
$U_{0.9}Zr_{0.1}C_{1.01}$-4w/oW	1700	7000	48.3	0.02	0.48	9.29×10^{-5}	48.0
$U_{0.9}Zr_{0.1}C_{1.01}$-4w/oW	1700	9000	62.1	0.02	0.42	1.53×10^{-4}	24.0

* Strain in first two minutes.

samples are found in Table 9. Listed in these tables are the test temperature and applied stress, strain during the first two minutes, total strain, total time at temperature, and the steady-state creep rate for each test. In general, the high-density samples were found to follow classical time dependent creep curves, with an instantaneous deformation, followed by a period of primary creep where the creep rate decreased with time, and finally a region of minimum or steady-state creep behavior (see Figures 11 to 14). The data shown in each of these figures were obtained by changing the applied stress in the order indicated, after steady state had been achieved for the preceding stress. In some cases, particularly when the applied stress was decreased, long periods of nearly zero deformation were noted while recovery to the equilibrium creep structure occurred.

Although the maximum temperature specified in the test matrix was 1700 C, some tests on the high-density $U_{0.9}Zr_{0.1}C_{1.01}$ + 4 w/o W specimens were conducted at 1800 C because of the very low creep rates observed at lower temperatures.

In order to determine the suitability of the second vacuum creep unit for testing the low-density carbide specimen without oxidation, and to determine the degree of densification of the carbide specimens at elevated temperature, a series of 75 percent dense carbide samples representative of the compositions being examined were annealed in this unit for 72 hours at 1750 C. The samples were not oxidized after this treatment, as established by X-ray diffraction and optical metallography. However, each of the three 75 percent dense carbide specimens so annealed was found to have densified to greater than 90 percent theoretical density and to have undergone major microstructural modification (compare Figures 6, 7, and 9 with Figures 15 to 17 which show the structures of the three alloys before and after annealing at 1750 C). Thus, it appeared that creep testing could be performed in this creep unit, but that tests with low-density specimens would have to be conducted at temperatures below 1700 C. Therefore, all tests on low-density specimens were conducted at 1400 and 1550 C. At these temperatures, under all applied loads, no specimen

TABLE 9. TEST INFORMATION FOR LOW-DENSITY CARBIDE SPECIMENS TESTED IN VACUUM OF 6.65×10^{-4} N/m^2 (5×10^{-6} torr)

Spec. No.	Composition	Density, % TD	Temp., C	Stress, psi	Stress, MN/m^2	Strain on Loading*, %	Total Strain, %	Steady-State Creep Rate, hr^{-1}	Total Time at Temp., min.
PA4	$UC_{1.01}$	75.1	1400	4000	27.6	1.29	2.15	3.22×10^{-1}	5.5
PA4	$UC_{1.01}$	75.1	1400	2000	13.8	0.35	1.41	7.92×10^{-2}	10.5
PA4	$UC_{1.01}$	75.1	1400	1000	6.9	0.13	2.02	2.02×10^{-2}	60
PA4	$UC_{1.01}$	75.1	1400	660	4.55	0.06	1.71	6.00×10^{-3}	284
PA5	$UC_{1.01}$	76.6	1550	1000	6.9	0.53	3.18	5.50×10^{-2}	25
PA5	$UC_{1.01}$	76.6	1550	2000	13.8	0.30	3.11	1.10×10^{-1}	16
PA6	$UC_{1.01}$	73.7	1550	4000	27.6	-	2.67	9.54×10^{-1}	1.3
PA6	$UC_{1.01}$	73.7	1550	2000	13.8	0.54	2.91	1.89×10^{-1}	9
PB1	$UC_{1.01}$ + 4w/oW	75.9	1400	4000	27.6	0.85	6.14	9.42×10^{-2}	33
PB2	$UC_{1.01}$ + 4w/oW	76.7	1400	1000	6.9	0.13	3.52	9.40×10^{-3}	180
PB7	$UC_{1.01}$ + 4w/oW	76.7	1400	2000	13.8	0.21	2.80	3.28×10^{-2}	50
PB7	$UC_{1.01}$ + 4w/oW	76.7	1400	1000	6.9	0.05	2.97	1.07×10^{-2}	190
PB5	$UC_{1.01}$ + 4w/oW	76.9	1550	1000	6.9	0.30	3.30	3.06×10^{-2}	50
PB5	$UC_{1.01}$ + 4w/oW	76.9	1550	2000	13.8	0.40	2.90	5.80×10^{-2}	30
PB6	$UC_{1.01}$ + 4w/oW	77.1	1550	4000	27.6	1.42	3.12	3.40×10^{-1}	5

* Strain in first two minutes.

TABLE 9. (Continued)

Spec. No.	Composition	Density, % TD	Temp., C	Stress, psi	Stress, MN/m^2	Strain on Loading*, %	Total Strain, %	Steady-State Creep Rate, hr^{-1}	Total Time at Temp., min.
PB6	$UC_{1.01}$ + 4w/oW	77.1	1550	2000	13.8	0.31	3.05	1.17×10^{-1}	16
PC3	$U_{0.9}Zr_{0.1}C_{1.01}$ + 4w/oW	76.6	1400	4000	27.6	0.45	2.90	5.88×10^{-2}	27
PC3	$U_{0.9}Zr_{0.1}C_{1.01}$ + 4w/oW	76.6	1400	2000	13.8	0.05	2.98	2.45×10^{-2}	78
PC4	$U_{0.9}Zr_{0.1}C_{1.01}$ + 4w/oW	73.8	1400	2000	13.8	0.30	2.77	1.20×10^{-2}	105
PC4	$U_{0.9}Zr_{0.1}C_{1.01}$ + 4w/oW	73.8	1400	1000	6.9	0.00	1.04	2.50×10^{-3}	262
PC5	$U_{0.9}Zr_{0.1}C_{1.01}$ + 4w/oW	76.2	1550	1000	6.9	0.21	2.77	1.92×10^{-2}	68
PC5	$U_{0.9}Zr_{0.1}C_{1.01}$ + 4w/oW	76.2	1550	2000	13.8	0.34	3.08	3.06×10^{-2}	62
PC7	$U_{0.9}Zr_{0.1}C_{1.01}$ + 4w/oW	75.8	1550	4000	27.6	1.51	3.21	3.78×10^{-1}	4.7
PC7	$U_{0.9}Zr_{0.1}C_{1.01}$ + 4w/oW	75.8	1550	2000	13.8	0.25	2.82	1.25×10^{-1}	17
PB11	$UC_{1.01}$ + 4w/oW	85.7	1400	4000	27.6	0.73	3.16	6.72×10^{-2}	21
PB11	$UC_{1.01}$ + 4w/oW	85.7	1400	2000	13.8	0.05	1.31	2.67×10^{-2}	31
PB11	$UC_{1.01}$ + 4w/oW	85.7	1400	1000	6.9	0.01	1.82	1.00×10^{-2}	113
PB14	$UC_{1.01}$ + 4w/oW	86.1	1550	4000	27.6	0.69	2.86	1.19×10^{-1}	12
PB14	$UC_{1.01}$ + 4w/oW	86.1	1550	2000	13.8	0.10	2.55	4.50×10^{-2}	33

* Strain in first two minutes.

TABLE 9. (Continued)

Spec. No.	Composition	Density, % TD	Temp., C	Stress, psi	Stress, MN/m^2	Strain on Loading*, %	Total Strain, %	Steady-State Creep Rate, hr^{-1}	Total Time at Temp., min.
PB15	$UC_{1.01}$ + 4w/oW	85.9	1550	4000	27.6	0.47	2.90	1.03×10^{-1}	16
PB15	$UC_{1.01}$ + 4w/oW	85.9	1550	1000	6.9	0.09	3.14	1.82×10^{-2}	92
PC11	$U_{0.9}Zr_{0.1}C_{1.01}$ + 4w/oW	87.0	1400	4000	27.6	0.20	1.60	2.16×10^{-2}	43
PC11	$U_{0.9}Zr_{0.1}C_{1.01}$ + 4w/oW	87.0	1400	2000	13.8	0.04	2.19	1.07×10^{-2}	137
PC12	$U_{0.9}Zr_{0.1}C_{1.01}$ + 4w/oW	86.4	1400	1000	6.9	0.10	2.27	3.30×10^{-3}	335
PC13	$U_{0.9}Zr_{0.1}C_{1.01}$ + 4w/oW	87.2	1550	1000	6.9	0.12	3.05	9.20×10^{-3}	195
PC13	$U_{0.9}Zr_{0.1}C_{1.01}$ + 4w/oW	87.2	1550	2000	13.8	0.13	3.06	1.30×10^{-2}	160
PC15	$U_{0.9}Zr_{0.1}C_{1.01}$ + 4w/oW	87.6	1550	4000	27.6	0.41	3.02	6.99×10^{-2}	25
PC15	$U_{0.9}Zr_{0.1}C_{1.01}$ + 4w/oW	87.6	1550	2000	13.8	0.09	3.09	3.20×10^{-2}	60

* Strain in first two minutes.

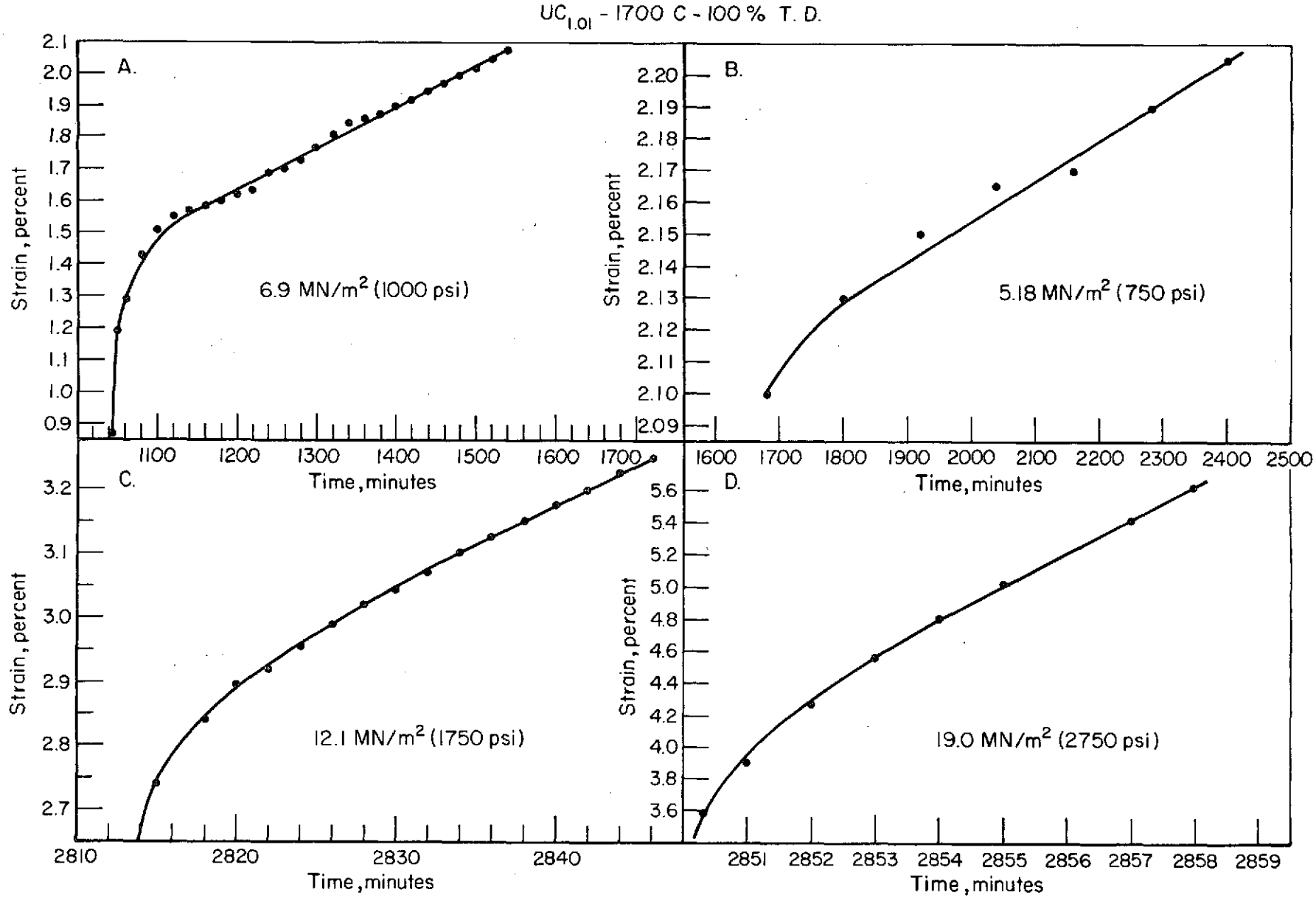

FIGURE 11. COMPRESSION CREEP STRAIN VERSUS TIME FOR THEORETICALLY DENSE $UC_{1.01}$ TESTED AT 1700 C

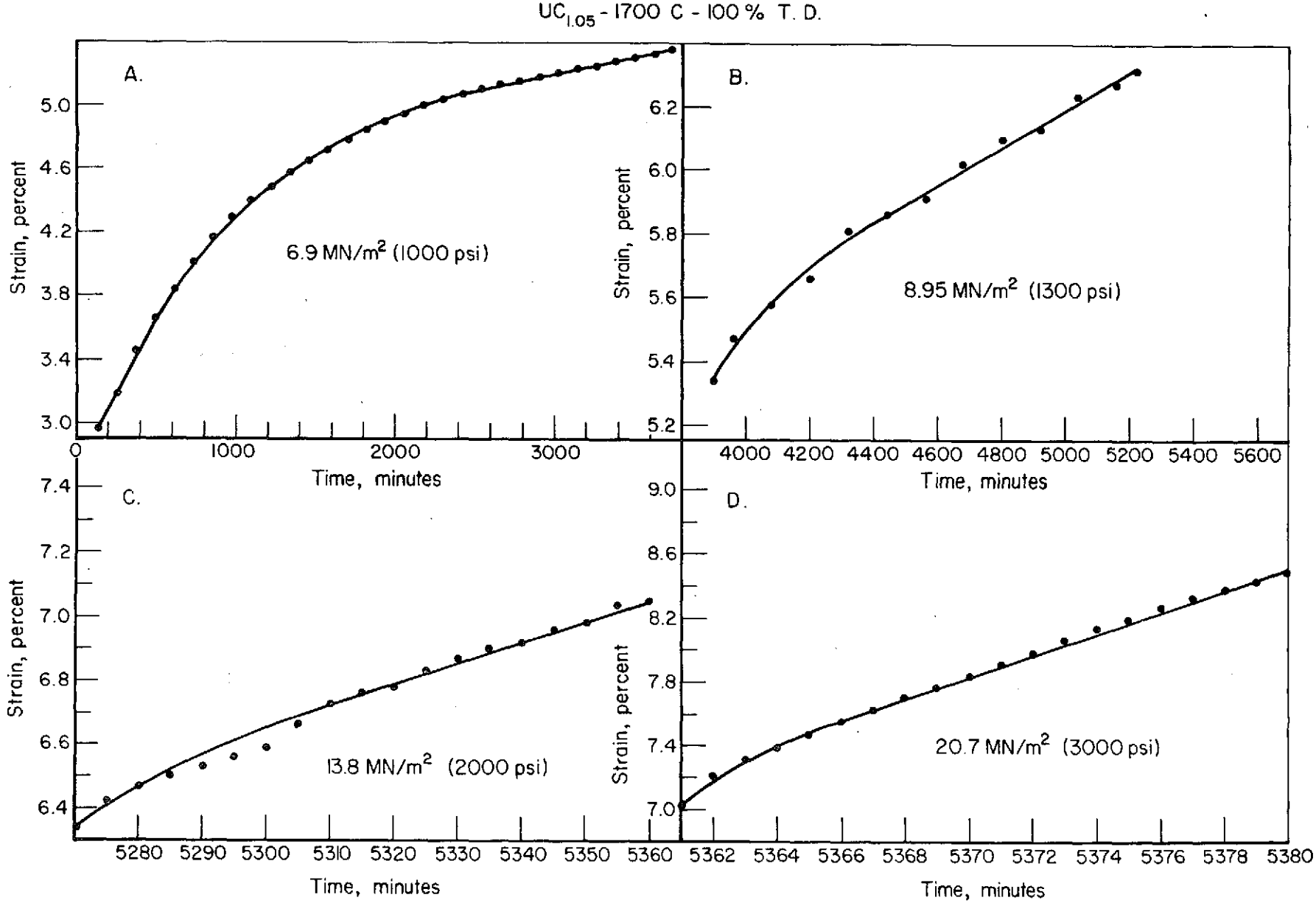

FIGURE 12. COMPRESSION CREEP STRAIN VERSUS TIME FOR THEORETICALLY DENSE $UC_{1.05}$ TESTED AT 1700 C

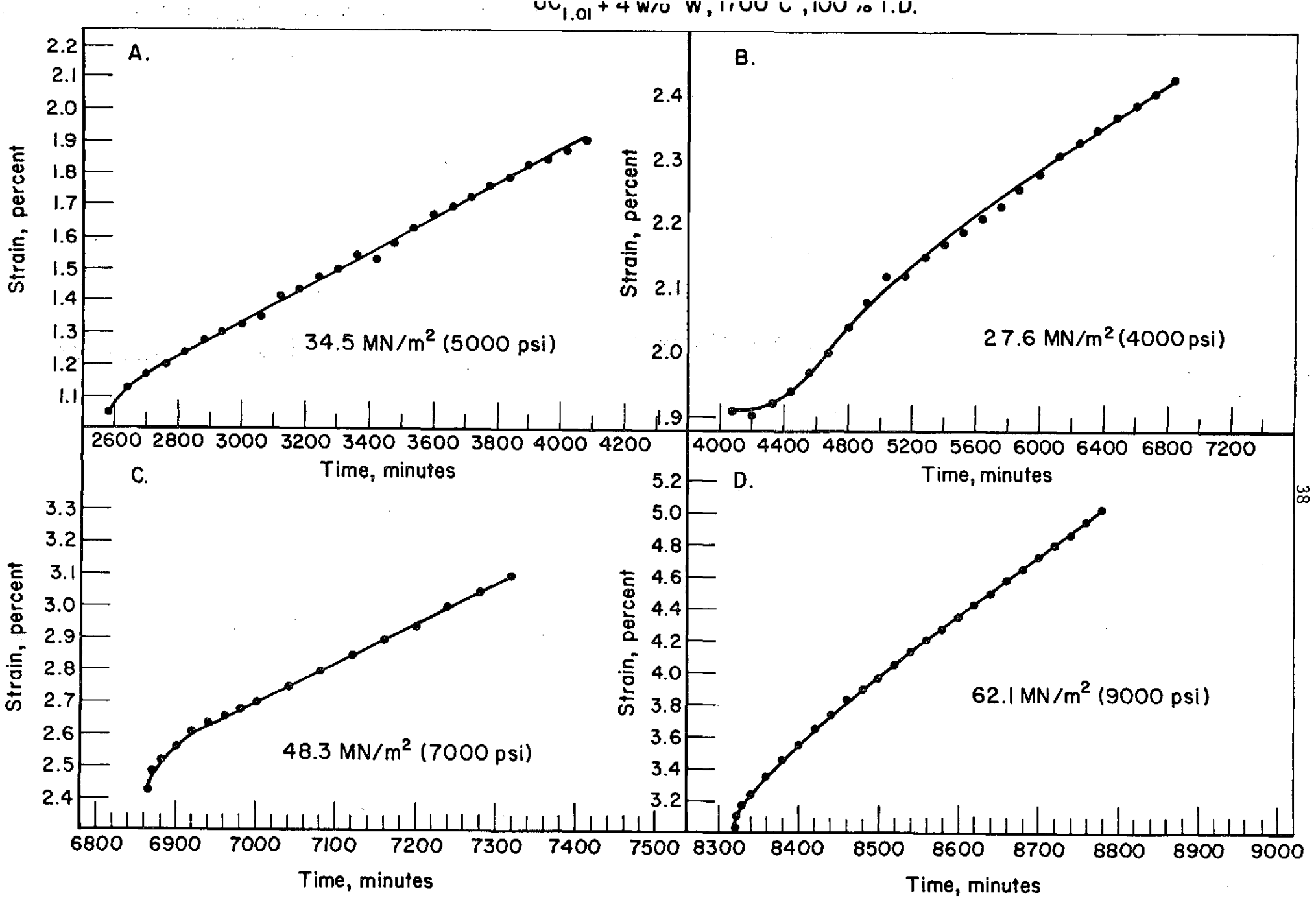

FIGURE 13. COMPRESSION CREEP STRAIN VERSUS TIME FOR THEORETICALLY DENSE $UC_{1.01}$ + 4 w/o W TESTED AT 1700 C

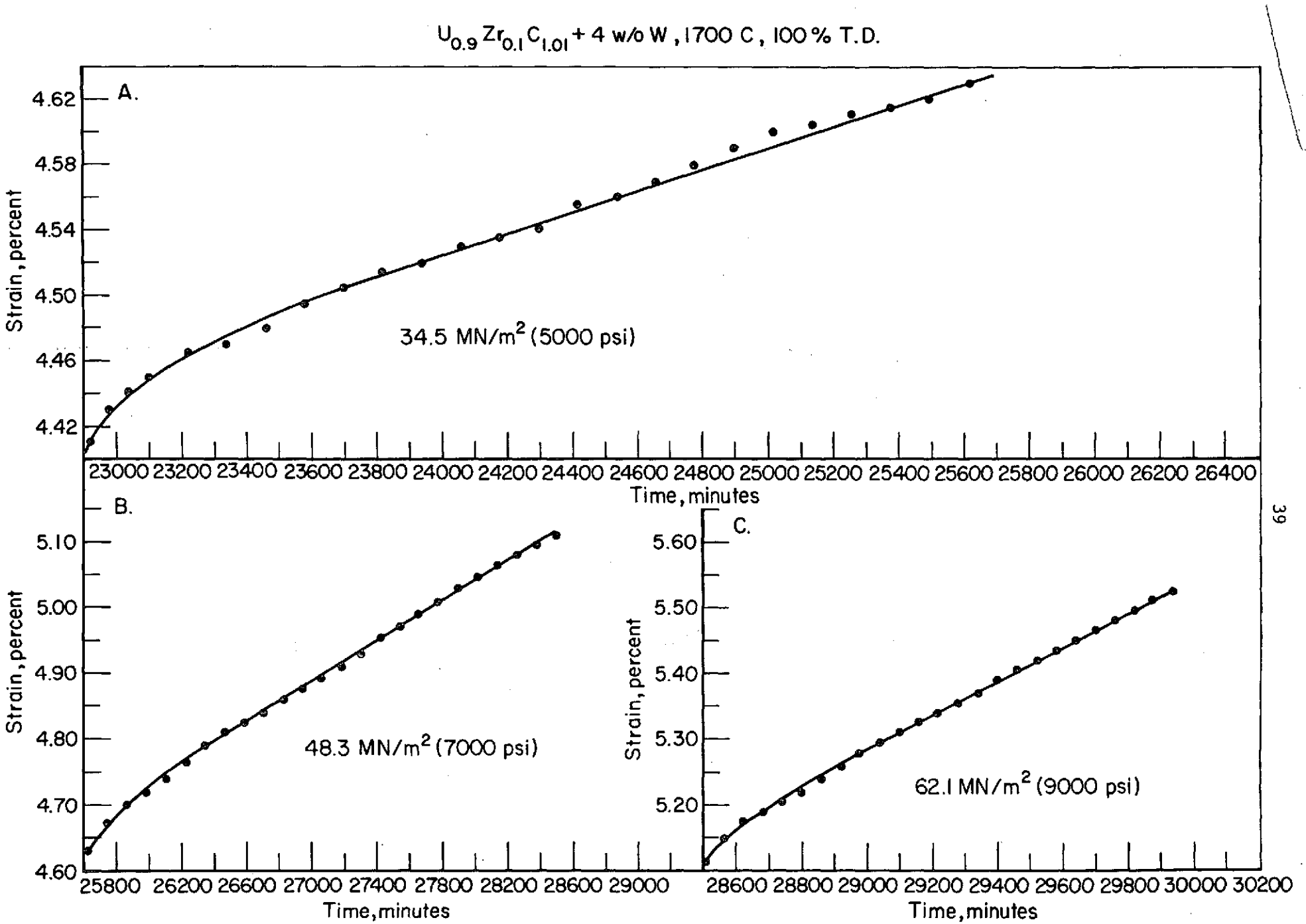

FIGURE 14. COMPRESSION CREEP STRAIN VERSUS TIME FOR THEORETICALLY DENSE $U_{0.9}Zr_{0.1}C_{1.01}$ + 4 w/o W TESTED AT 1700 C

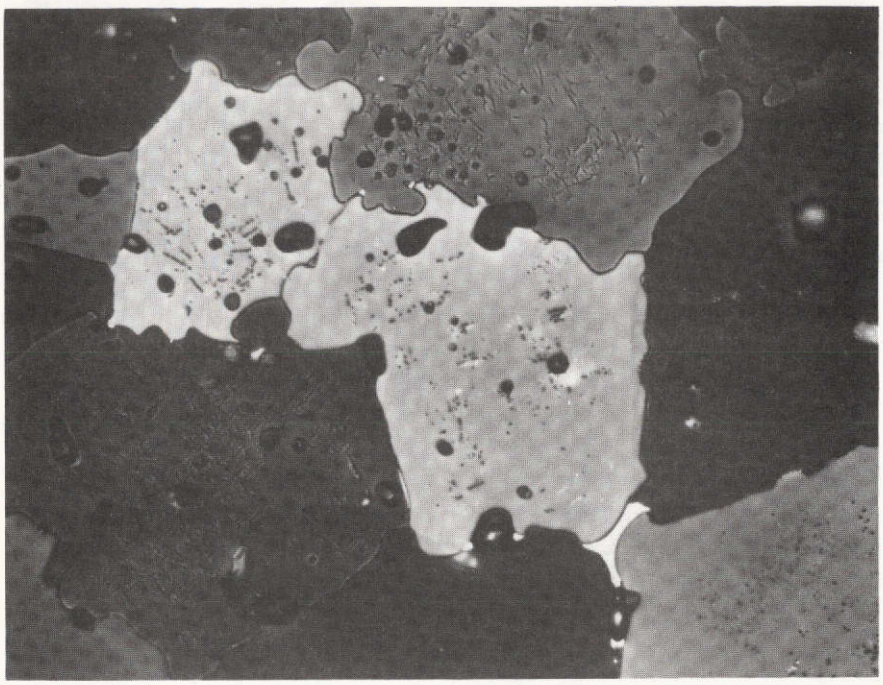

750X 5G678

FIGURE 15. PA9. $UC_{1.01}$, 72 HRS. AT 1750 C. INITIAL DENSITY - 77 % TD. FINAL DENSITY - 94.5% TD

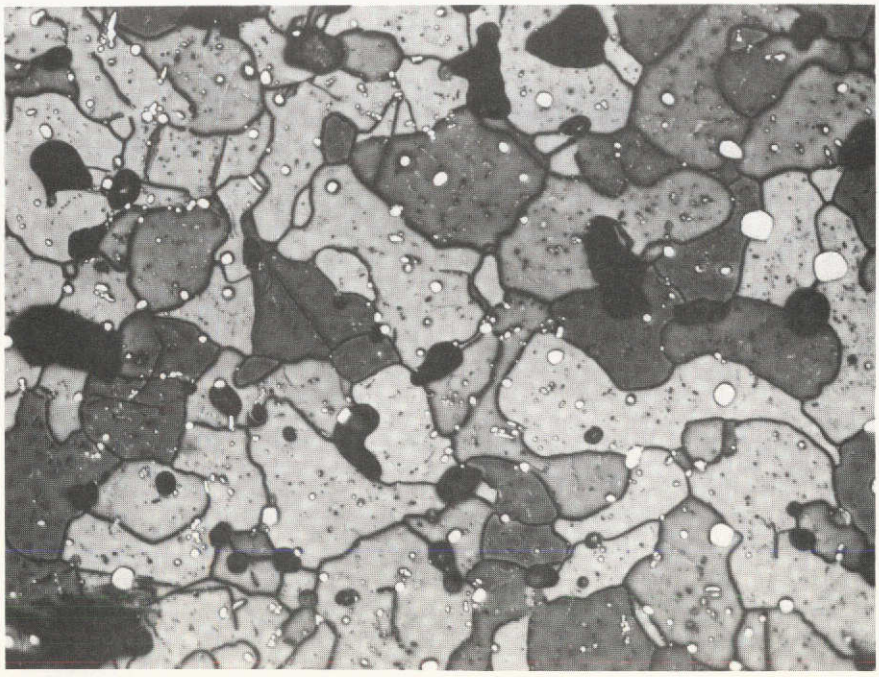

750X 5G380

FIGURE 16. PB9. $UC_{1.01}$ + 4 w/o W, 72 HRS AT 1750 C. INITIAL DENSITY - 77.1% TD. FINAL DENSITY - 90.0% TD

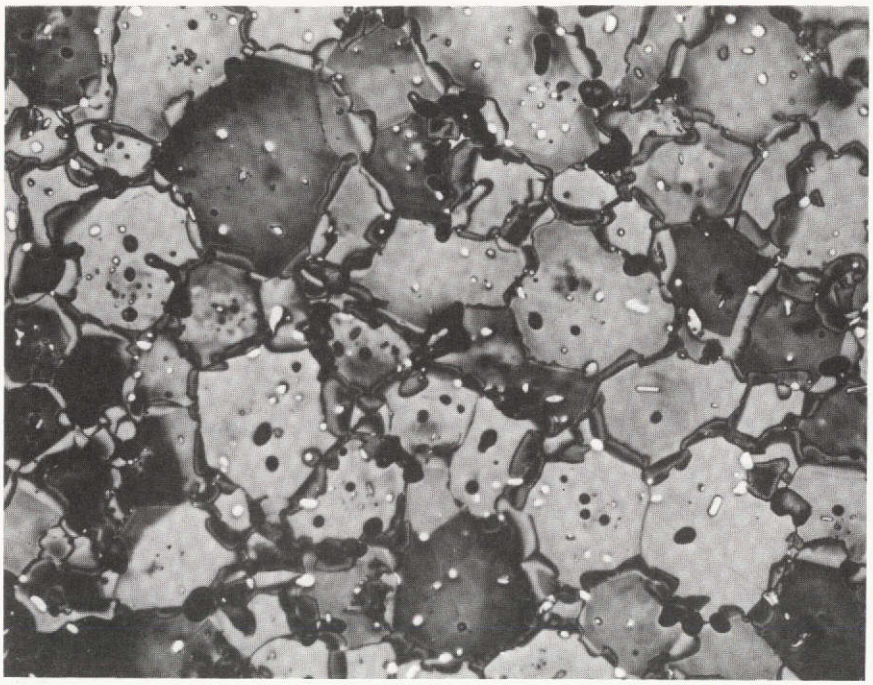

750X 5G383

FIGURE 17. PC9. $U_{0.9}Zr_{0.01}$ + 4 w/o W, 72 HRS AT 1750 C. INITIAL DENSITY - 77.2% TD. FINAL DENSITY - 90.5% TD

was found to densify by more than one percent an in no case was any oxidation detected. Typical curves of strain versus time for the tests conducted on low-density specimens are presented in Figures 18 to 21. It can be seen from examination of Table 9 that some specimens have been stress-cycled while others have been subjected to a single stress. The results are characterized by large contributions to the total strain by primary creep behavior and steady-state creep rates several orders of magnitude higher than those found for high-density specimens.

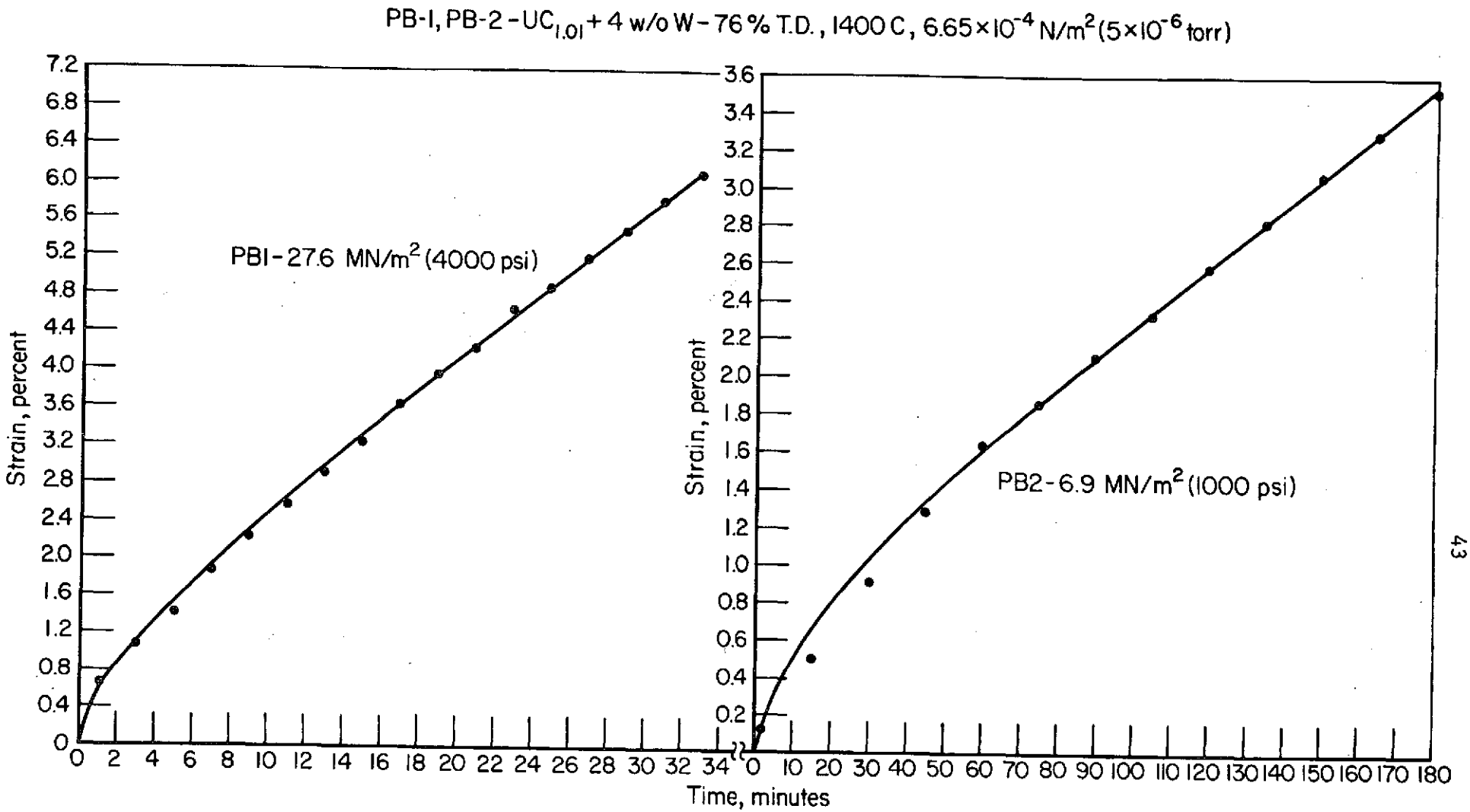

FIGURE 18. COMPRESSION CREEP STRAIN VERSUS TIME FOR SPECIMENS PB1 AND PB 2 76% TD, $UC_{1.01}$ + 4 w/o W TESTED AT 1400 C

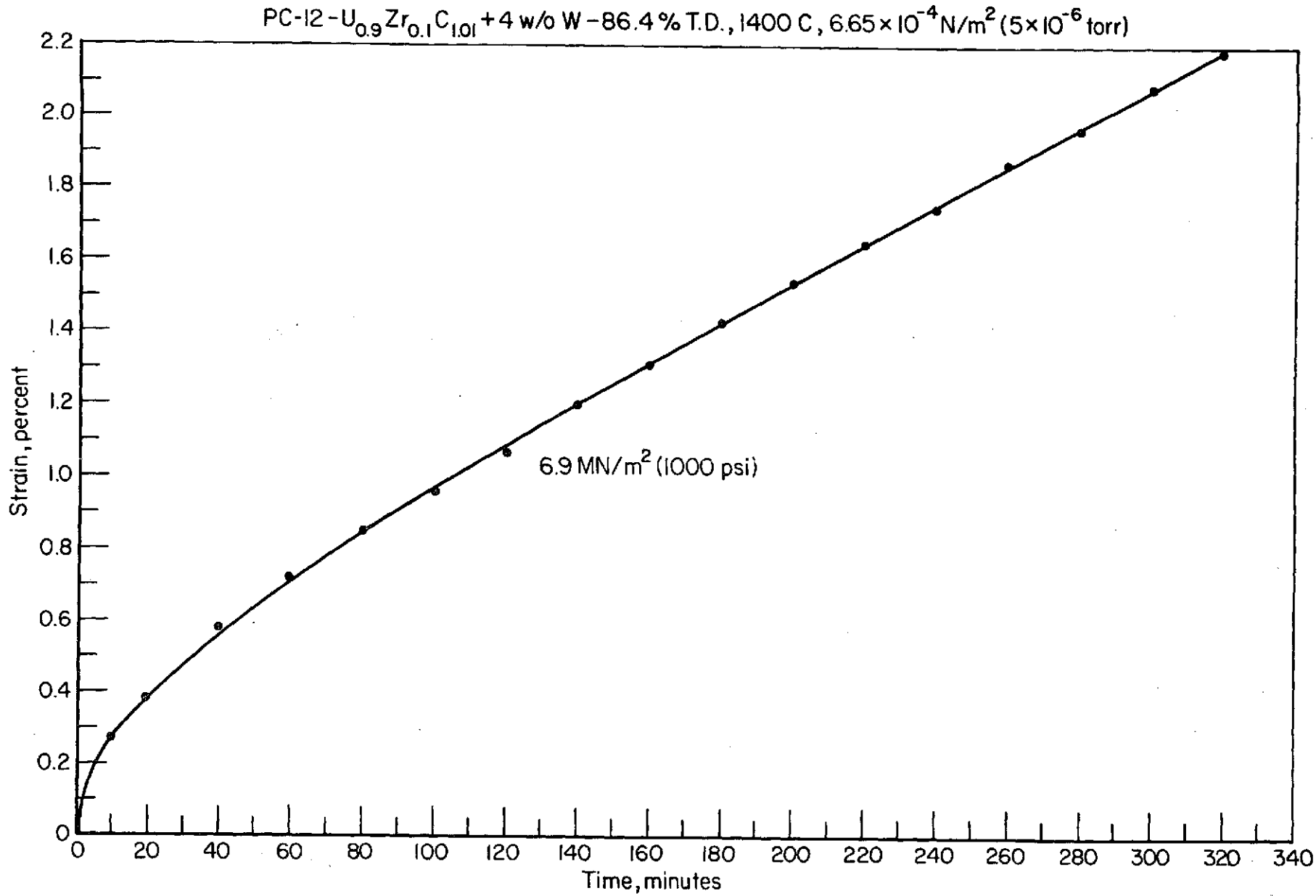

FIGURE 19. COMPRESSION CREEP STRAIN VERSUS TIME FOR SPECIMEN PC12, 86.4% TD, $U_{0.9}Zr_{0.1}C_{1.01}$ + 4 w/o W TESTED AT 1400 C

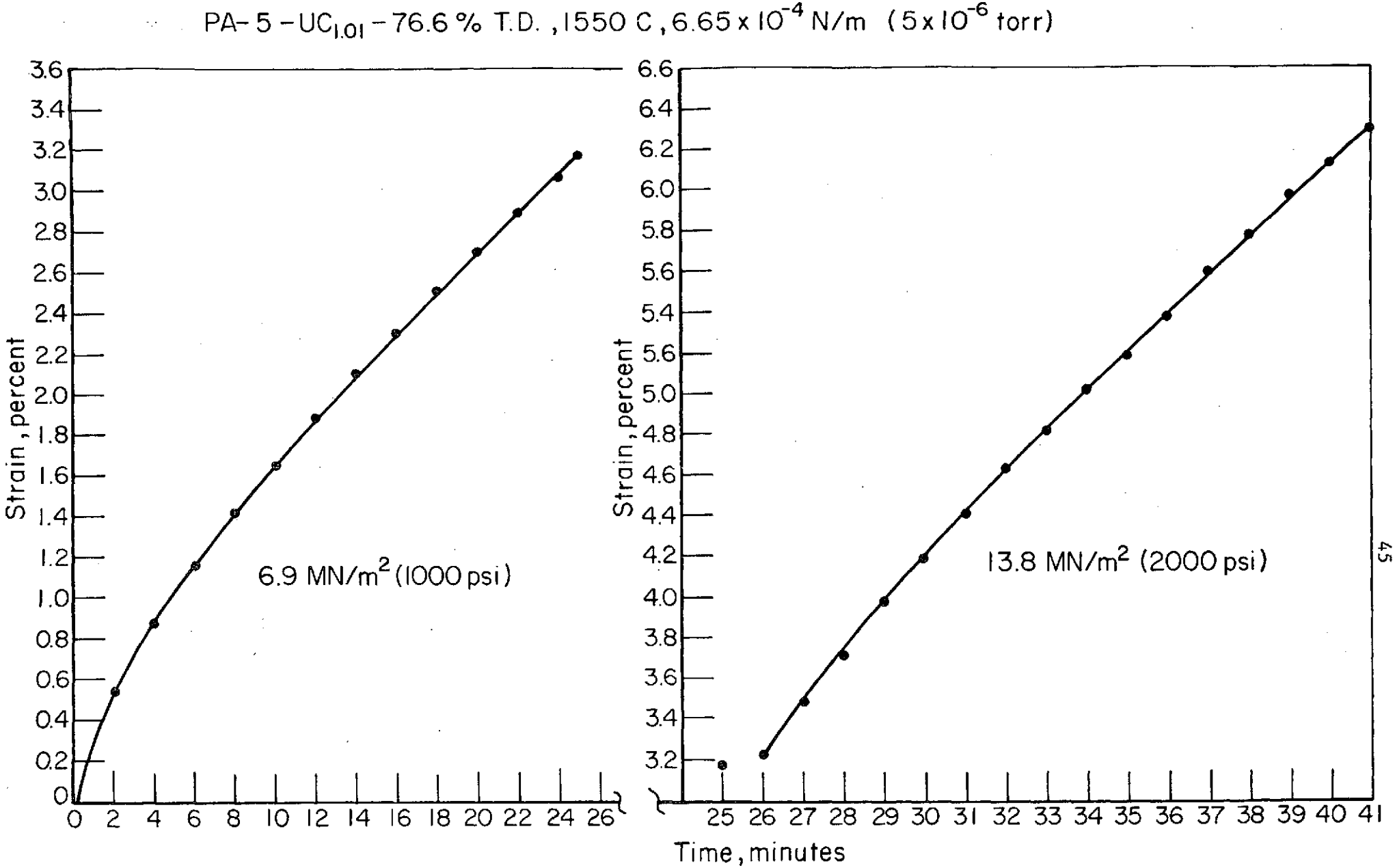

FIGURE 20. COMPRESSION CREEP STRAIN VERSUS TIME FOR SPECIMEN PA5, 76.6% TD, $UC_{1.01}$ TESTED AT 1550 C

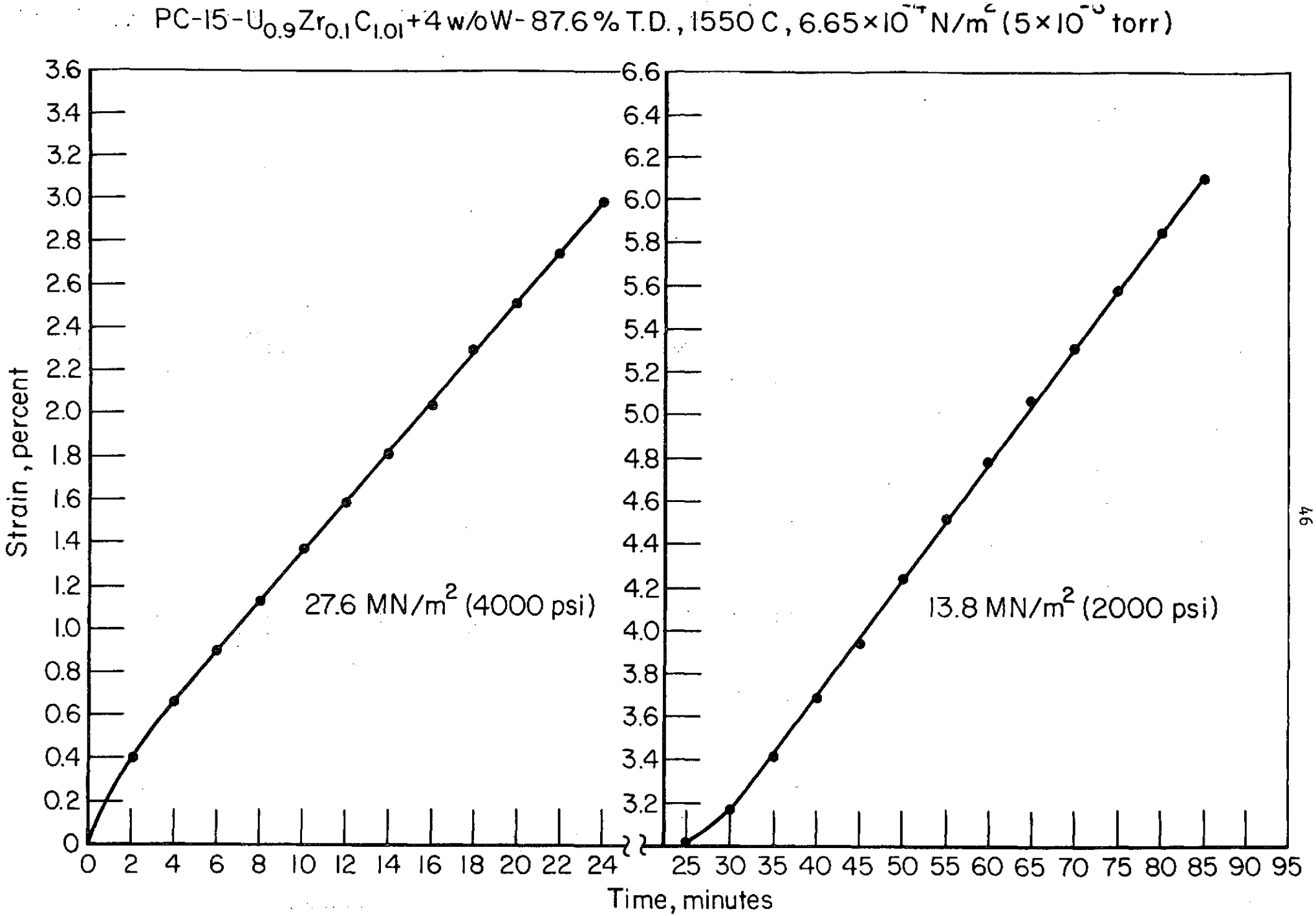

FIGURE 21. COMPRESSION CREEP STRAIN VERSUS TIME FOR SPECIMEN PC15, 87.6%TD, $U_{0.9}Zr_{0.1}C_{1.01}$ + 4 w/o W TESTED AT 1550 C

TASK III. ANALYSIS OF CREEP DATA

M. S. Seltzer and B. A. Wilcox

I. INTRODUCTION

The purpose of this task was to analyze and interpret the creep data generated in Task II in order to examine how the creep rate is influenced by alloy content, stoichiometry, density, temperature, and stress. Steady-state creep rates, $\dot{\varepsilon}$, were determined and constitutive equations were developed for each material.

In order to put the results obtained in the present study in proper prospective, the literature on creep of uranium carbide and on diffusion of uranium and carbide in this compound will be reviewed in the following section. This review is followed by presentation of the experimental creep data, as a function of stress, temperature, and U/C ratio. Finally the data are analyzed and discussed in terms of operative creep mechanisms.

II. PREVIOUS STUDIES

Uranium carbide has the NaCl structure with a melting temperature of 2400 ± 50 C.[1]* The width of the homogeneity range varies with temperature, but it extends roughly from 4.75 to 4.90 w/o carbon in the temperature region of 1300 to 1900 C, with the stoichiometric composition corresponding to 4.80 w/o carbon.[3] At carbon levels below 4.8 w/o, U forms in the microstructure on cooling to room temperature; and at carbon levels above 4.8 w/o, U_2C_3 or UC_2 forms in the microstructure.

The available creep data for uranium monocarbide have been recently reviewed by Seltzer, et al.[2] An updated version of that review is given below. Most high-temperature creep studies of UC have been performed in

---

* References at end of section.

compression[3-11] under vacuums from 1.33×10^{-2} to 1.33×10^{-4} N/m^2 (10^{-4} to 10^{-6} torr). See Table 10. Recently, a few tensile creep experiments have been reported.[12] Except for two studies on single crystals[5,10], the creep experiments have been conducted on high-density arc-cast polycrystals.

Table 10 reveals that for a power-law stress dependence of the creep rate, i.e., $\dot{\epsilon} = A\sigma^n$, the stress exponent, n, varies from 2.3 to 6. The low value of 2.3 was estimated from creep rates at only two stresses, 41.4 and 55.2 MN/m^2 (6000 and 8000 psi), at 1300 C, on the finest grain size uranium carbide tested. This may be in a transition region from the linear dependence associated with a diffusional creep or grain-boundary sliding process to the high power-law dependence of dislocation creep models. Norreys[6] found that minimum creep rates in the range of 13.8 to 55.2 MN/m^2 (2000 to 8000 psi) at 1300 C could best be fit by an exponential stress dependence. However, replotting his data to a power law gave n = 1.8. The stress exponents of 1.79 and 4.18 found by Killey[10] also result from a power-law treatment of data which could be fit by an exponential stress dependence.

Uranium diffusivities are some three orders of magnitude lower than are those for carbon diffusion in uranium carbide[13, 14], and it is therefore expected that the high-temperature creep of UC will be controlled by an uranium-diffusion process. Although considerable data are available on both creep and self-diffusion activation energies for uranium carbide, it is not possible to simply relate all creep activation energies to atomic diffusion. Careful study of Table 10 suggests that the creep activation energies increase from 37.5 kcal per mole to 141.6 kcal per mole as the U/C ratio decreases from a carbon-deficient composition where free uranium is present to a carbon-excess composition in which a carbon-rich second phase is expected. According to Table 11, the activation energies for carbon diffusion either decrease with or are independent of any decreasing U/C ratio.[14,16] The trend is no different, however, for uranium diffusion[15,16], although at high temperatures Lindner, et al,[15] did find that the uranium activation energy increased from 70 kcal per mole to 90 kcal per mole as the carbon content increased from 4.68 to 4.83 w/o. The absolute values of the activation energies for creep and diffusion, however, are not in good agreement in this case.

TABLE 10. CREEP PROPERTIES OF UC[a]

Reference	Temperature °C	Atmosphere	Grain Size, μ	Purity	Carbon w/o	n[b]	Q_c kcal/mole	Remarks
Chang [4]	1500-1900	10^{-5} torr vacuum	300-400	50 ppm Fe 40 ppm Si 15 ppm Ni		5	37.5	Arc-cast, some metallic uranium. For transient creep, Q = 80 kcal/mole. Voids on grain boundaries parallel to compression axis.
Chang [5]	1600-2000	10^{-4} torr vacuum	Single		Stoichiometric	5-6	69-92	Grown by electron-beam, floating zone technique.
Norreys [6]	1200-1400	5×10^{-5} torr vacuum	300	0.05 w/o Al 0.01 w/o Ti 0.005 w/o Fe 200 ppm O_2 100 ppm N_2	4.9	1.8	49±8	Free U increases $\dot{\epsilon}$ at 1300 C W decreases $\dot{\epsilon}$ Arc cast
Fassler, et al [7]	1100-1300	10^{-6} torr vacuum	30	0.05 w/o Si 0.05 w/o Fe 0.02 w/o Cr 0.02 w/o Ni	4.9	2.3	44	1850 ppm O_2, 400 ppm N_2, 95% TD
					4.5		51.7	3200 ppm O_2, 1150 ppm N_2
Magnier, et al [24]	1600-2300	10^{-5} torr vacuum		300 ppm (O_2+N_2)	4.5 to 5.0			Specimens are strengthened as C increases from 4.5 to 5.0 w/o.
Stellrecht, et al [8]	1200-1600	10^{-5} torr vacuum		50 ppm O_2 50 ppm N_2 100 ppm metals	5.2	3	90	Arc cast
Killey [9]	900-1100	2×10^{-5} torr vacuum	150-500	100 ppm N_2 200 ppm O_2 500 ppm Al 100 ppm Ni	4.7-4.78	1	45±3	Arc cast
Killey [11]	1225-1600	2×10^{-5} torr vacuum	120	100 ppm N_2 200 ppm O_2 500 ppm Al 100 ppm Ni	4.81-5.18	1.79 4.18	68.6 141.6	Low temperature; low stress High temperature; high stress Single crystals also tested.

(a) All the tests are in compression.
(b) The creep data are fitted to the relation $\dot{\epsilon} \propto \sigma^n$.

TABLE 11. SELF-DIFFUSION IN UC

Reference	Element	Temperature °C	Atmosphere	Purity	Carbon w/o	Do, cm^2/sec	Q, kcal/mole	Comments[a]
Chubb, et al[13]	C^{14}	1200-1940	Vacuum in graphite holder		5.0	0.02	50±20	Sectioning method for U and C. Arc-cast
	U^{235}	1600-2120			5.0	0.0013	64±20	
Lee & Barrett[14]	C^{14}	1266-1684	10^{-5} torr vacuum in UC capsule		4.7	32.3	89±6	Sectioning method for U and C, 97% TD. All Arc-cast except 5.1 w/o C which was sintered.
				~ 100 ppm oxygen	4.82	1.75	63±1	
				~ 125 ppm nitrogen	5.0	3.21×10^{-2}	55±8	
				100 ppm tungsten	5.1	2.95×10^{-2}	54±15	
				150 ppm iron	5.6	2.76×10^{-3}	45±6	
	U^{235}	1505-1863			4.82	8.47	104±7	
Lindner, et al[15]	U^{233}	1600-2100	10^{-5} to 10^{-6} torr vacuum		4.68	6.53×10^{-6}	70±5	Arc-cast and single xtals
		800-1600			4.68	6.33×10^{-11}	33±2	Alpha energy degradation
		1400-2000		1000 ppm oxygen	4.83	1.85×10^{-4}	90±6	Same results for single crystals and arc cast
		1000-1400			4.83	1.21×10^{-12}	28±4	
Bentle & Ervin[16]	U^{235}	1700-2050	10^{-5} to 10^{-6} mm Hg vac.	500-700 ppm non-metallic	4.4		125±15	ZM Sectioning
		1700-2050			4.6		125±15	ZM
		1750-2050			4.8		125±15	ZM
		1350-1700	1500°C		4.4		32±2	ZM
		1150-1750	10^{-8} - 10^{-9} mm Hg vacuum below 1500°C		4.6		32±2	ZM
		1150-1750			4.8		32±2	ZM, A.C.
		1400-2050			4.9		70±5	ZM, A.C.
Bentle & Ervin[16]	C^{14}	1500-1900			4.6		94±6	ZM
		1600-1900			4.7		92±6	ZM
		1500-1900			4.8		84±6	ZM
		1150-1500			4.6		53±6	ZM
		1150-1600			4.7		54±4	ZM
		1150-1500			4.8		51±4	ZM
		1100-1900			4.9		60±5	ZM
Villaine[17]	U^{235}	1450-2000		250-500 ppm O_2 100 ppm N_2	4.63 to 5.00	7.5×10^{-5}	81±10	Diffusivities decrease with increase in % C Sectioning, autoradiography Alpha-spectrometry
Krakowski[18]	C^{14}	1065-1499	10^{-5} torr vacuum	60-1250 ppm oxygen	4.68 to 4.75	0.1	62.5±2	Decrease in surface activity
Hirsch & Scheff[19]	U^{233}	1700-2300	10^{-5} torr vacuum	50-100 ppm oxygen	4.62	3.6×10^{-2}	107±3	Decrease in surface activity
	U^{233}	1700-2050		125 ppm metallic impurities	5.14	4.0×10^{-4}	106±1.5	Arc cast
	U^{233}	2050-2300			5.14	9.0×10^{2}	174±6	
Fyodorov, et al[20]	U^{235}	1900-2200	10^{-6} torr vacuum		4.86	2.7×10^{-2}	100	Sectioning method

(a) S.C. = single crystal
P.C. = polycrystal
A.C. = arc cast
Z.M. = zone melted

Killey[9-11] has performed the most extensive investigation of the influence of stoichiometry on the creep behavior of uranium monocarbide. He suggests that at temperatures between 900 and 1100 C and for stresses in the range of 27.6 to 55.2 MN/m^2 (4000 to 8000 psi), where $\epsilon = A\sigma$, creep of slightly hypostoichiometric UC (4.70 to 4.78 w/o carbon) is controlled by the diffusion of carbon vacancies. However, such samples should contain some uranium metal. Differences between the creep activation energy of 45 kcal per mole and carbon diffusion activation energies of 62 to 89 kcal per mole for this range of UC compositions may be explained by the presence of uranium metal acting as a lubricant at the UC grain boundaries in creep tests; whereas this effect would not be present in diffusion measurements. This finding is in agreement with the recent results of Bentle and Erwin[16], shown in Table 11 where the carbon activation energies are in the range of 51 to 54 kcal per mole for temperatures of 1150 to 1600 C where the solubility of uranium in UC is low and in the range of 84 to 94 kcal per mole for 1500 to 1900 C where the solubility of uranium in UC is increasing.

Killey[10] has also performed a series of compressive creep tests on arc-cast, polycrystalline (120-μ grain size) hyperstoichiometric UC (4.81 to 5.18 w/o carbon) in the temperature range of 1225 to 1600 C and under stresses of 10.3 to 69.0 MN/m^2 (1500 to 10,000 psi). It was found that the creep data could be fit to an expression of the form

$$\dot{\epsilon} = A\sigma^n \exp\left(-\frac{Q}{RT}\right),$$

where, for low temperatures and low stresses,

$$A = 2.28 \times 10^{-2}\ hr^{-1}$$

$$n = 1.79 \pm 0.67$$

$$Q = 68.6 \pm 23.4 \text{ kcal per mole,}$$

while at high temperatures and high stresses,

$$A = 1.13 \times 10^{-1}\ hr^{-1}$$

$$n = 3.18 \pm 1.36$$

$$Q = 141.6 \pm 21.6 \text{ kcal per mole.}$$

At a stress of 41.4 MN/m^2 (6000 psi) the transition occurs in the temperature range of 1300 to 1400 C.

Under equivalent conditions of stress and temperature, the creep rates for hyperstoichiometric UC are several orders of magnitude lower than are those for hypostoichiometric material. Such a difference is expected since free uranium appears in the grain boundaries of UC at carbon contents of 4.75 w/o corresponding to a C/U ratio of 0.98. However, if the observed dependence of creep rates on carbon concentration is attributed to variations in diffusion rates rather than to the presence of varying amounts of a second phase, then the diffusion data suggest uranium diffusion is the rate-controlling process. Lindner, et al[15], Bentle and Erwin[16], and Villaine[17] all found that uranium diffusion coefficients decreased with increasing carbon content, which is the behavior consistent with decreasing creep rates, while Lee and Barrett[14] and Bentle and Ervin[16] found that carbon diffusivities increased with increasing carbon concentration.

There have been no systematic studies of the influence of grain size or density on the creep behavior of uranium carbide. Of major concern for the present program was the influence of ZrC and tungsten on the creep properties of uranium carbide. There have been no studies in the literature of the quantitative effect of these additions on the creep behavior of UC, but Norreys[6] and others have shown that small additions of tungsten improve the creep resistance of hyperstoichiometric alloys considerably. Thus, at 1400 C and 40 MN/m^2 (5800 psi), the creep strain for UC containing 0.9 w/o W was less than 1 percent after 120 hours as compared with a creep strain of 10 percent for the tungsten-free alloy. In an earlier study performed at Battelle, it was found that at 1500 C and 69.0 MN/m^2 (10,000 psi), the creep rate of a hyperstoichiometric UC-5 mole percent WC alloy was 6×10^{-5} per hr compared to a creep rate in excess of 1 percent per hr for unalloyed UC.[22]

A program has been conducted at Battelle-Columbus to perform several compressive creep tests on an alloy of UC-4 w/o W prepared by Gulf General Atomic (GGA). Specimens of this alloy, which had a density of 78 percent theoretical, C/U ratio of 1.02, and an average grain size of 10μm, were tested in the temperature range of 1500 to 1900 C. For completeness, the results of this work are included in the following section.

III. EXPERIMENTAL RESULTS

High-Density Materials

Stress Dependence

The creep data for fully dense $UC_{1.01}$ are presented in Figure 22 as a steady-state creep rate versus applied stress. These data were subjected to a least squares analysis in order to determine the best values for the stress exponent and the creep activation energy. It was found that the data for fully dense $UC_{1.01}$ could best be fit by the equation:

$$\dot{\varepsilon} = 1773\ \sigma^{6.024\pm0.283}\ \exp\left(-\frac{106.5\pm8.4}{RT}\right), \qquad (1)$$

where $\dot{\varepsilon}$ is in hr^{-1}, σ is in MN/m^2, T is in °K, and the creep activation energy is in kcal/mole. The confidence limits given represent one standard error. The least squares lines from equation 1 for 1400, 1550, and 1700 C are drawn in Figure 22 which also includes the experimental data for these temperatures. The stress exponent of 6 is typical of values found for coarse grained or single crystal materials, while the creep activation energy is in good agreement with values for uranium self-diffusion in hyperstoichiometric uranium carbide.[14,19,20]

Creep rates for fully dense $UC_{1.05}$ are presented in Figure 23 as a function of the applied stress. These data could not be fit to a regression analysis because the stress exponent for creep clearly decreases with decreasing temperature. The values for n are 5.7, 4.3, and 3.3 at 1700, 1550, and 1400 C. The increased creep strength of $UC_{1.05}$ as compared with $UC_{1.01}$, particularly evident at the lower temperatures, is discussed in more detail in the section Stoichiometry Effects.

Creep rates for $U_{0.9}Zr_{0.1}C_{1.01}$ + 4 w/o W are plotted versus applied stress in Figure 24. These data were found to be best fit by the equation:

$$\varepsilon = 1.137 \times 10^{10}\ \sigma^{1.854\pm0.096}\ \exp\left(-\frac{155.2\pm4.8}{RT}\right), \qquad (2)$$

where the units are the same as those used in Equation 1. The great differences in creep strength, stress exponent, and creep activation energy between unalloyed

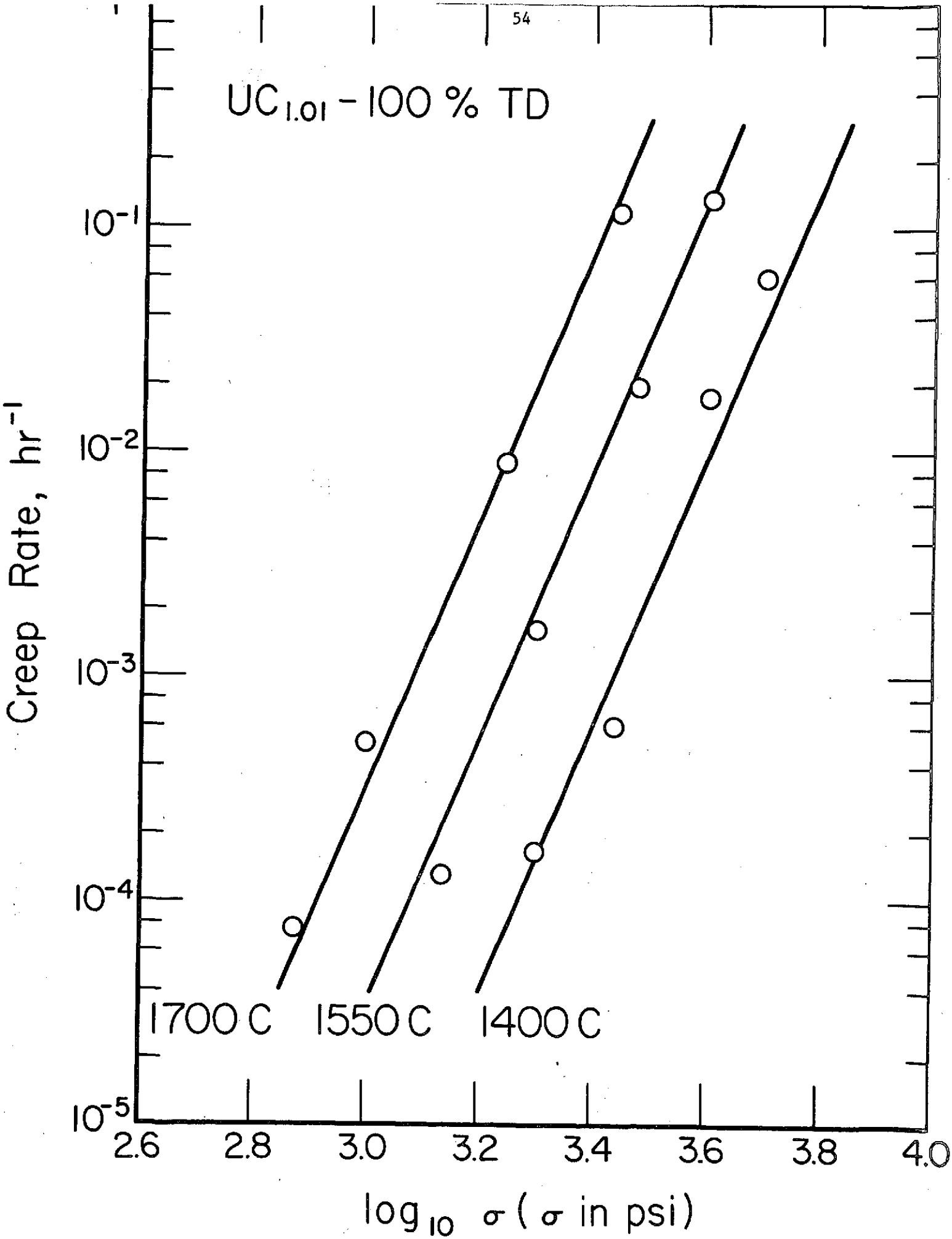

FIGURE 22. STEADY-STATE CREEP RATE VERSUS APPLIED STRESS FOR FULLY DENSE $UC_{1.01}$

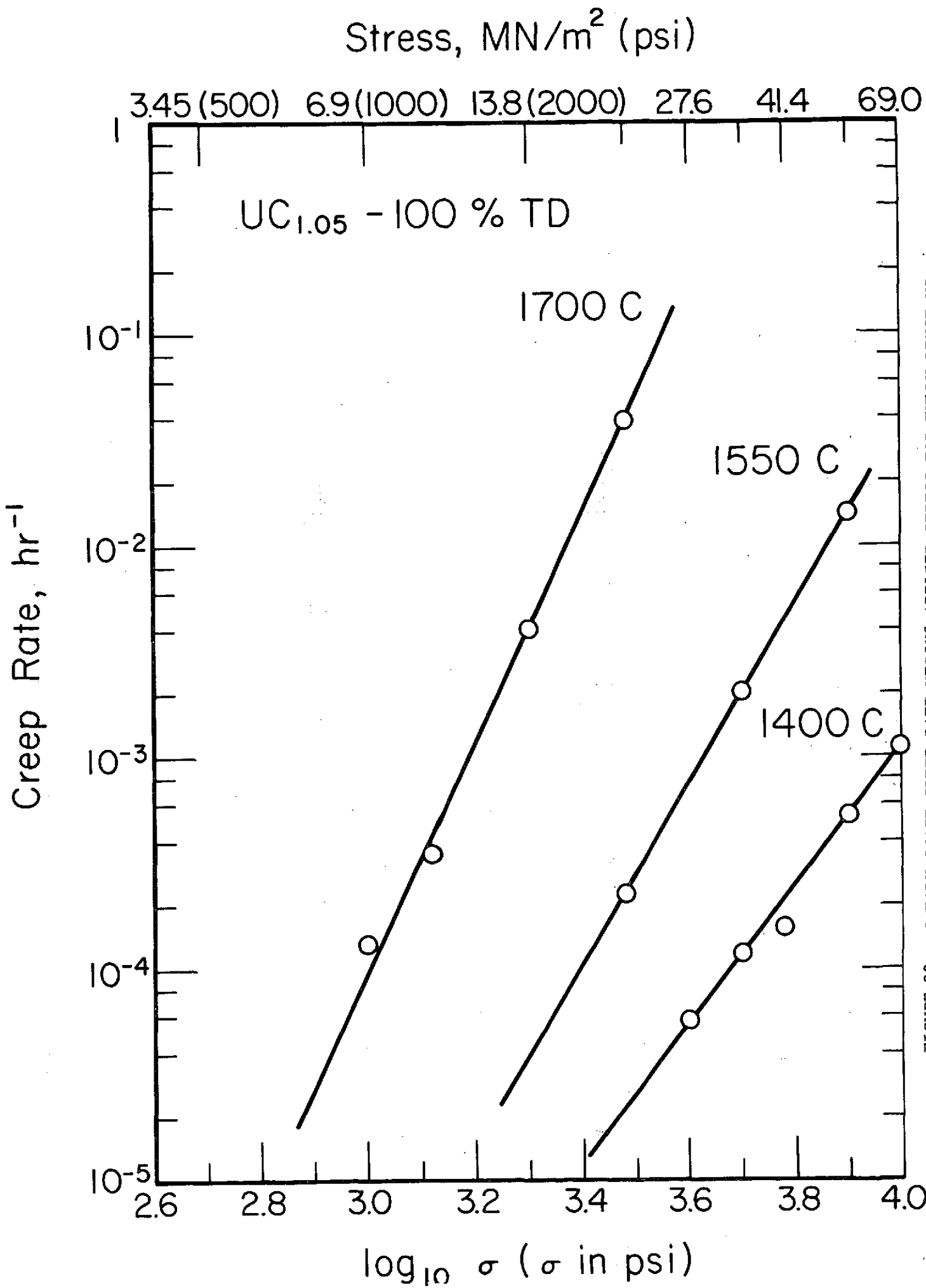

FIGURE 23. STEADY-STATE CREEP RATE VERSUS APPLIED STRESS FOR FULLY DENSE $UC_{1.05}$

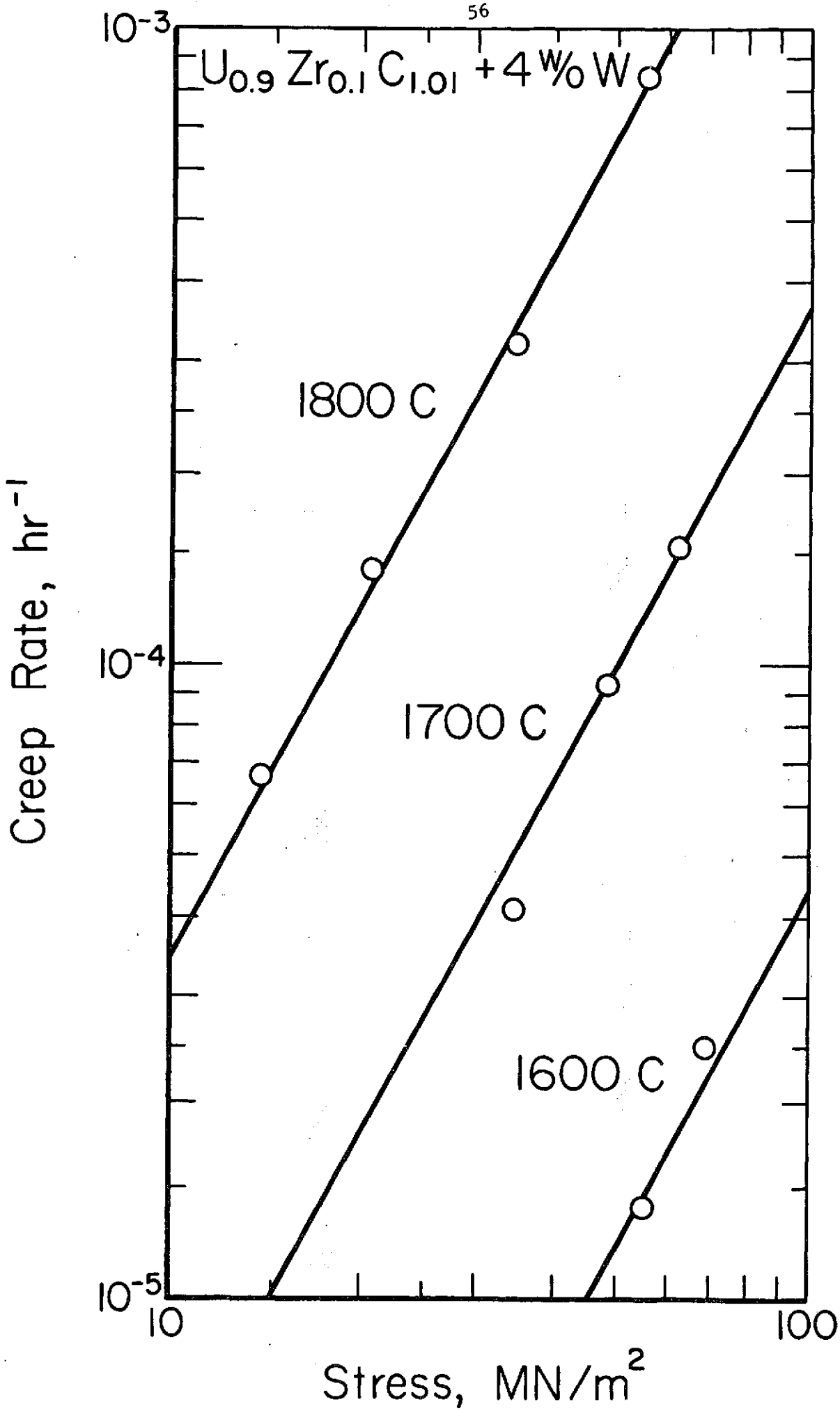

FIGURE 24. STEADY-STATE CREEP RATE VERSUS APPLIED STRESS FOR FULLY DENSE $U_{0.9}Zr_{0.1}C_{1.01}$ + 4 w/o W

uranium carbide, and the carbide containing ZrC and tungsten dispersoid are common to many metallic systems containing dispersoids, as for example, nickel or nickel-20 w/o chromium compared with TD Ni or TD NiCr[21] (nickel-2 v/o ThO_2 or nickel-20 w/o chromium-2 w/o ThO_2). In these cases, the measured creep activation energy is considerably higher than the self-diffusion activation energies, and the creep strength for the dispersoid containing material is greater than that for the nondispersion strengthened material. The stress exponent appears to be dependent on the crystalline grain size, with very high values for n being found when coarse grained specimens are tested.

The same high creep strengths found for $U_{0.9}Zr_{0.1}C_{1.01}$ + 4 w/o W have also been measured for uranium carbide containing approximately 4 w/o W, but without the zirconium addition. Figure 25 includes creep rates measured as a function of stress for fully dense $UC_{1.01}$ + 4 w/o W (prepared for this study) obtained under a vacuum of 1.33×10^{-3} N/m^2 (10^{-5} torr) at 1700 C as well as values for $UC_{1.02}$ + 4 w/o W with an initial density of 78 percent TD (prepared by GGA) obtained in an argon atmosphere at 1750 and 1900 C. Both kinds of specimens yielded a stress exponent of approximately 3, and as will be shown later in this section, the creep rates measured from these specimens are in reasonably good agreement with regard to the temperature dependence for creep.

All of the data obtained in this study at 1700 C are presented in Figure 26 as a function of applied stress to illustrate the difference in creep strength between alloyed and unalloyed uranium carbide. At 27.6 MN/m^2 (4000 psi) creep rates for the tungsten-bearing compounds are some four to five orders of magnitude lower than that measured for $UC_{1.01}$. As a result of the different stress dependencies for creep of the various carbide alloys, this great disparity in creep strength is reduced somewhat at lower stresses, although still amounting to some three orders of magnitude at 6.9 MN/m^2 (1000 psi).

Temperature Dependence

The temperature dependence for creep of the various carbide alloys is shown in Figure 27 which includes creep rates measured at 27.6 MN/m^2

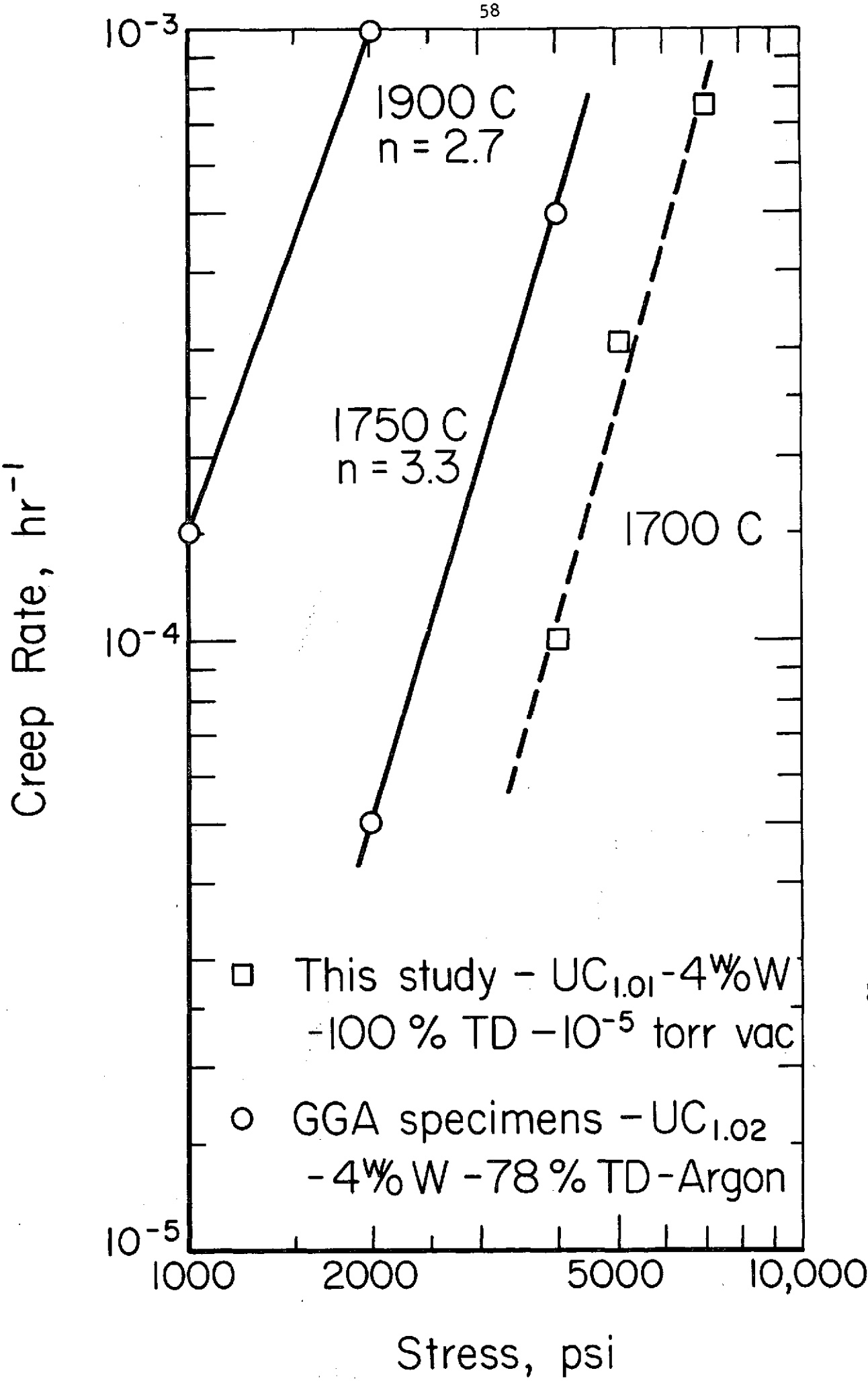

FIGURE 25. STEADY-STATE CREEP RATE VERSUS APPLIED STRESS FOR FULLY DENSE AND LOW-DENSITY URANIUM CARBIDE CONTAINING 4 w/o W

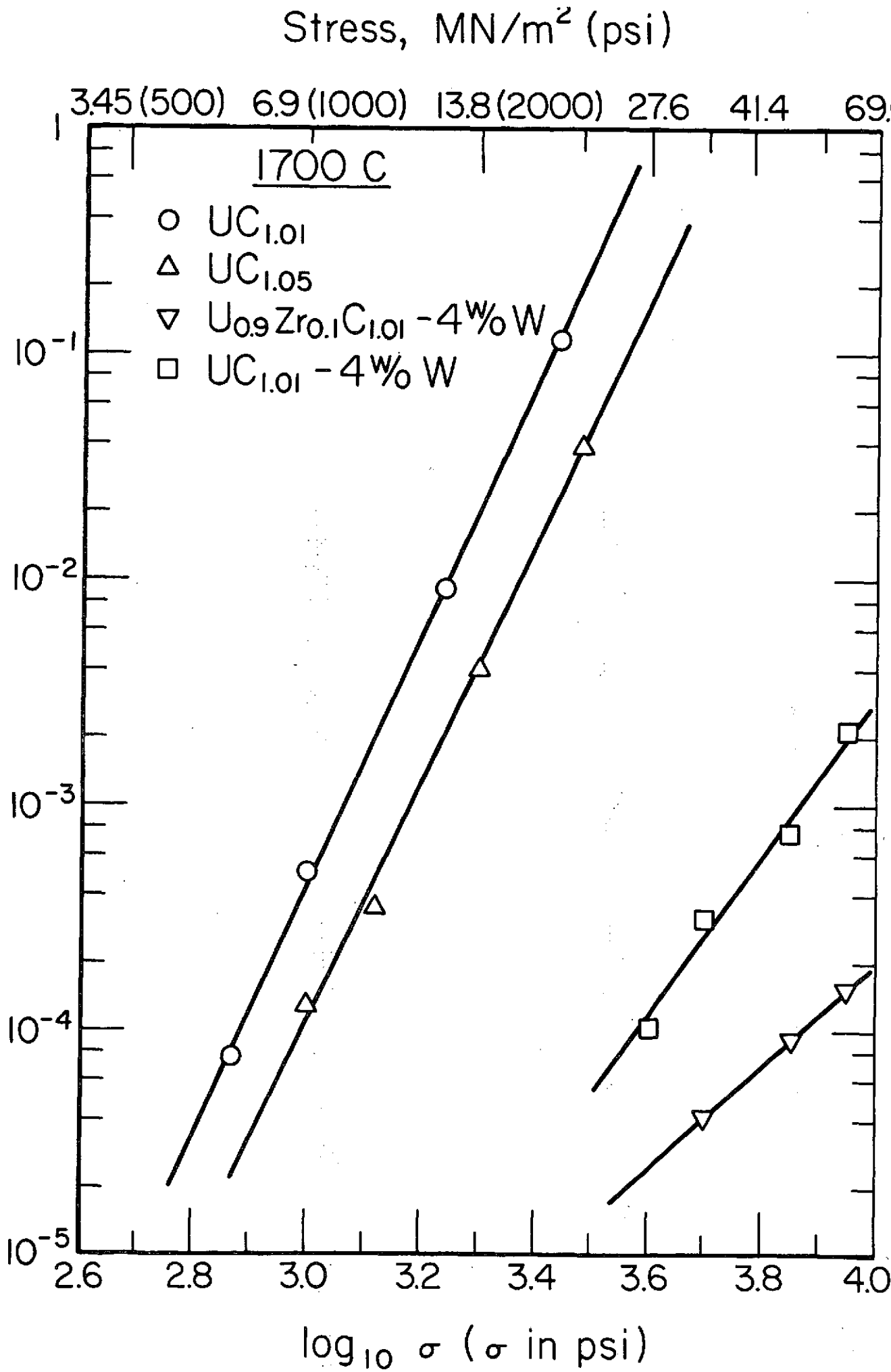

FIGURE 26. STEADY-STATE CREEP RATES MEASURED AT 1700 C VERSUS APPLIED STRESS FOR FULLY DENSE $UC_{1.01}$, $UC_{1.05}$, $UC_{1.01}$ + 4 w/o W AND $U_{0.9}Zr_{0.1}C_{1.01}$ + 4 w/o W

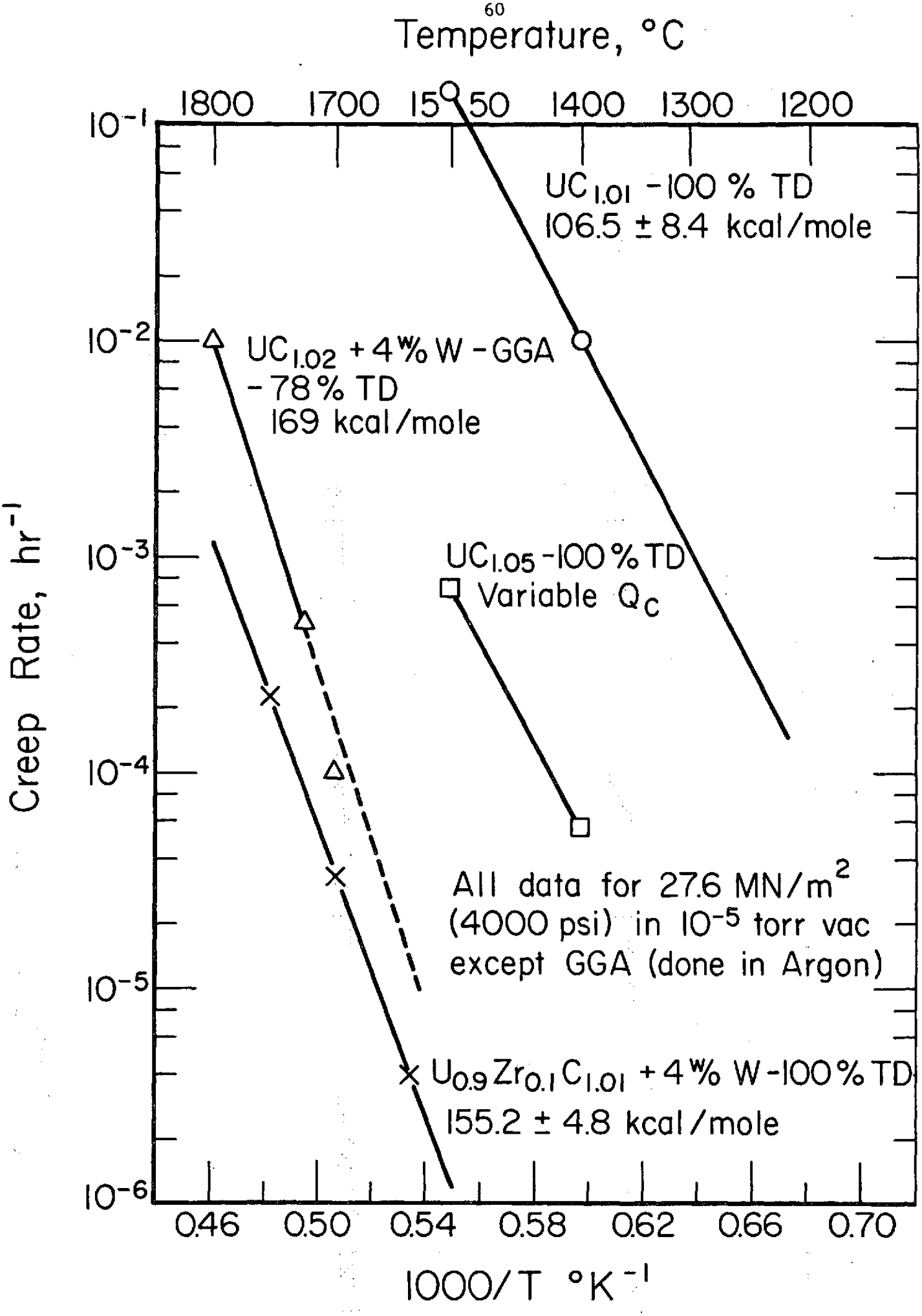

FIGURE 27. STEADY-STATE CREEP RATE VERSUS RECIPROCAL OF ABSOLUTE TEMPERATURE FOR VARIOUS CARBIDE FUELS

(4000 psi) as a function of reciprocal absolute temperature. The variable stress exponent for $UC_{1.05}$ precludes evaluation of a meaningful activation energy, but data obtained at 1400 and 1550 C have been included to place the creep rates for this material in relation to other creep data. The results presented in Figure 27 clearly reveal that the great differences in creep strength for the materials tested exist over a wide temperature range.

Stoichiometry Effects

Although creep measurements in the current program have been limited to two compositions of unalloyed uranium carbide, $UC_{1.01}$ and $UC_{1.05}$, it has been possible, using creep data obtained in previous studies[6,8,10], to construct diagrams of creep rates as a function of U/C ratio for various temperatures and stresses. Figure 28 includes data obtained at 1400 C under stresses of 20.7 MN/m^2 (3000 psi) and 41.4 MN/m^2 (6000 psi). At this temperature creep, rates are seen to decrease by several orders of magnitude as the C/U ratio is increased from 1.01 to 1.05 and then to increase as the C/U level is increased further to 1.08. The paucity of data and the fact that the information available was obtained in different laboratories under different conditions requires that these diagrams be used with some care until more extensive data are obtained. Furthermore, as shown in Figure 29 where creep rates are plotted as function of C/U ratio for several different temperatures, the large effect of stoichiometry observed at 1400 C, may be all but eliminated at 1700 C where second-phase precipitates are not present to strengthened the fuel. It is expected that only small differences in creep rates, due to changes in point defect concentrations rather than second phases, will be observed at temperatures above 1700 C for unalloyed uranium carbide of different stoichiometric compositions.

Microstructural Studies

Typical microstructures for the four carbide materials which were tested in this program were reproduced in Figure 30. The $UC_{1.01}$ starting material had

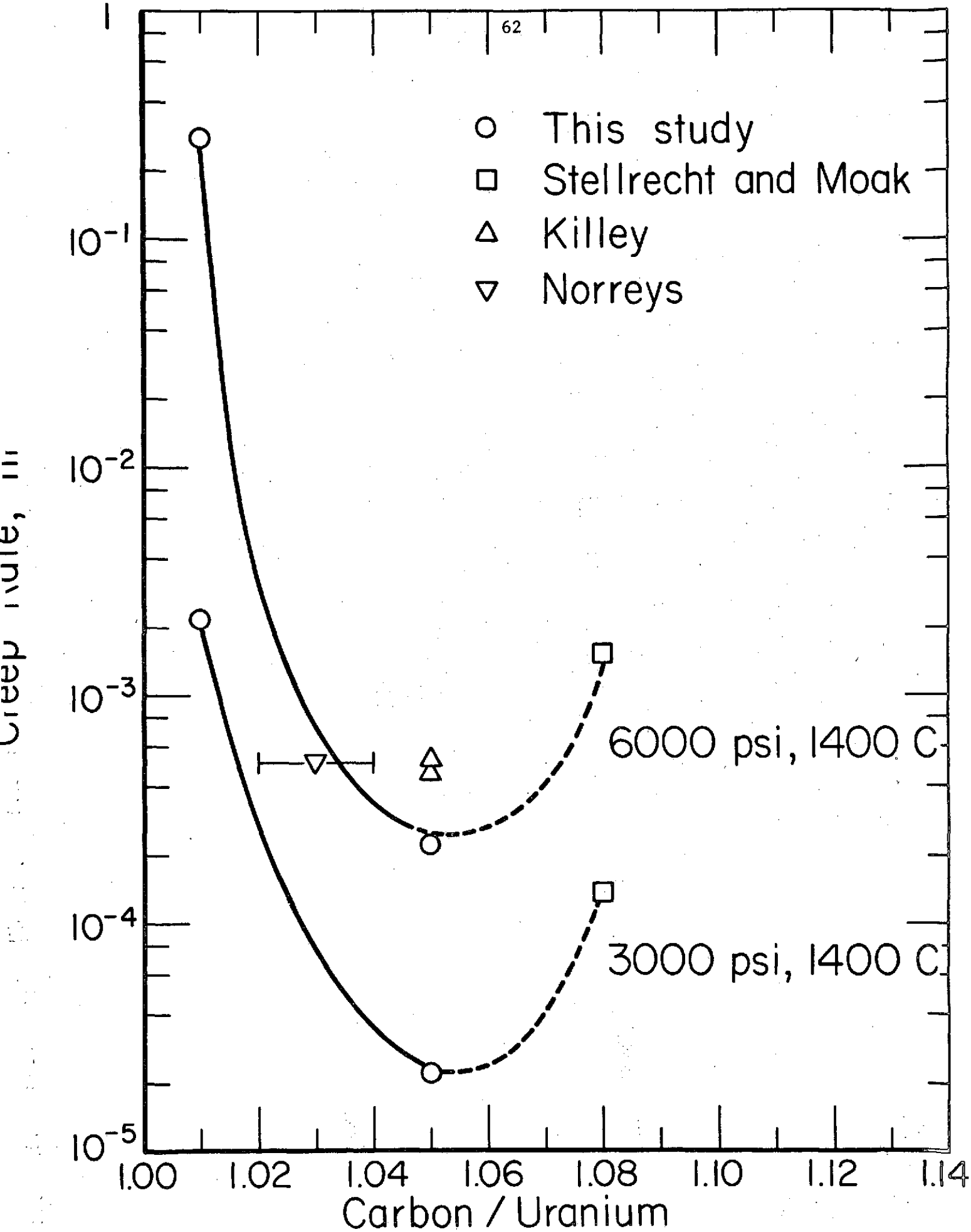

FIGURE 28. STEADY-STATE CREEP RATE VERSUS C/U RATIO FOR URANIUM CARBIDE TESTED AT 1400 C UNDER STRESSES OF 20.7 MN/m^2 (3000 psi) AND 41.4 MN/m^2 (6000 psi)

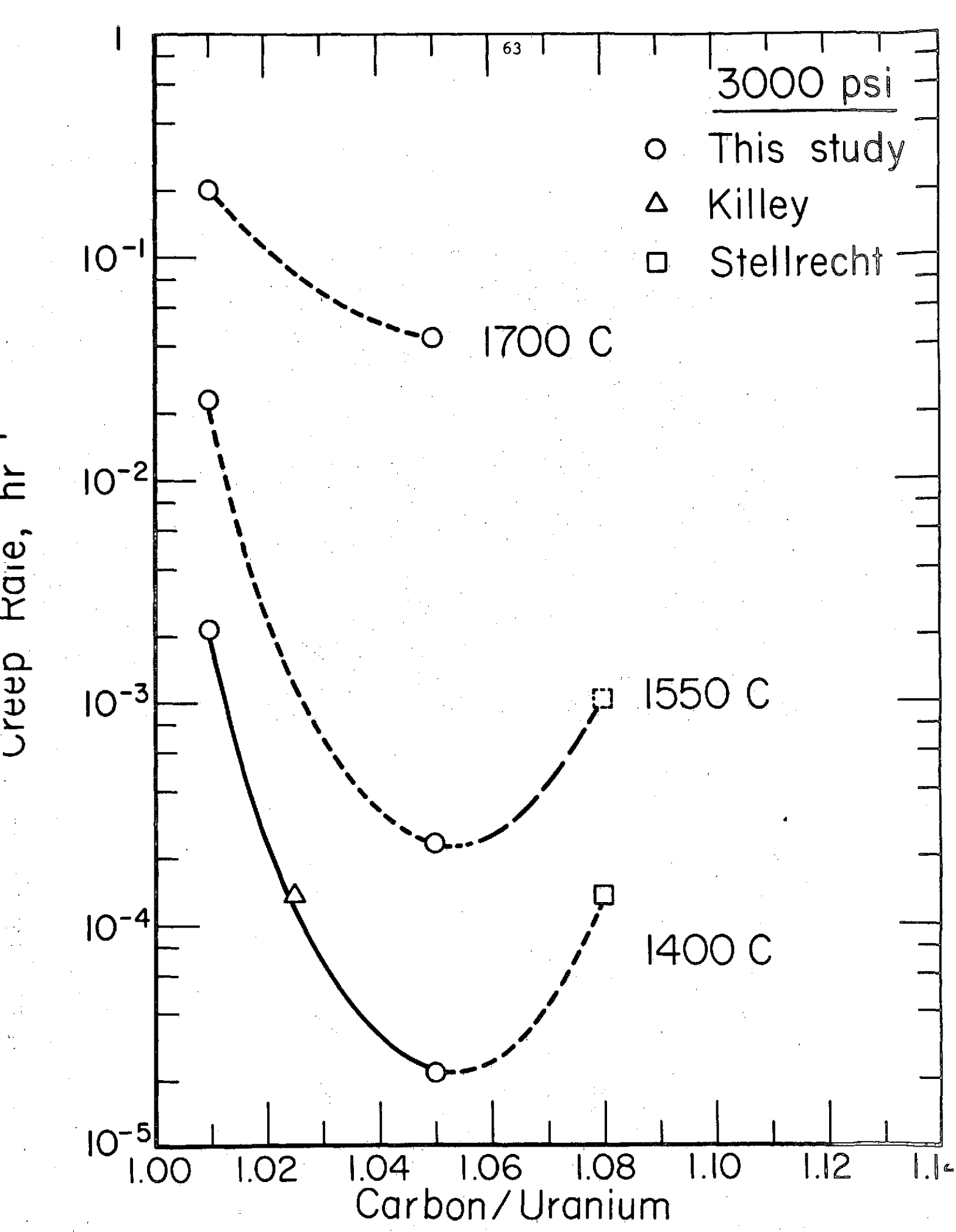

FIGURE 29. STEADY-STATE CREEP RATE VERSUS C/U RATIO FOR URANIUM CARBIDE TESTED UNDER STRESS OF 20.7 MN/m^2 (3000 psi) AT 1400, 1550, AND 1700 C

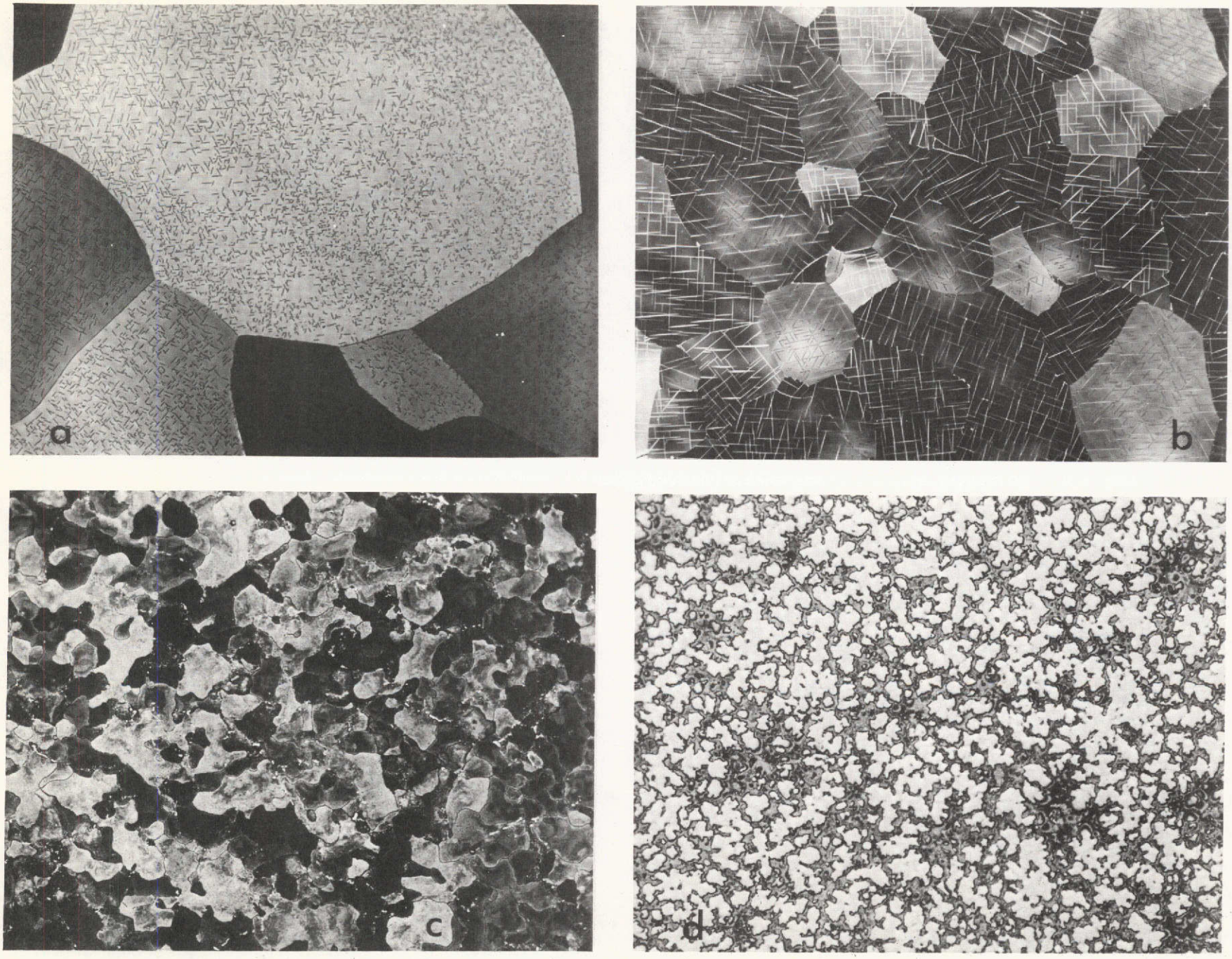

FIGURE 30. MICROSTRUCTURE OF 100% DENSE AS-CAST CARBIDE SPECIMENS, 250X (a) $UC_{1.01}$, (b) $UC_{1.05}$, (c) $UC_{1.01}$ + 4 w/o W, (d) $U_{0.9}Zr_{0.1}C_{1.01}$ + 4 w/o W

very large grains with a fine distribution of UC_2 platelets, while the $UC_{1.05}$ had a somewhat smaller grain size and a more dense platelet distribution. The structures for $U_{0.9}Ar_{0.1}C_{1.01}$ + 4 w/o W and $UC_{1.01}$ + 4 w/o W appear to be quite complex with a much smaller grain size and containing several different phases.

Microstructures at the same magnification (250X) taken from transverse sections after creep are shown in Figure 31. No UC_2 platelets are visible in the $UC_{1.01}$ and the concentration of platelets in the $UC_{1.05}$ is greatly reduced. In their stead is found a white phase, probably U_2C_3, which has accumulated mostly at the grain boundaries. This same phase can also be seen in the $UC_{1.01}$ + 4 w/o W. The phase may have formed during the slow cooling after creep which occurs in the creep furnace. The high creep strength of these carbides, particularly of $UC_{1.01}$ + 4 w/o W, precludes the possibility that the grain boundary phase is free uranium or some other compound which would be liquid or have little creep strength at the creep temperatures. The microstructure of $U_{0.9}Ar_{0.1}C_{1.01}$ + 4 w/o W appears to have changed the least during creep, although changes on a fine scale may have occurred in this complex structure.

More potentially important effects of the creep test environment on the structure of the materials tested are shown in the longitudinal sections shown at 20X in Figures 32 and 33. The outer layers of these specimens have been oxidized, apparently while at temperature in the creep apparatus. The oxidation is very slight for $UC_{1.01}$ and moderate for $UC_{1.05}$, while more extensive attack has occurred for the fine-grained tungsten doped carbides. Evidence for oxygen in the outer portion of the specimens was obtained from electron microprobe analysis. In addition, X-ray diffraction of a sample taken from the outer portion of the $U_{0.9}Zr_{0.1}C_{1.01}$ + 4 w/o W revealed the presence of uranium dioxide. Additional electron probe studies of the $U_{0.9}Zr_{0.1}C_{1.01}$ + 4 w/o W revealed that the outer band contained zirconium and tungsten in the same proportions and distribution as found in the unoxidized portions as well as carbon at a lower level than was found in the unoxidized central portion.

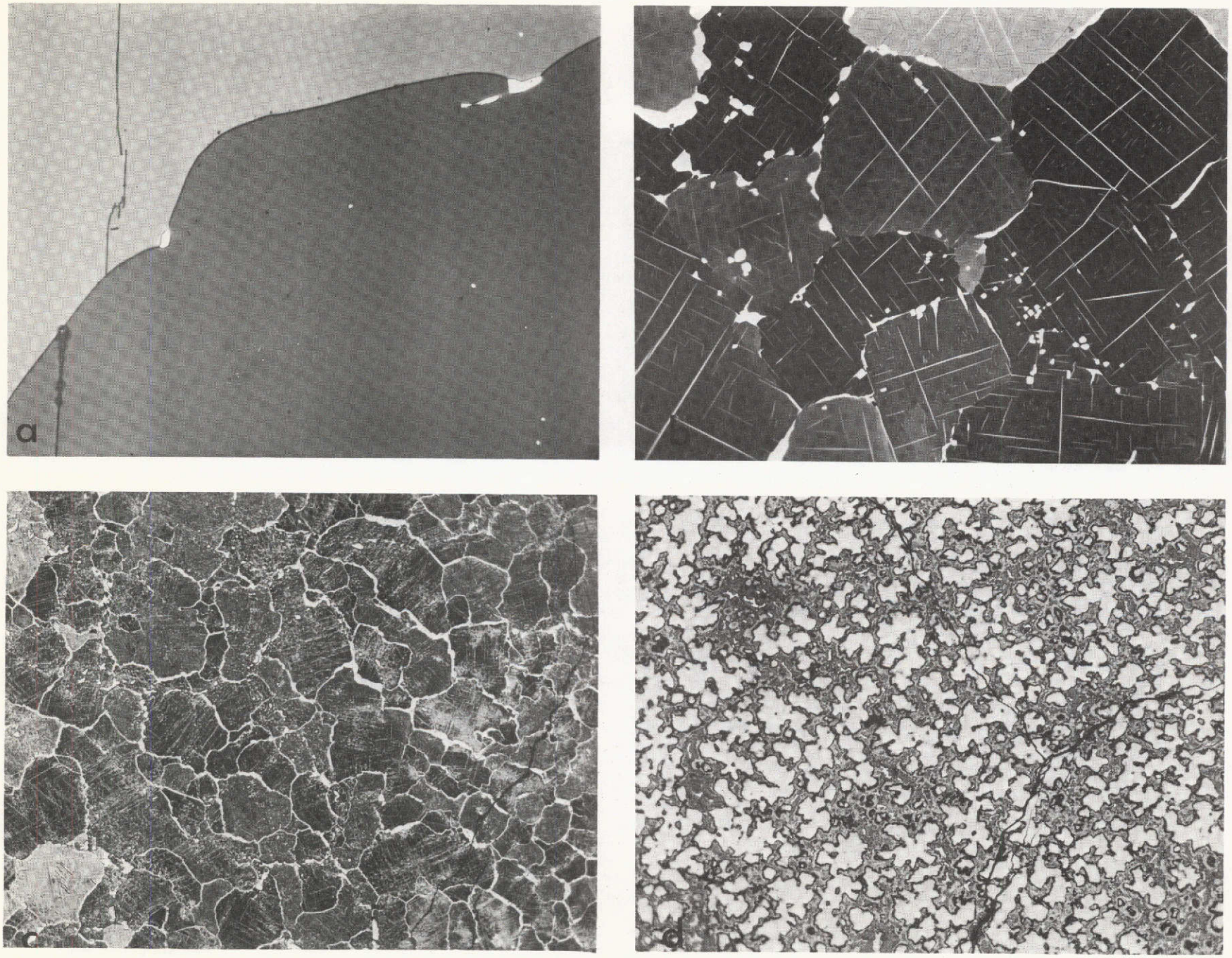

FIGURE 31. MICROSTRUCTURE OF 100% DENSE CARBIDE SPECIMENS AFTER CREEP, 250X (a) $UC_{1.01}$, (b) $UC_{1.05}$, (c) $UC_{1.01}$ + 4 w/o W, (d) $U_{0.9}Zr_{0.1}C_{1.01}$ + 4 w/o W

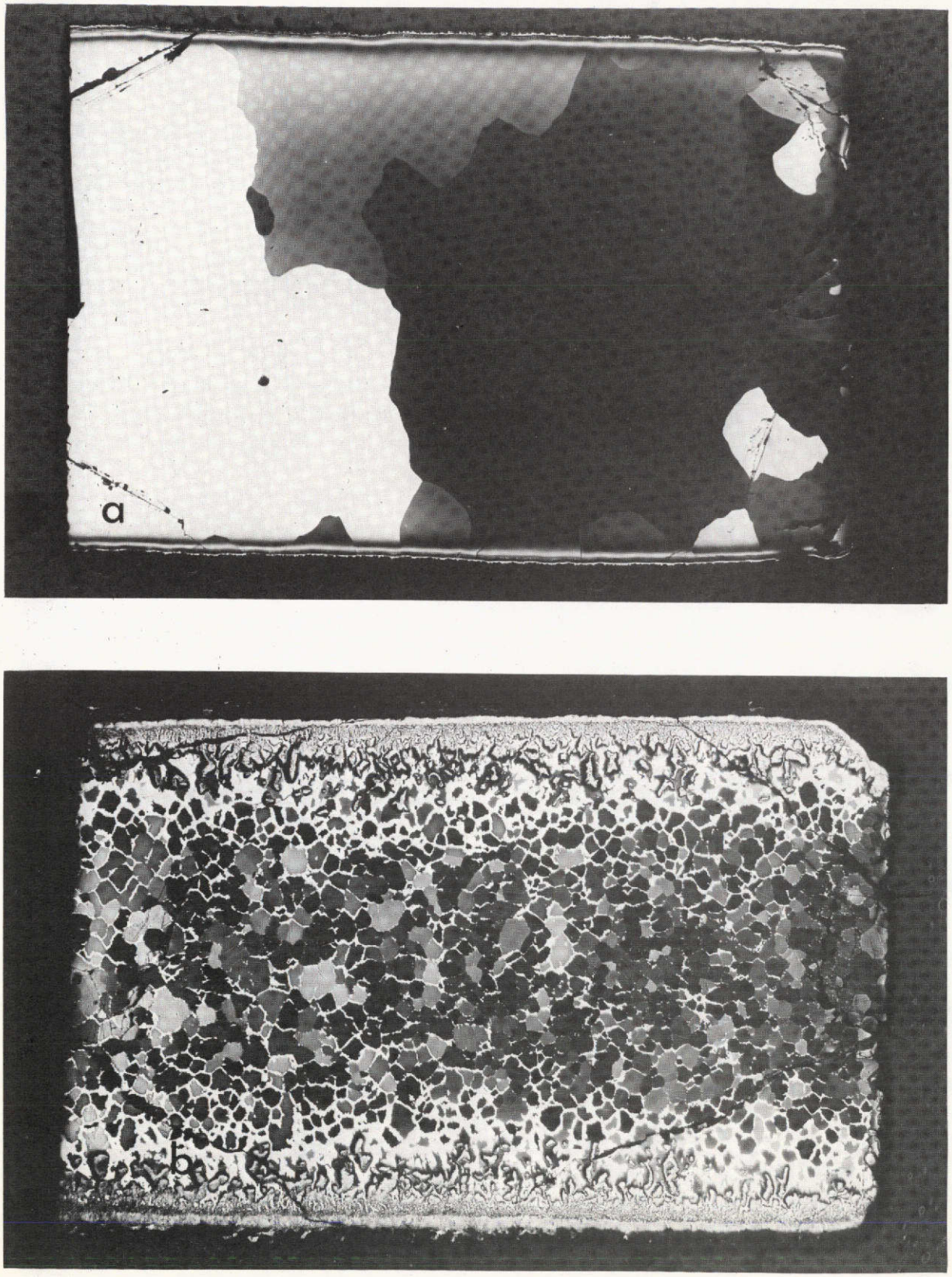

FIGURE 32. MICROSTRUCTURE OF 100% DENSE CARBIDE SPECIMENS AFTER CREEP, 20X (a) $UC_{1.01}$, (b) $UC_{1.05}$

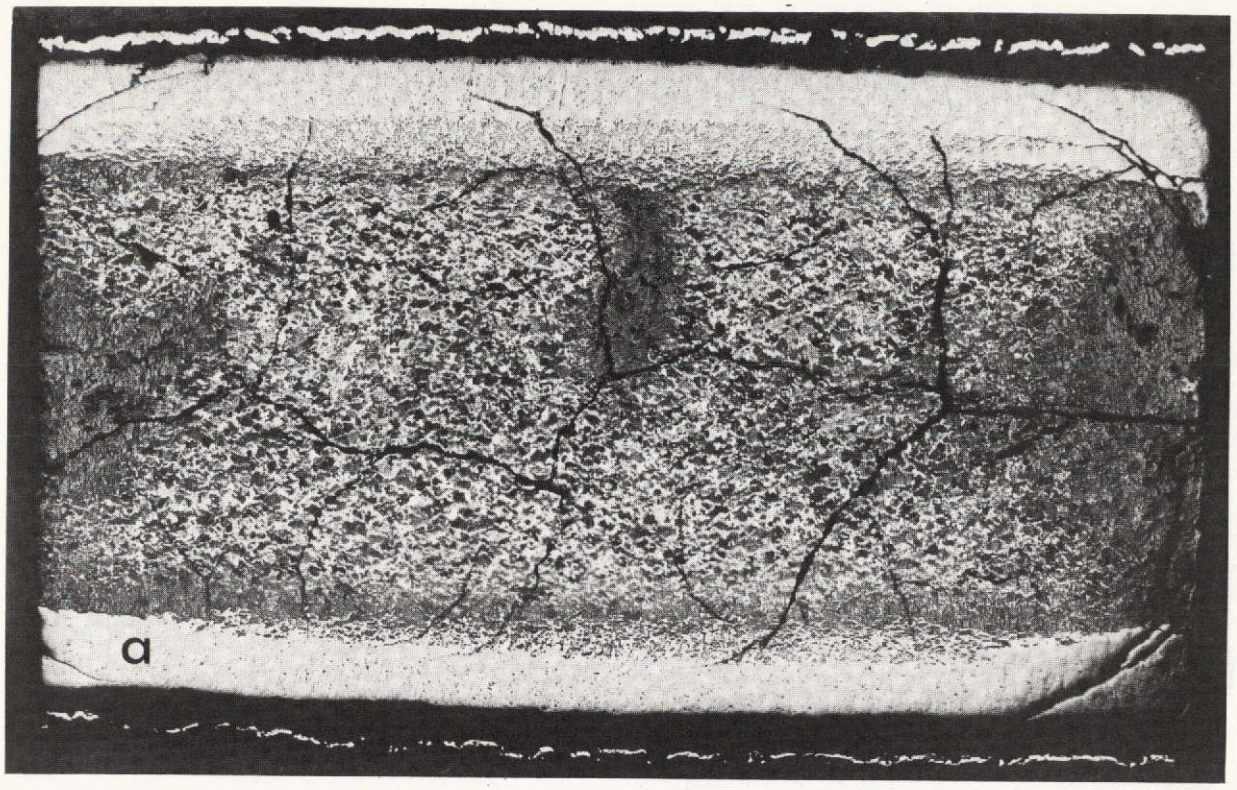

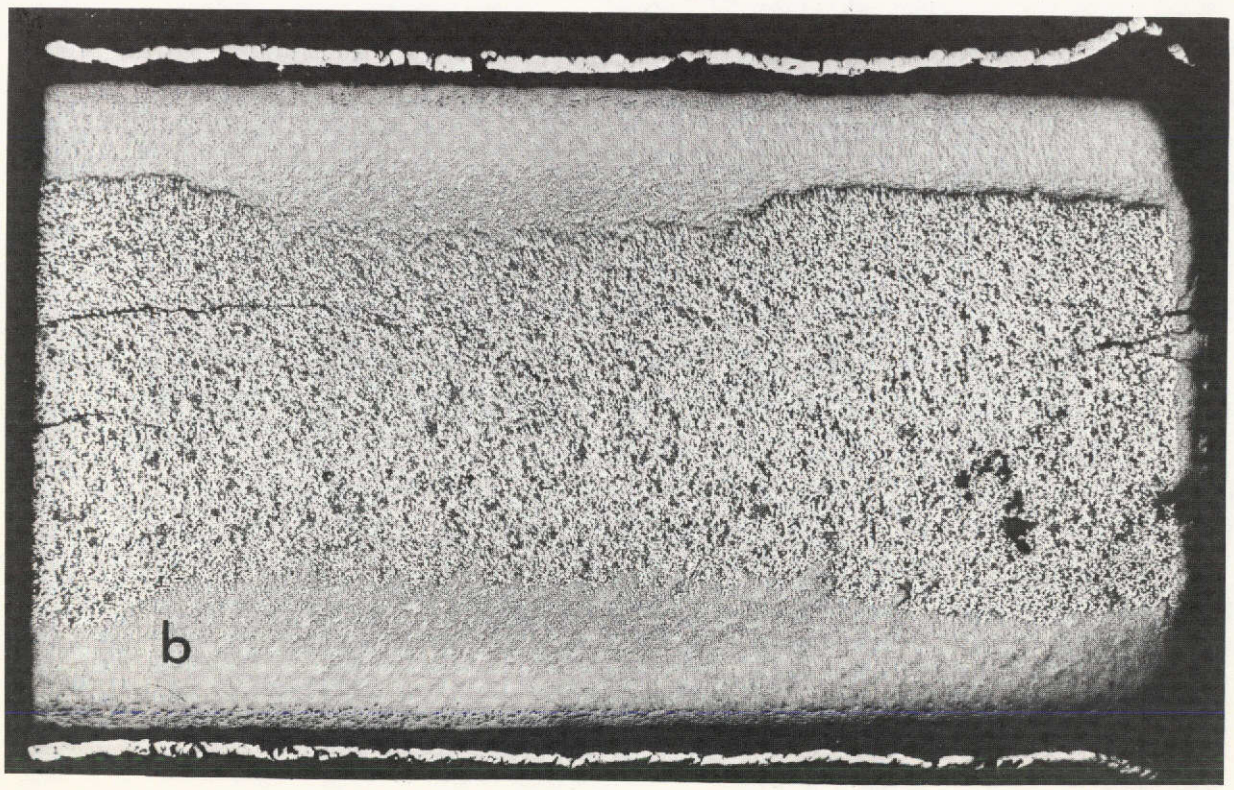

FIGURE 33. MICROSTRUCTURE OF 100% DENSE CARBIDE SPECIMENS AFTER CREEP, 20X
(a) $UC_{1.01}$ + 4 w/o W, (b) $U_{0.9}Zr_{0.1}C_{1.01}$ + 4 w/o W

In an attempt to determine what effect the oxidation layer had on the creep properties, high-density carbide specimens containing tungsten were tested at 1700 C in the same creep unit used for the low-density specimens. Under these test conditions, no oxidation of the carbide specimens was observed. The "Bracermet" material placed between the specimens and the platens was indented by the specimens. In contrast, the "Bracermet" material was not indented in the previous tests where oxidation occurred. These results suggest that the oxidation of the carbide specimens resulted in some reduction in strength and, therefore, the results obtained on the high-density carbide alloys containing tungsten should be taken as the lower limit on creep strength.

Low-Density Materials

Stress and Temperature Dependence

Steady-state creep rates for approximately 75 percent dense $UC_{1.01}$, $UC_{1.01}$ + 4 w/o W and $U_{0.9}Zr_{0.1}C_{1.01}$ + 4 w/o W obtained as a function of applied stress at 1400 and 1550 C are presented in Figures 34 to 36 while similar data for the latter two alloys with densities of about 85 percent of the theoretical value are given in Figures 37 and 38. In these figures the specimen designation from which each data point was obtained is given. The numbers after the specimen designation refer to the order in which the stress changes were made for a given specimen. For example, the creep rates for specimen PA5 were measured first at 6.9 MN/m^2 and then at 13.8 MN/m^2. Examination of Figures 34 to 38 reveals that data points obtained after increasing the applied stress from some lower value were often lower than might be predicted (PA5-2, PB5-2, PC5-2, PC13-2), while creep rates measured under conditions of decreasing stress were in good agreement with those measured initially at the same lower stress. For both 75 and 85 percent TD specimens the order of increasing creep strength is the same as that found for theoretically dense specimens, i.e., unalloyed UC is the weakest material

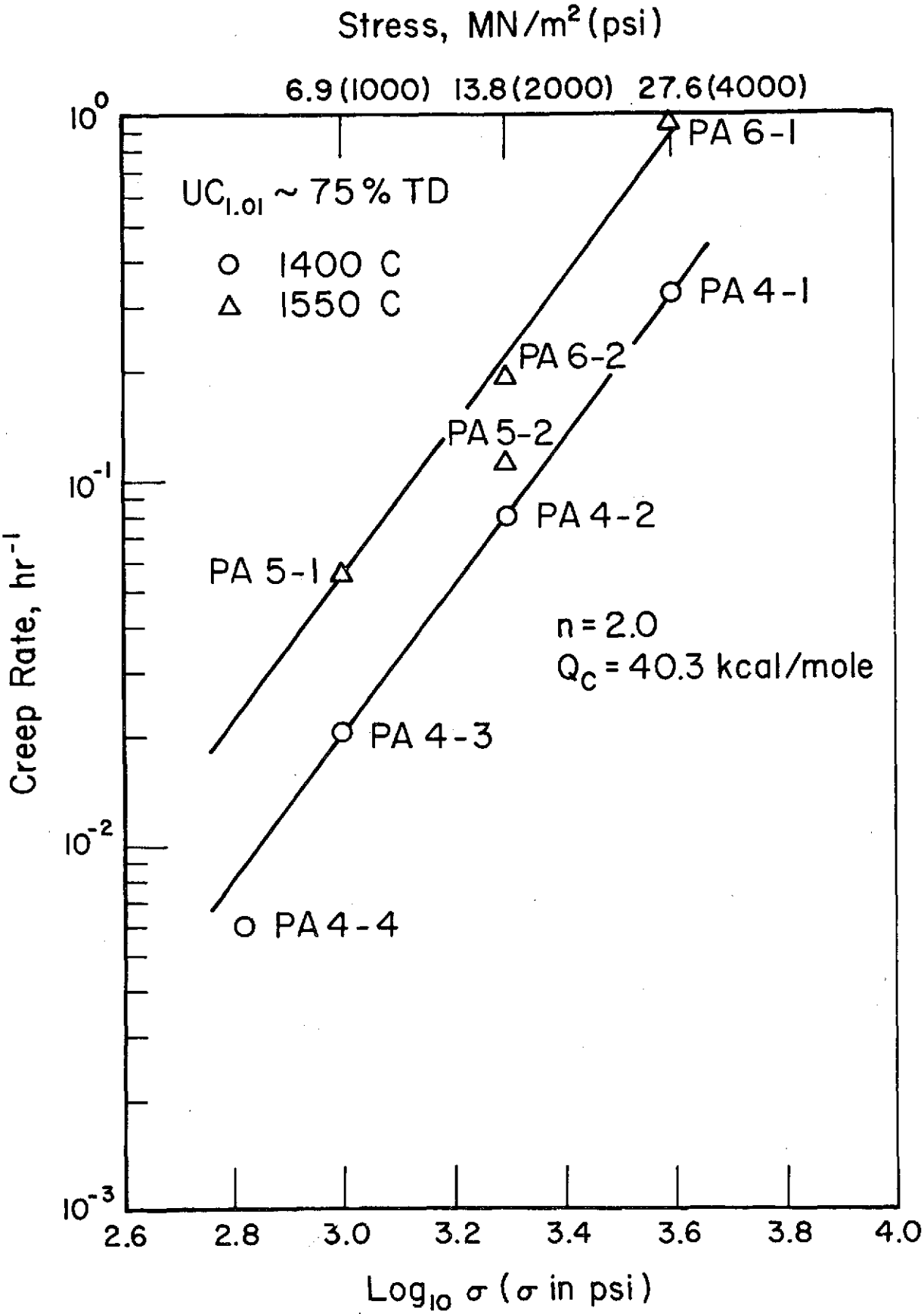

FIGURE 34. STEADY-STATE CREEP RATE VERSUS APPLIED STRESS FOR $UC_{1.01}$, 75% TD

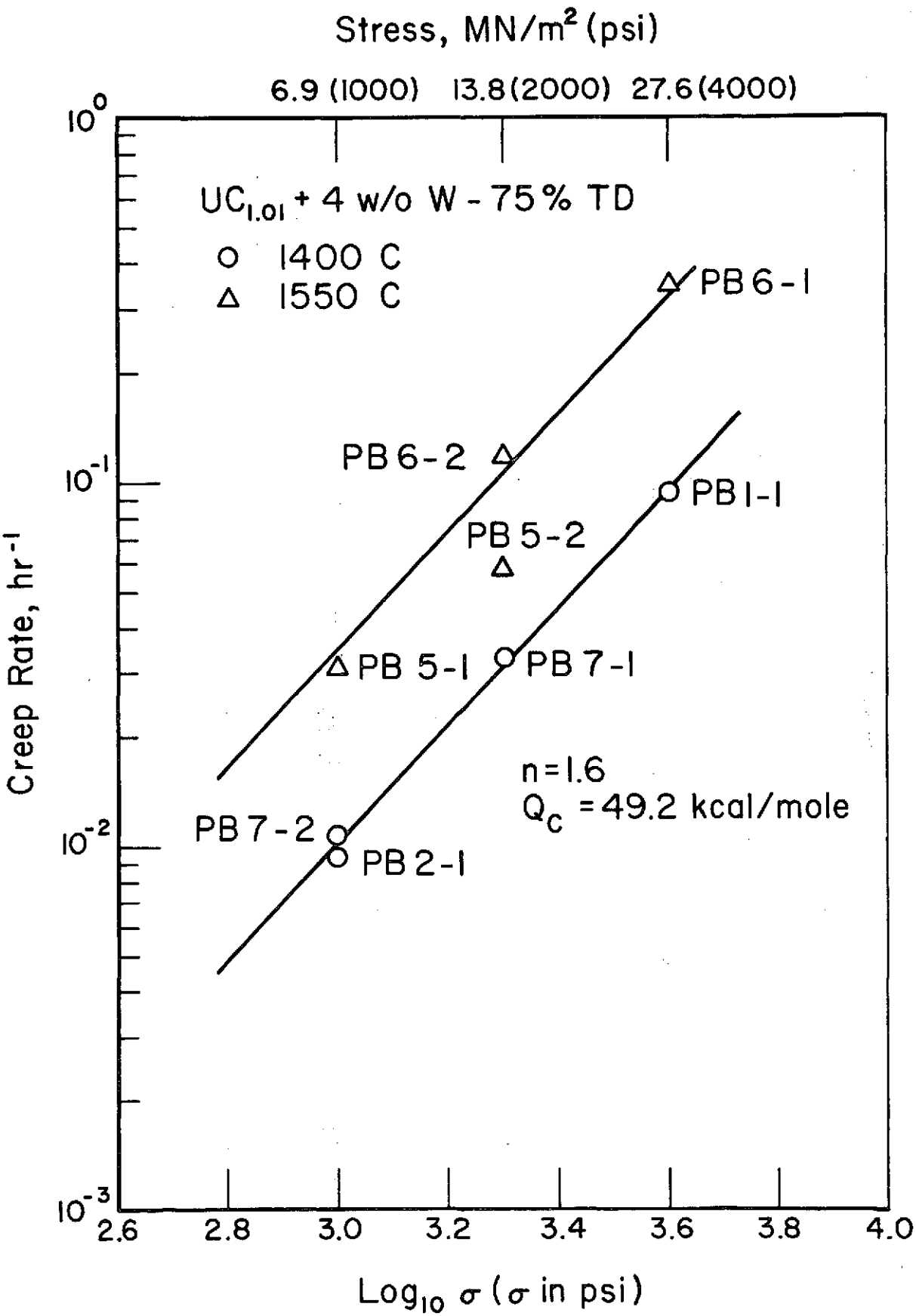

FIGURE 35. STEADY-STATE CREEP RATE VERSUS APPLIED STRESS FOR $UC_{1.01}$ + 4 w/o W, 75% TD

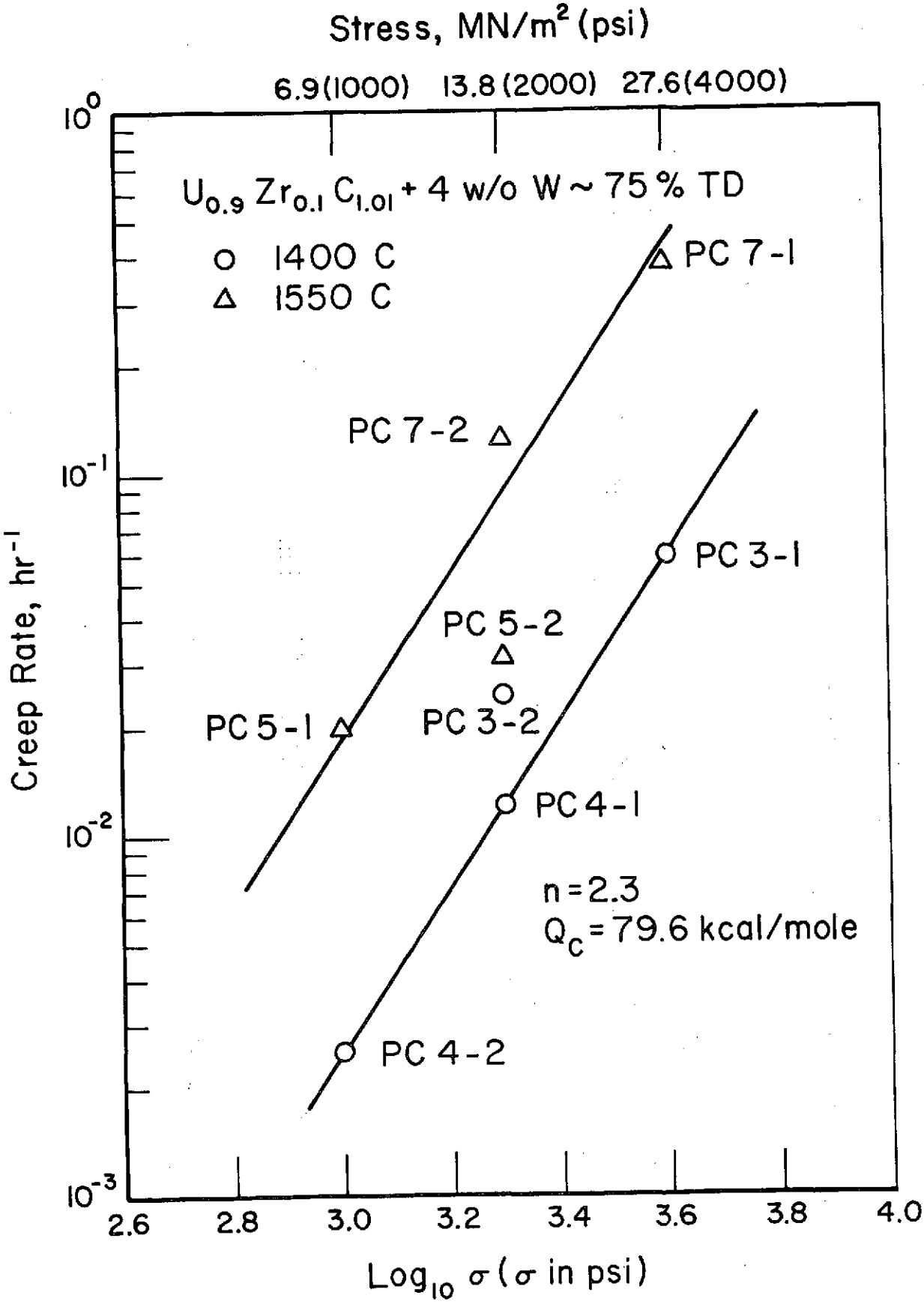

FIGURE 36. STEADY-STATE CREEP RATE VERSUS APPLIED STRESS FOR $U_{0.9}Zr_{0.1}C_{1.01}$ + 4 w/o W, 75% TD

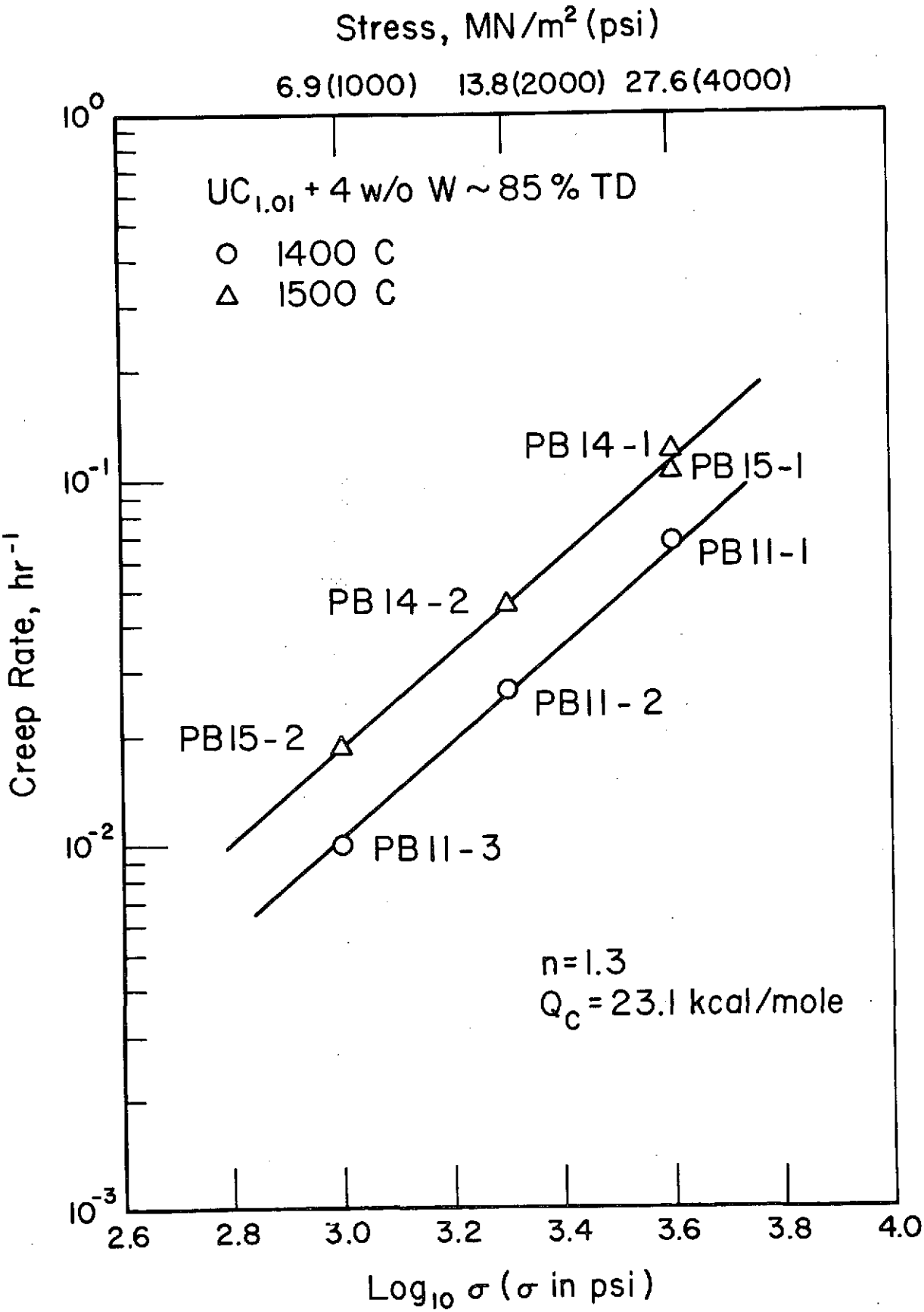

FIGURE 37. STEADY-STATE CREEP RATE VERSUS APPLIED STRESS FOR $UC_{1.01}$ + 4 w/o W, 85% TD

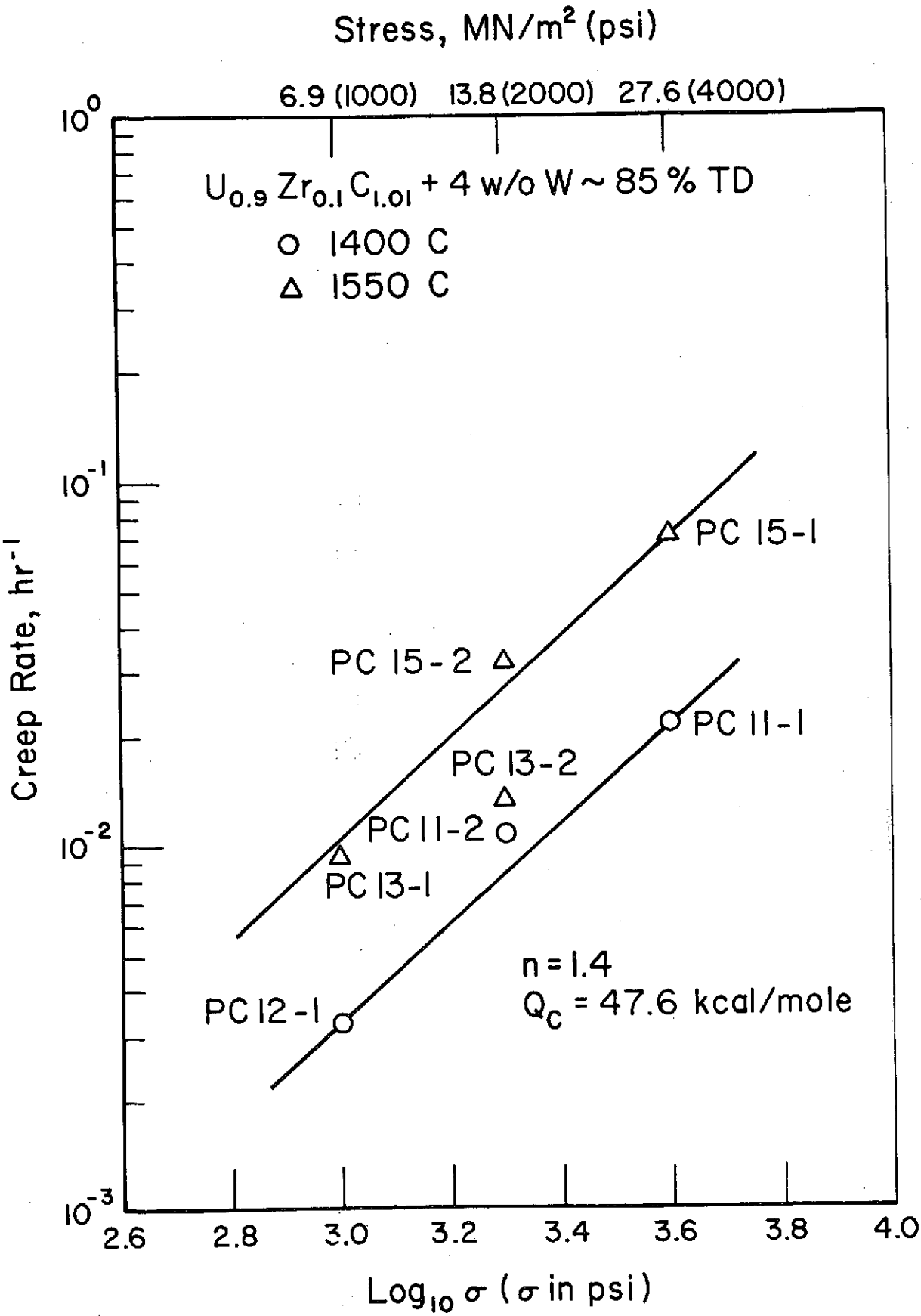

FIGURE 38. STEADY-STATE CREEP RATE VERSUS APPLIED STRESS FOR $U_{0.9}Zr_{0.1}C_{1.01}$ + 4 w/o W, 85% TD

followed by $UC_{1.01}$ + 4 w/o W and the $U_{0.9}Zr_{0.1}C_{1.01}$ + 4 w/o W. The differences in steady-state creep behavior among the low-density specimens are much smaller, however, as compared with high-density specimens. This is a reflection of the similarity in grain size and microstructure of the low-density specimens. Compare for example the relative uniformity of the microstructures of 75 percent TD crept specimens shown in Figures 39 to 44 with the diverse structures of the theoretically dense crept samples presented in Figure 30. Creep rates for 75 percent TD specimens were found to be a factor of three or less higher than those measured for 85 percent TD samples. This again is a reflection in the similarity of microstructures for the test specimens (compare Figures 41 and 45 which are representative microstructures for 75 percent TD and 85 percent TD $UC_{1.01}$ + 4 w/o W).

In all cases the stress exponents, n, for creep of low-density carbide specimens at 1400 C have values between 1.3 and 2.3. The low stress exponents found for $UC_{1.01}$ + 4 w/o W and $U_{0.9}Zr_{0.1}C_{1.01}$ + 4 w/o W are similar to those reported for high-density dispersoid-containing specimens.

From creep rates obtained at a given stress at 1400 C and 1550 C approximate creep activation energies could be obtained for each composition studied. Activation energies, Q_c, and stress exponents, n, for low density carbide fuels were obtained as follows:

Composition	n	Q_c (kcal/mole)
$UC_{1.01}$ - 75 percent TD	2.0	40.2
$UC_{1.01}$ + 4 w/o W - 75 percent TD	1.6	49.2
$U_{0.9}Zr_{0.1}C_{1.01}$ + 4 w/o W - 75 percent TD	2.3	79.6
$UC_{1.01}$ + 4 w/o W - 85 percent TD	1.3	23.1
$U_{0.9}Zr_{0.1}C_{1.01}$ + 4 w/o W - 85 percent TD	1.4	47.6

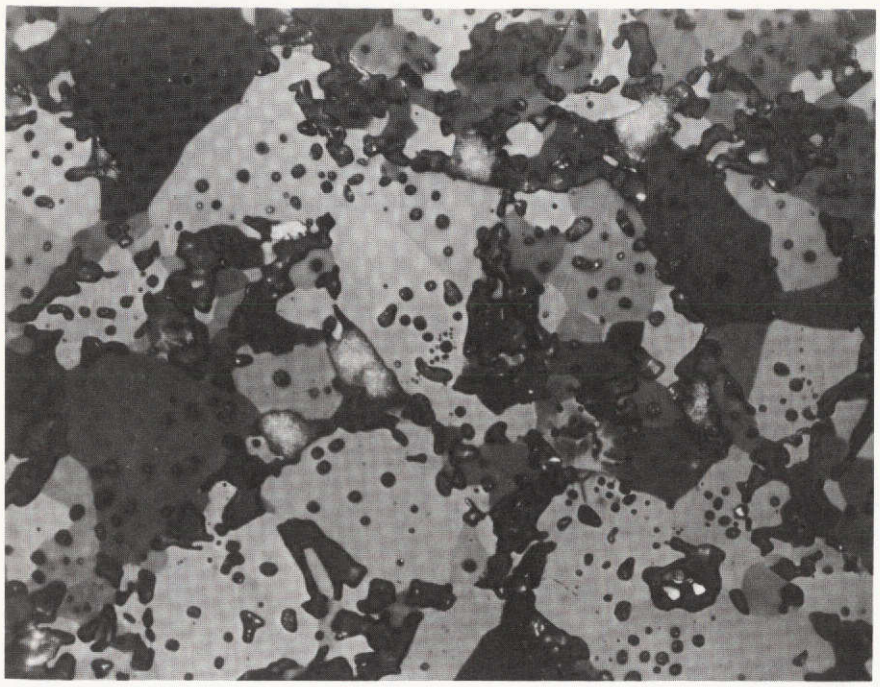

500X

7G187

FIGURE 39. PA4, $UC_{1.01}$, 75.1% TD, TESTED AT 1400 C

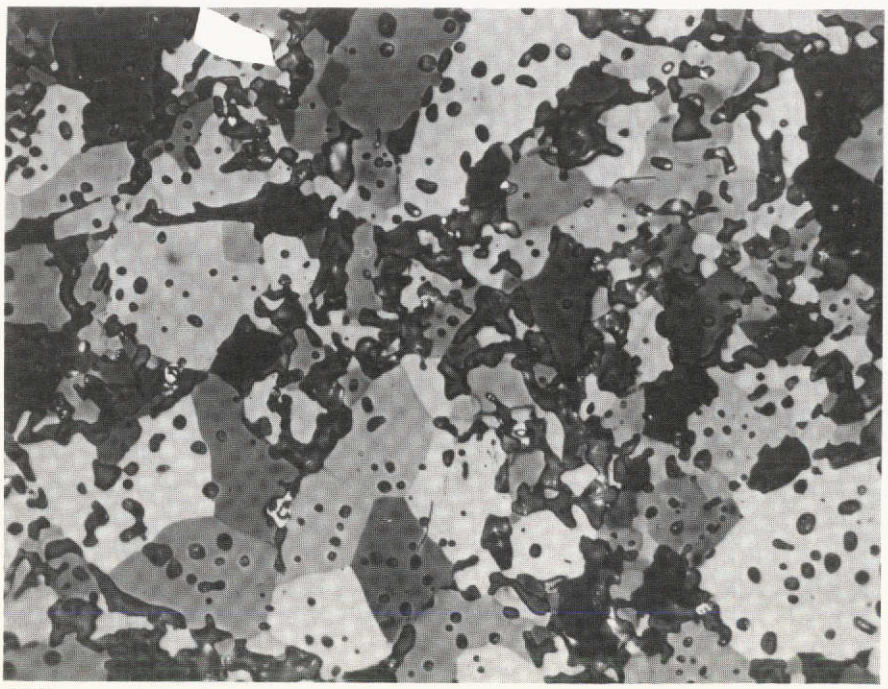

500X

7G189

FIGURE 40. PA5, $UC_{1.01}$, 76.6% TD, TESTED AT 1550 C

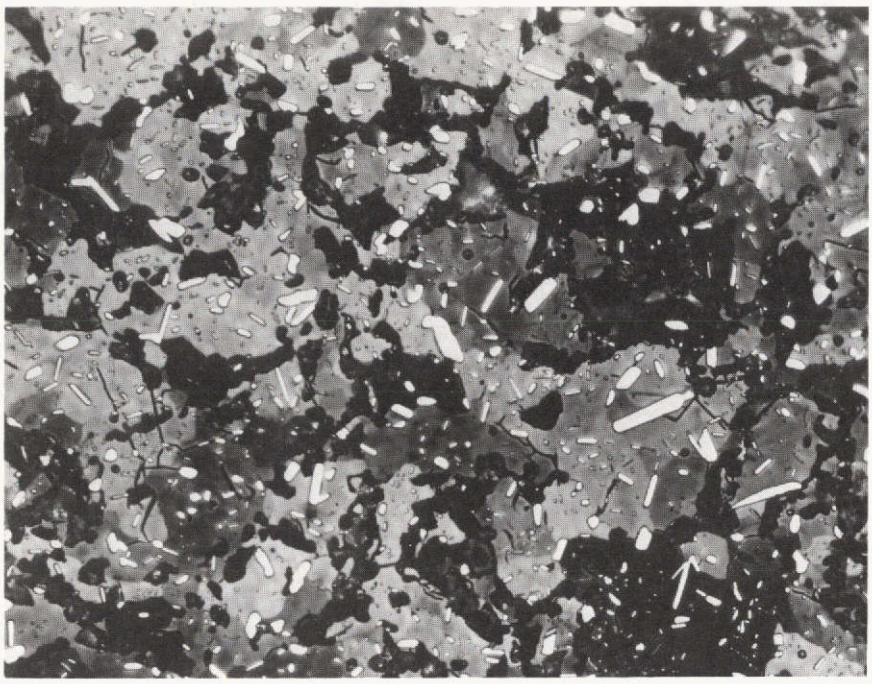

500X 5G635

FIGURE 41. PB1, $UC_{1.01}$ + 4 w/o W, 75.9% TD, TESTED AT 1400 C

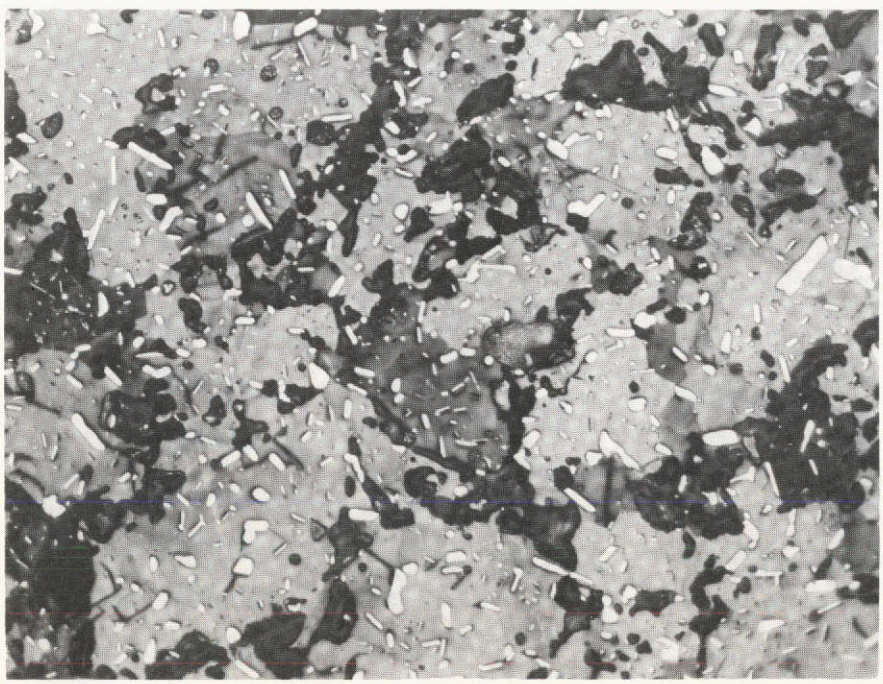

500X 7G191

FIGURE 42. PB5, $UC_{1.01}$ + 4 w/o W, 77.1% TD, TESTED AT 1550 C

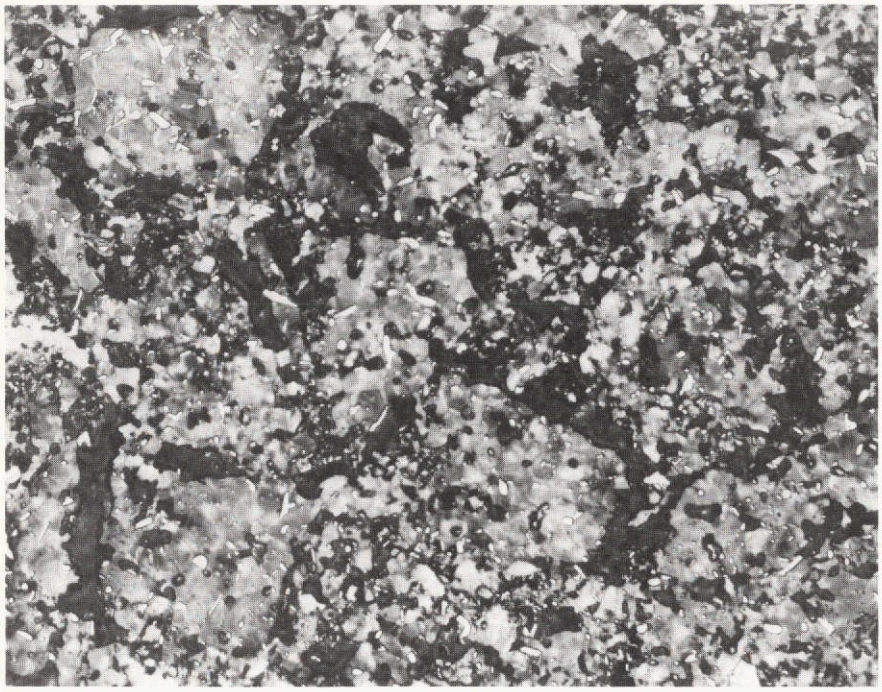

500X 5G645

FIGURE 43. PC3, $U_{0.9}Zr_{0.1}C_{1.01}$ + 4 w/o W, 76.6% TD, TESTED AT 1400 C

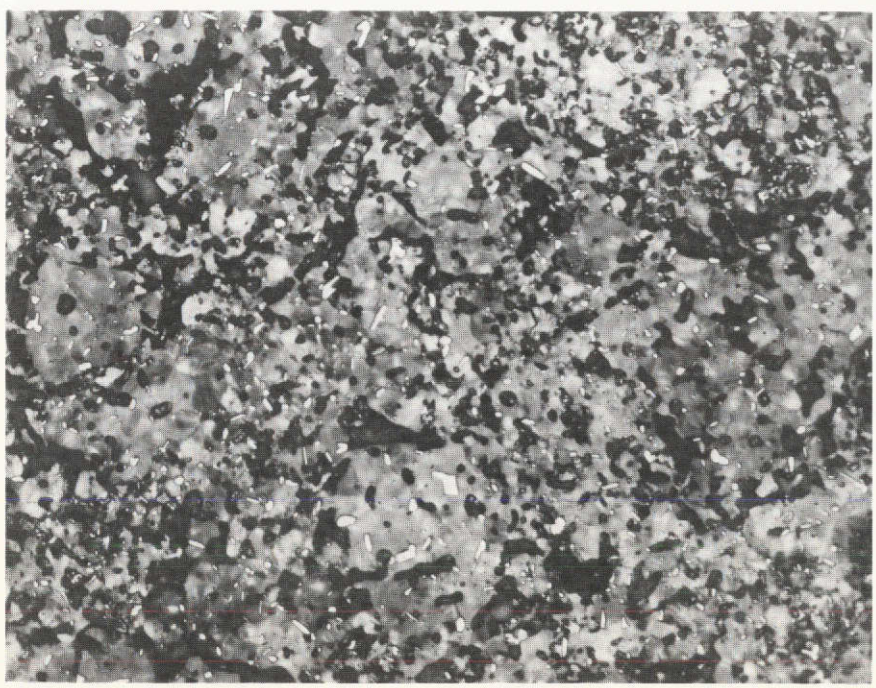

500X 7G195

FIGURE 44. PC5, $U_{0.9}Zr_{0.1}C_{1.01}$ + 4 w/o W, 76.2% TD, TESTED AT 1550 C

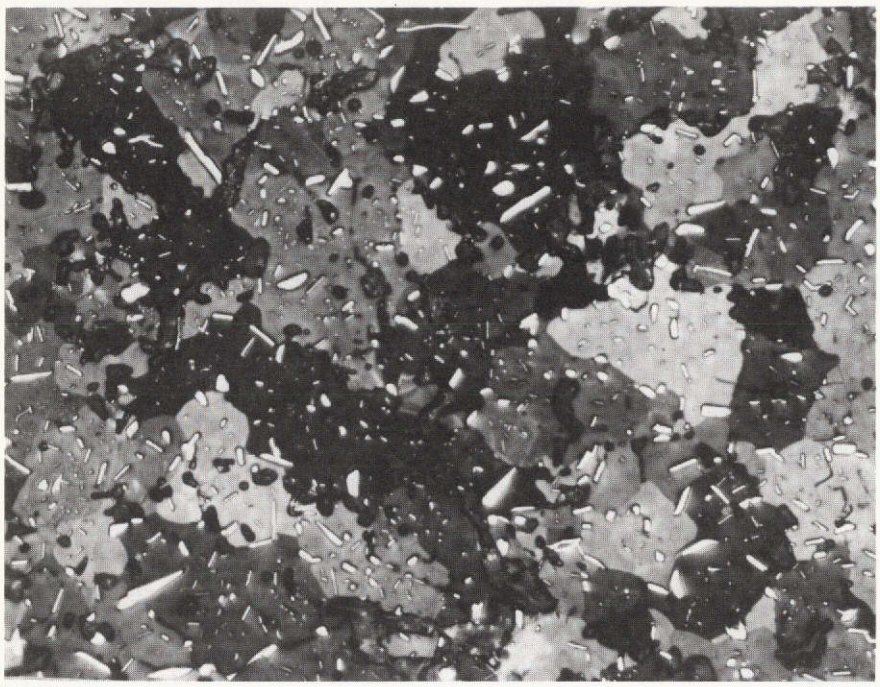

500X 5G697

FIGURE 45. PB11, $UC_{1.01}$ + 4 w/o W, 85.7% TD, TESTED AT 1400 C

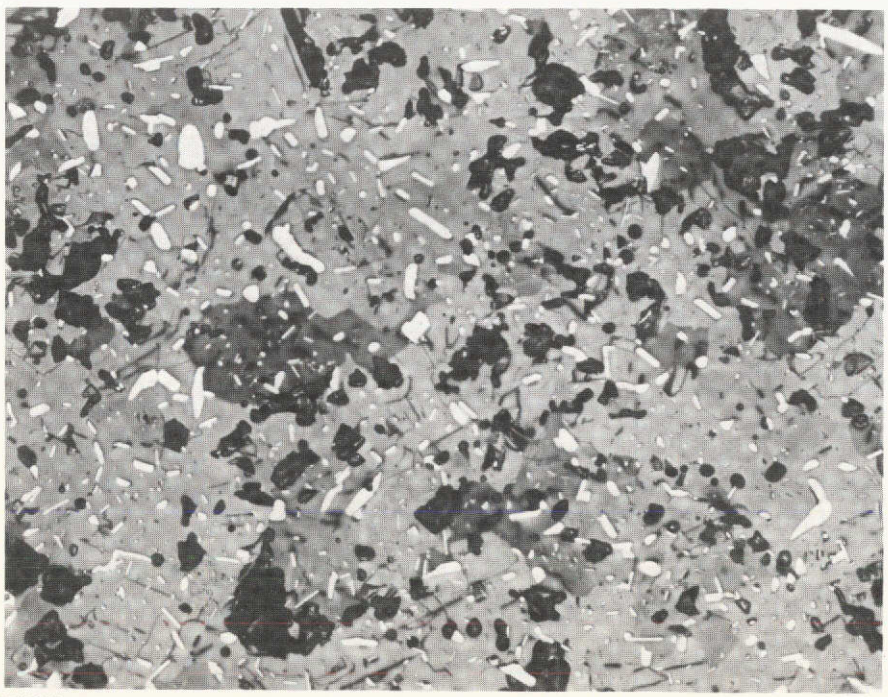

500X 7G193

FIGURE 46. PB14, $UC_{1.01}$ + 4 w/o W, 86.1% TD, TESTED AT 1550 C

Microstructural Studies

The microstructures of the low-density carbide specimens prior to creep testing were presented in Figures 6 to 10. Typical structures obtained from low-density specimens crept at 1400 and 1550 C are shown in Figures 39 to 48. The size and distribution of grains and various phases was not greatly altered after creep, except for the disappearance of the UC_2 platelets in the $UC_{1.01}$ specimens. Furthermore, there is little apparent difference in the structures of 75 and 85 percent TD alloys. Compare Figures 43 and 41 with Figures 45 and 47. The entire cross section of specimen PB1, $UC_{1.01}$ + 4 w/o W tested at 1400 C is shown in Figure 49. No evidence of oxidation was found on this specimen or on any other specimen tested in the Brew Unit.

IV. DISCUSSION

The data obtained for fully dense $UC_{1.01}$ appear to be in accord both with current theories of high-temperature creep and with other experimental results for deformation of coarse grained ceramic materials. Thus, the stress exponent of 6 found in this study is in agreement with the value found by Chang[5] for stoichiometric UC in the temperature range of 1500-2000 C, while the creep activation energy of 106 kcal/mole compares favorably with the values of 104, 107, and 100 kcal/mole measured for uranium diffusion in uranium carbide by Lee and Barrett[14], Hirsch and Scheff[19], and Fyodorov, et al[20], respectively. These results suggest that the creep behavior of high density $UC_{1.01}$ is controlled by a dislocation mechanism limited by uranium diffusion. Chang[5] has discussed several theories of high-temperature creep of intermetallic compounds and ceramic oxides and suggested a mechanism of steady-state creep based on diffusion-controlled dissolution of trails left behind by moving screw dislocations. Verification

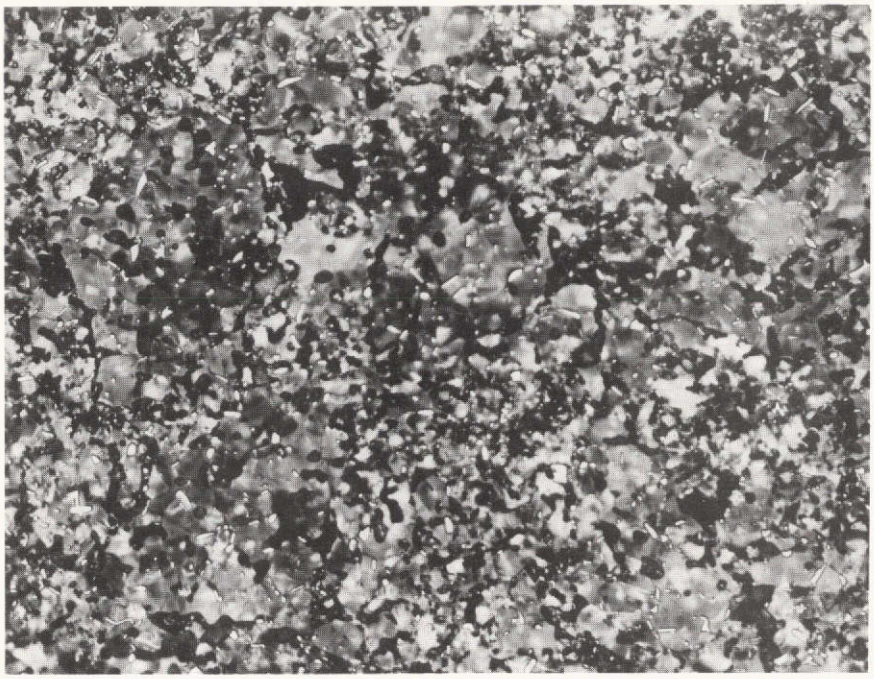

500X 5G699

FIGURE 47. PC11, $U_{0.9}Zr_{0.1}C_{1.01}$ + 4 w/o W, 87.0% TD, TESTED AT 1400 C

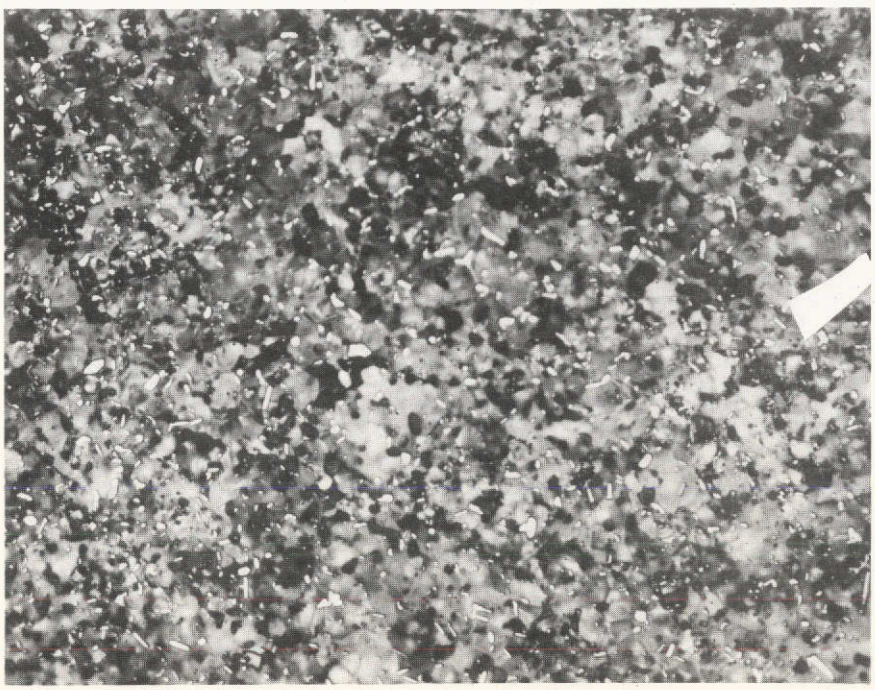

500X 7G196

FIGURE 48. PC13, $U_{0.9}Zr_{0.1}C_{1.01}$ + 4 w/o W, 87.2% TD, TESTED AT 1550 C

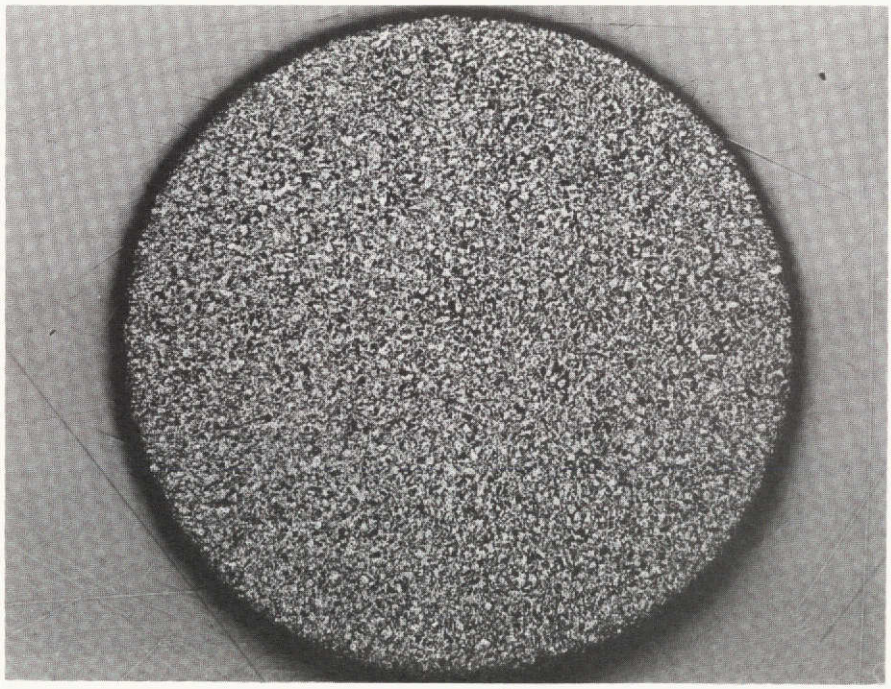

20X 5G634

FIGURE 49. PB1, $UC_{1.01}$ + 4 w/o W, 75.9% TD, TESTED AT 1400 C

of such a model for the materials studies in this program would have required detailed electron microscopy studies of crept samples; work which was beyond the scope of the program.

The creep data for $UC_{1.05}$ could not be treated in terms of a single stress exponent and a simple activation energy. These results, as well as the increased creep strength of $UC_{1.05}$ as compared with $UC_{1.01}$ which is found at lower temperatures can be attributed to second-phase precipitation at temperature in $UC_{1.05}$. This is illustrated by the phase diagram for the U-C system shown in Figure 50. The phase boundary between single phase UC_{1+x} and $UC + U_2C_3$ for the composition $UC_{1.05}$ occurs just below 1700 C, while for $UC_{1.01}$ a single UC phase may be expected even at 1400 C. Photographs showing the higher carbide acicular platelets in $UC_{1.05}$ as compared with $UC_{1.01}$, both before and after creep are shown in Figures 30 and 31. At temperatures above 1700 C, only small variations in creep strength should be expected for unalloyed UC_{1+x} fuels, but changes in stoichiometry can be expected to significantly influence creep behavior at lower temperatures. This was amply demonstrated in Figures 28 and 29 which included results of creep rate versus U/C ratio obtained by several different investigators.

The significant increase in creep strength of high-density uranium carbide containing tungsten additions as compared with unalloyed hyper-stoichiometric UC has now been observed in at least three independent studies. In the earlier Battelle study[22], creep rates for UC + 5 w/o W were some five orders of magnitude lower than those for unalloyed UC, while from Norrey's work[6], it appeared that as little as 0.9 w/o W sharply increases the creep strength of this compound. Norreys found that the presence of 0.9 w/o W reduced the lattice parameter of UC from 4.960 to 4.954Å and suggested that this certain amount of solubility of tungsten in UC causes a reduction in plasticity within the grains. More probably, the strengthening is due to the presence of particles of intermetallic compounds dispersed throughout the crystals. The most likely strengthening agent is UWC_2, a very hard (1900 kg/mm^2) compound which has been identified in previous studies

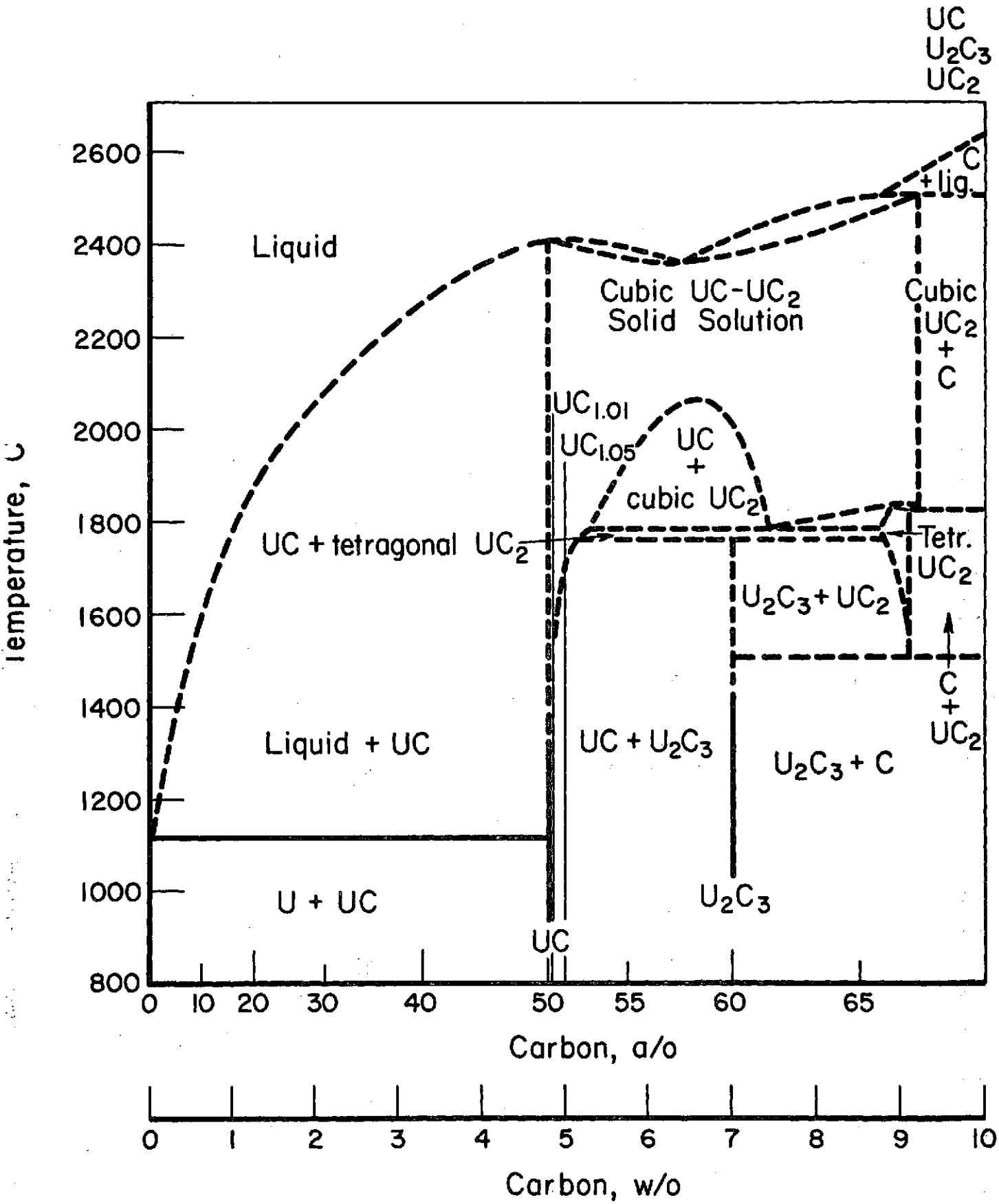

FIGURE 50. U-C CONSTITUTIONAL DIAGRAM

of uranium carbide containing tungsten additions.[23] Some additional strengthening may be expected in the alloys containing ten percent ZrC and this was indeed found in the present study.

In view of the differences in method of preparation, microstructure and oxygen concentration as well as porosity content and distribution, it is difficult to attribute variations in creep behavior for low- and high-density carbides to specific causes. For $UC_{1.01}$ creep rates of low-density specimens were some three orders of magnitude higher than those for fully dense specimens at 1400 C, while the difference amounted to some six orders of magnitude for $U_{0.9}Zr_{0.1}C_{1.01}$ + 4 w/o W at 1500-1600C.

The operative creep mechanisms appear to be different in all cases for high- and low-density specimens of a given alloy. This is seen most clearly from comparison of the creep activation energies, and for the unalloyed $UC_{1.01}$ by the differences in stress exponent. While creep of fully dense $UC_{1.01}$ has been attributed to an uranium volume diffusion-controlled dislocation mechanism, the low apparent creep activation energy of 40.2 kcal/mole for 75 percent dense $UC_{1.01}$ is indicative of a creep process controlled by a "short-circuit" diffusion mechanism such as uranium grain boundary diffusion or by carbon diffusion. Similarly, the low activation energies for creep of 75 and 85 percent dense carbide specimens containing tungsten suggests that dispersion strengthening is not applicable in these cases. While the low density specimens containing tungsten are stronger than those without the tungsten addition, the effect is minimal, amounting to a factor of three at high stresses (27.6 MN/m^2; 4000 psi) and being less than a factor of two at 6.9 MN/m^2 (1000 psi).

V. CONCLUSIONS

1. The creep behavior of high-density carbide samples was found to follow the classical time dependence, comprising an instantaneous deformation, followed by a primary creep region and then a period during which steady-state creep was measured.

2. Results for low-density specimens were characterized by large contributions to the total strain by primary creep behavior. Steady-state creep rates were several orders of magnitude higher for low-density specimens than those found for high-density specimens.
3. The creep data for fully dense $UC_{1.01}$ in the temperature range of 1400-1700 C could best be fit by the equation:

$$\dot{\varepsilon} = 1773\ \sigma^{6.024\pm0.283}\ \exp\left(-\frac{106.5\pm8.4}{RT}\right),$$

where $\dot{\varepsilon}$ is in hr^{-1}, σ is in MN/m^2, T is in °K, and creep activation energy is in kcal/mole.

The activation energy of 106 kcal/mole is in good agreement with values for uranium self-diffusion in uranium carbide.

4. Creep rates for fully dense $U_{0.9}Zr_{0.1}C_{1.01}$ + 4 w/o W were best fit by the equation:

$$\dot{\varepsilon} = 1.137 \times 10^{10}\ \sigma^{1.854\pm0.096}\ \exp\left(-\frac{155.2\pm4.8}{RT}\right).$$

5. Creep rates for fully dense $UC_{1.05}$ could not be fit by a simple Arrhenius equation because the stress exponent for creep decreased with decreasing temperature in the range 1700 to 1400 C.
6. Creep rates for unalloyed $UC_{1.01}$ and $UC_{1.05}$ are orders of magnitude greater than those measured for carbide alloys containing ZrC and/or tungsten dispersoid. The difference in creep strength between alloyed and unalloyed materials varies with temperature and applied stress.
7. At 1400 C, the creep rates for unalloyed UC_{1+x} decrease by several orders of magnitude as the C/U ratio is increased from 1.01 to 1.05 and then increase slightly as the C/U level is increased further to 1.08. This increase in creep strength at1400 C with increasing C/U ratio apparently results from precipitation strengthening. The effect is all but eliminated at 1700 C.
8. The possibility that some of the high-density carbide alloys may have been oxidized during testing suggests that the data obtained represent a lower limit on creep strength for the materials containing ZrC and/or tungsten.

9. The order of increasing creep strength was the same for low-density specimens as that found for fully dense samples, i.e., unalloyed UC is the weakest material, followed by $UC_{1.01}$ + 4 w/o W and $U_{0.9}Zr_{0.1}C_{1.01}$ + 4 w/o W. The differences in creep strength among the low-density specimens are much smaller, however, as compared with high-density materials.
10. In the temperature range of 1400-1550 C stress exponents for low-density alloys were found to vary from 1.3 to 2.6 while creep activation energies were measured in the range of 23.1 to 49.2 kcal/mole.

REFERENCES

(1) Ervin, G., Smalley, A. K., and Nadler, H., "Control of Stoichiometry in the Growth of Crystals and Uranium Monocarbide", Mater. Res. Bull., 1, 151 (1966).

(2) Seltzer, M. S., Perrin, J. S., Clauer, A. H., and Wilcox, B. A., "A Review of Creep Behavior of Ceramic Nuclear Fuels", Reactor Technology, 14, 99 (1971).

(3) Boncoeur, M., Magnier, P., and Accory, A., "Effect of Oxygen on the UC Phase Existence Domain", J. Nucl. Mat., 28, 233 (1968).

(4) Chang, R., "Flow and Recovery Properties of Nearly Stoichiometric Polycrystalline Uranium Carbide and the Mechanism of Work Hardening of Crystalline Solids", J. Appl. Phys., 33, 858 (1962).

(5) Chang, R., in Physics and Chemistry of Ceramics, edited by C. Klingsberg, Gordon and Breach, New York (1963), p 282.

(6) Norreys, J. J., in Carbides and Nuclear Energy, Vol 1, edited by L. E. Russell, MacMillan and Co., Ltd., London (1964), p 435.

(7) Fassler, M. H., Huegel, F. J., and DeCrescente, M. A., "Compressive Creep of UC and UN", PWAC-482, Part I (October, 1965).

(8) Stellrecht, D. E., Farkas, M. S., and Moak, D. P., "Compressive Creep of Uranium Carbide", J. Am. Ceram. Soc., 51, 455 (1968).

(9) Killey, N. M., "The Secondary Creep Behaviour of Uranium Monocarbide in Compression, I: Hypostoichiometric Uranium Monocarbide", J. Nucl. Mater., 41, 178 (1971).

(10) Killey, N. M., private communication to M. S. Seltzer (1971).

(11) Killey, N. M., King, E., and Hedger, H. J., "Creep of Uranium and Uranium-Plutonium Monocarbides in Compression", J. Brit. Nuc. Energy Soc., 65 (1971).

(12) Stellrecht, D. E., and Moak, D. P., "Creep Rupture of High-Temperature Fuels", in BMI-1870 (August, 1969), p 164.

(13) Chubb, W., Getz, R. W., and Townley, C. W., "Diffusion in Uranium Monocarbide", J. Nucl. Mater., 13, 63 (1964).

(14) Lee, H. M, and Barrett, L. R., "Measurements of Self-Diffusion in Uranium Carbide and Their Application to Related Activated Processes", Proc. Brit. Ceram. Soc., 7, 159 (1967).

(15) Lindner, R., Riemer, G., and Scherff, H. L., "Self-Diffusion of Uranium in Uranium Monocarbide", J. Nucl. Mater., 23, 222 (1967).

(16) Bentle, G. G., and Ervin, G., Jr., "Self-Diffusion of Uranium and Carbon in Uranium Monocarbide", AI-AEC-12726 (August, 1968).

(17) Villaine, P., "Uranium Self-Diffusion in Uranium Monocarbide", CEA-R-3436, in French (September, 1968).

REFERENCES (Cont.)

(18) Krakowski, R. A., "Self-Diffusion of Carbon in Uranium Monocarbide", J. Nucl. Mater., 32, 120 (1969).

(19) Hirsch, H. J., and Scherff, H. L., "Actinide Diffusion in Uranium Monocarbide", J. Nucl. Mater., 45, 123 (1973).

(20) Fyodorov, G. B., Gusev, V. N., Smirnov, E. A., Solovyev, G. I., and Yankulev, S. S., "An Investigation of Diffusion in the System UC-ZrC", Atomic Energy (USSR), 33, 584 (1972).

(21) Wilcox, B. A., and Clauer, A. C., "Dispersion Strengthening" in The Superalloys, C. T. Sims and W. C. Hagel, EDS., John Wiley and Sons, New York, 1972, p. 197.

(22) BMI-1848, August 1968.

(23) BMI-1732, June 29, 1965.

(24) Magnier, P., Marchal, M., and Accary, A., "High-Temperature Compressive Creep and Hot Extrusion of Uranium-Carbon Alloys", Proc. Brit. Ceram. Soc., 7, 141 (1967).